UNITED STATES PATENT AND TRADEMARK OFFICE

UNITED STATES DEPARTMENT OF COMMERCE
United States Patent and Trademark Office
Address: COMMISSIONER FOR PATENTS
P.O. Box 1450
Alexandria, Virginia 22313-1450
www.uspto.gov

APPLICATION NO.	FILING DATE	FIRST NAMED INVENTOR	ATTORNEY DOCKET NO.	CONFIRMATION NO.
10/005,168	12/04/2001	Thomas J. Brennan	R-10	6874

7590 10/21/2003

DELTAGEN, INC.
740 Bay Road
Redwood Ciity, CA 94063

EXAMINER	
WILSON, MICHAEL C	
ART UNIT	PAPER NUMBER
1632	

DATE MAILED: 10/21/2003

Please find below and/or attached an Office communication concerning this application or proceeding.

Office Action Summary	Application No.	Applicant(s)	
	10/005,168	BRENNAN, THOMAS J.	
	Examiner	Art Unit	
	Michael C. Wilson	1632	

-- The MAILING DATE of this communication appears on the cover sheet with the correspondence address --

Period for Reply

A SHORTENED STATUTORY PERIOD FOR REPLY IS SET TO EXPIRE 3 MONTH(S) FROM THE MAILING DATE OF THIS COMMUNICATION.

- Extensions of time may be available under the provisions of 37 CFR 1.136(a). In no event, however, may a reply be timely filed after SIX (6) MONTHS from the mailing date of this communication.
- If the period for reply specified above is less than thirty (30) days, a reply within the statutory minimum of thirty (30) days will be considered timely.
- If NO period for reply is specified above, the maximum statutory period will apply and will expire SIX (6) MONTHS from the mailing date of this communication.
- Failure to reply within the set or extended period for reply will, by statute, cause the application to become ABANDONED (35 U.S.C. § 133).
- Any reply received by the Office later than three months after the mailing date of this communication, even if timely filed, may reduce any earned patent term adjustment. See 37 CFR 1.704(b).

Status

1)☐ Responsive to communication(s) filed on _____ .

2a)☐ This action is **FINAL**. 2b)☒ This action is non-final.

3)☐ Since this application is in condition for allowance except for formal matters, prosecution as to the merits is closed in accordance with the practice under *Ex parte Quayle*, 1935 C.D. 11, 453 O.G. 213.

Disposition of Claims

4)☒ Claim(s) *1-37* is/are pending in the application.

4a) Of the above claim(s) *1,2,13 and 35-37* is/are withdrawn from consideration.

5)☐ Claim(s) _____ is/are allowed.

6)☒ Claim(s) *3-12 and 14-34* is/are rejected.

7)☐ Claim(s) _____ is/are objected to.

8)☐ Claim(s) _____ are subject to restriction and/or election requirement.

Application Papers

9)☐ The specification is objected to by the Examiner.

10)☐ The drawing(s) filed on _____ is/are: a)☐ accepted or b)☐ objected to by the Examiner.

Applicant may not request that any objection to the drawing(s) be held in abeyance. See 37 CFR 1.85(a).

11)☐ The proposed drawing correction filed on _____ is: a)☐ approved b)☐ disapproved by the Examiner.

If approved, corrected drawings are required in reply to this Office action.

12)☐ The oath or declaration is objected to by the Examiner.

Priority under 35 U.S.C. §§ 119 and 120

13)☐ Acknowledgment is made of a claim for foreign priority under 35 U.S.C. § 119(a)-(d) or (f).

a)☐ All b)☐ Some * c)☐ None of:

1.☐ Certified copies of the priority documents have been received.

2.☐ Certified copies of the priority documents have been received in Application No. _____ .

3.☐ Copies of the certified copies of the priority documents have been received in this National Stage application from the International Bureau (PCT Rule 17.2(a)).

* See the attached detailed Office action for a list of the certified copies not received.

14)☐ Acknowledgment is made of a claim for domestic priority under 35 U.S.C. § 119(e) (to a provisional application).

a) ☐ The translation of the foreign language provisional application has been received.

15)☐ Acknowledgment is made of a claim for domestic priority under 35 U.S.C. §§ 120 and/or 121.

Attachment(s)

1) ☒ Notice of References Cited (PTO-892)
2) ☐ Notice of Draftsperson's Patent Drawing Review (PTO-948)
3) ☒ Information Disclosure Statement(s) (PTO-1449) Paper No(s) *5* .
4) ☐ Interview Summary (PTO-413) Paper No(s). _____ .
5) ☐ Notice of Informal Patent Application (PTO-152)
6) ☐ Other: .

DETAILED ACTION

New Fig. 3 has been entered. The amendment to the description of Fig. 3 has been entered.

Election/Restrictions

Applicant's election without traverse of Group II (claims 3-12, 14-34) in the paper filed 7-20-03 is acknowledged.

Claims 1, 2, 13 and 35-37 are withdrawn from further consideration pursuant to 37 CFR 1.142(b) as being drawn to a nonelected invention, there being no allowable generic or linking claim. The requirement is made FINAL.

Claims 3-12 and 14-34 are under consideration in the instant office action.

Claim Rejections - 35 USC § 101

35 U.S.C. 101 reads as follows:

> Whoever invents or discovers any new and useful process, machine, manufacture, or composition of matter, or any new and useful improvement thereof, may obtain a patent therefor, subject to the conditions and requirements of this title.

Claims 3-12 and 14-34 are rejected under 35 U.S.C. 101 because the claimed invention is not supported by either a specific or substantial asserted utility or a well-established utility.

Claims 6, 7 and 14-33 are directed toward a transgenic animal having a disruption of an A2D2 calcium channel subunit gene. Claims 10 and 34 are directed toward methods of using the mice to identify compounds. The specification teaches making A2D2 -/- mice. The specification lists numerous tests to run on the mice to

determine their phenotype (pg 21-27). The mice had perinatal lethality and abnormal behavior, posture, body shape, eyes, growth and immune system. Heterozygous mice were not tested (pg 53, lines 7-24; pg 54 and 55, Tables 1-3). The specification suggests using the mice as a model of genetic disease but does not disclose a specific disease in humans linked to a disruption in A2D2 (pg 18, pg 20, lines 8-12).

The art at the time of filing taught "ducky mouse" had a disruption in A2D2 and a phenotype of "ataxic, wide-based gait and paroxysmal dyskinesia, small size and a failure to breed or survive beyond 35 days;" the art did not teach how to use such a mouse as a model of disease (Barclay, Aug. 15, 2001, J. Neurosci., Vol. 21, No. 16. pg 6095-6104; pg 6095, col. 2, 2nd ¶). Since the time of filing, Brodbeck (March 8, 2002, J. Biol. Chem., Vol. 277. No. 10, pg 7684-7693) taught mice having a disruption of the A2D2 gene are a model for "absence epilepsy," which is not taught or suggested in the instant application.

The mouse claimed does not have a specific utility. The specification does not teach a disruption in A2D2 correlates to any specific disease in humans. For example, A2D2 has not been linked to dwarfism (claim 22) in humans. While claims 14-33 are directed toward mice having particular characteristics, the characteristics are not specific to any disease. For example, abnormal gait (claim 19) is not specific to any disease. Using the mice claimed to identify compounds is not specific to the mouse claimed because wild-type mice may be used to identify such compounds. Therefore, using the mouse claimed to identify compounds is not specific to that mouse, and the mouse claimed does not have a use that is specific to any disease in humans.

The mouse claimed does not have a substantial utility. The mice die shortly after birth (perinatally); the specification does not teach how to use a mouse that dies perinatally (claim 20). Such mice are not useful in testing compounds because a phenotype in the mouse would have to be observed over a significant period of time. The specification does not teach how to use a mouse that has abnormal organ weight (claims 24-27), posture (claim 29-30), small eyes (claim 32) or squinting eyes (claim 33). Claims 10-11, step c) require administering compounds to the mice and determining whether A2D2 gene expression is modulated. Compounds that modulate A2D2 expression cannot be found using the mice because A2D2 is not expressed in the mice. Claim 34 requires administering compounds to the mice and determining whether a particular phenotype is ameliorated. The specification states the mouse may be used to test compounds relating to behavioral phenotypes (pg 20, line 8-12). Compounds that modulate behavioral phenotypes in the mice described in the specification are not useful because no behavioral phenotypes are linked with A2D2 in humans. No human genetic diseases, such as neurological, neuropsychological or psychotic illnesses (pg 20, line 12), are linked to the A2D2 gene. The specification does not identify any compounds that alter behavioral phenotypes using the mice. Therefore, using the mouse to identify compounds is not substantial.

Claim 9 is included because it is directed toward making the mouse, which lacks utility for reasons above. Claims 3-5, 8 and 15, directed toward cells having a disrupted A2D2 gene, and claims 11-12, directed toward using the cells to test compounds, are included because the cells lack a specific and substantial utility for the reasons above.

Claim Rejections - 35 USC § 112

The following is a quotation of the first paragraph of 35 U.S.C. 112:

> The specification shall contain a written description of the invention, and of the manner and process of making and using it, in such full, clear, concise, and exact terms as to enable any person skilled in the art to which it pertains, or with which it is most nearly connected, to make and use the same and shall set forth the best mode contemplated by the inventor of carrying out his invention.

Claims 3-12 and 14-34 are also rejected under 35 U.S.C. 112, first paragraph. Specifically, since the claimed invention is not supported by either a specific or substantial asserted utility or a well established utility for the reasons set forth above, one skilled in the art clearly would not know how to use the claimed invention.

In addition, the specification does not reasonably provide enablement for any animal, A2D2 gene, phenotype, cell, disruption, method of making a transgenic or method of using a transgenic as broadly claimed.

Claims 6, 7 and 14-33 are directed toward a transgenic animal having a disruption of an A2D2 calcium channel subunit gene. Claims 10 and 34 are directed toward methods of using the mice to identify compounds. The specification teaches making A2D2 -/- mice. The specification lists numerous tests to run on the mice to determine their phenotype (pg 21-27). The mice had perinatal lethality and abnormal behavior, posture, body shape, eyes, growth and immune system. Heterozygous mice were not tested (pg 53, lines 7-24; pg 54 and 55, Tables 1-3). The specification suggests using the mice as a model of genetic disease but does not disclose a specific disease in humans linked to a disruption in A2D2 (pg 18, pg 20, lines 8-12).

The specification does not enable making or using a transgenic with a wild-type phenotype as encompassed by the claims. The transgenics throughout many of the claims do not recite any phenotype and may, therefore, have any phenotype including wild-type phenotype. The specification does not provide any use for a transgenic having a disruption in A2D2 that has a wild-type phenotype. The only disclosed phenotype for the transgenic claimed is one that correlates to a mutation in A2D2. Therefore, the claims should recite a non-wild-type phenotype that correlates to a disruption in A2D2.

The specification does not teach how to make animals or cells having a disruption in an A2D2 gene other than mice (claims 3-8). Specifically, claims 4-5 encompass mice and rat cells. "Murine" encompasses mice and rats (http://www.m-w.com/cgi-bin/dictionary?book=Dictionary&va=murine). The only means of making a cell with a disruption in A2D2 taught in the specification is by using mouse embryonic stem cell technology. The state of the art at the time of filing was such that embryonic stem (ES) cell technology had only been successful in mice. Wagner (May 1995, Clin. and Experimental Hypertension, Vol. 17, pages 593-605) and Mullins (1996, J. Clin. Invest., Vol. 98, pages S37-S40) taught germline transmission of ES cells has not been demonstrated in species other than mice and the growth of ES cells from species other than mice is unreliable. Wall (1996, Theriogenology, Vol. 45, pg 57-68) taught transgene expression and the physiological result of such expression in livestock was not always accurately predicted in transgenic mice (page 62, line 7). The specification fails to provide sufficient guidance to make transgenics other than mice by teaching

obtaining ES cells in species other than mice. The specification does not teach the nucleic acid sequence of the A2D2 gene in non-mice, non-human species or correlate the A2D2 gene in mice to the A2D2 gene in other species. The specification does not teach how to make knockout animals other than mice or correlate making knockout mice to other species. Therefore, the specification does not provide adequate guidance for one of skill in the art to make a transgenic, non-human animal or cells having a disruption in A2D2 in any species other than mice.

The specification does not provide adequate correlation between the phenotype obtained in mice to the phenotype obtained in other species. The state of the art at the time of filing was that the phenotype of transgenic mice does not predict the phenotype in non-mice species. Models of human diseases have relied on transgenic rats when the development of transgenic mice having the desired phenotype was not feasible. Mullins (1990, Nature, Vol. 344, pg 541-544) produced outbred Sprague-Dawley x WKY rats with hypertension caused by expression of a mouse Ren-2 renin transgene. Hammer (1990, Cell, Vol. 63, pg 1099-1112) describes spontaneous inflammatory disease in inbred Fischer and Lewis rats expressing human class I major histocompatibility allele HLA-B27 and human b_2-microglobulin transgenes. Both investigations were preceded by the failure to develop human disease-like symptoms in transgenic mice (Mullins, 1989, EMBO, Vol. 8, pg 4065-4072; Taurog, 1988, J. Immunol., Vol. 141, pg 4020-4023) expressing the same transgenes that successfully caused the desired symptoms in transgenic rats. Therefore, the specification does not enable making transgenic having the disclosed phenotypes in species other than mice.

Claim 9 is directed toward a method of making a transgenic mouse having a disruption in A2D2 using a cell having a construct with two sequences of A2D2, introducing the cell into a blastocyst, implanting the blastocyst into a pseudopregnant mouse which gives birth to chimeric mice, and breeding the chimeric mouse to produce the transgenic mouse. The claim does not require using mouse cells or an embryonic stem cell, which is considered essential to the invention. A mouse ES cell is the only type of cell taught in the specification that can be introduced into a blastocyst and result in a chimeric mouse as claimed. The claim does not require the mouse have a non-wild type phenotype, which is required for reasons cited above. Given the unpredictability in the art taken with the guidance provided in the specification, the cell in a) should be a mouse ES cell, the blastocyst in b) should be a mouse blastocyst, and the transgenic mouse produced should have a genome comprising a homozygous disruption in A2D2, wherein said mouse lacks functional A2D2 and has a disclosed phenotype.

Claims 10-12 and 34 are directed toward methods of screening compounds using a cell or mouse having a disruption in an A2D2 gene. Step (c) requires determining whether the expression or function of A2D2 is modulated but the mice and cells do not express A2D2. The specification does not teach how to determine A2D2 expression in mice having a disruption in A2D2. While the specification teaches transgenics having particular characteristics, the specification does not teach how to use mice

having such characteristics in an assay to determine whether a compound modulates A2D2; the compound may modulate some other protein. Without such a disclosure, the specification does not provide adequate guidance for one of skill to use the mouse disclosed to determine compounds that modulate A2D2 expression or function.

The following is a quotation of the second paragraph of 35 U.S.C. 112:

> The specification shall conclude with one or more claims particularly pointing out and distinctly claiming the subject matter which the applicant regards as his invention.

Claim 12 and 14-34 are rejected under 35 U.S.C. 112, second paragraph, as being indefinite for failing to particularly point out and distinctly claim the subject matter which applicant regards as the invention.

The metes and bounds of what applicants consider "significant" expression cannot be determined making claim 14 unclear.

The metes and bounds of what applicants consider "abnormal" cannot be determined because the term has various meanings to those of skill in the art and because the term is not defined in the specification. Therefore, claims 16-34 are indefinite.

The term "derived" in claims 12 and 15 is indefinite. It cannot be determined if the claim is limited to cells having a disruption in A2D2 isolated from the transgenics or if the claim encompasses cells isolated from the mouse then made to have the disruption.

Claim Rejections - 35 USC § 102

The following is a quotation of the appropriate paragraphs of 35 U.S.C. 102 that form the basis for the rejections under this section made in this Office action:

A person shall be entitled to a patent unless –

(b) the invention was patented or described in a printed publication in this or a foreign country or in public use or on sale in this country, more than one year prior to the date of application for patent in the United States.

Claims 3, 4, 6-8 and 14-33 are rejected under 35 U.S.C. 102(b) as being anticipated by Snell (1955, J. Hered. Vol. 46, pg 27-29) as supported by Barclay (1998, J. Clin. Invest., Vol. 101, pg 689-695).

Snell taught the ducky mouse mutant. Barclay taught the ducky mouse mutant had a disruption in an A2D2 gene and had an "ataxic, wide-based gait and paroxysmal dyskinesia, small size and a failure to breed or survive beyond 35 days" (pg 6095, col. 2, 2nd ¶).

Conclusion

No claim is allowed.

Inquiry concerning this communication or earlier communications from the examiner should be directed to Michael C. Wilson who can normally be reached on Monday through Friday from 9:00 am to 5:30 pm at (703) 305-0120.

Questions of formal matters can be directed to the patent analyst, Dianiece Jacobs, who can normally be reached on Monday through Friday from 9:00 am to 5:30 pm at (703) 305-3388.

Questions of a general nature relating to the status of this application should be directed to the Group receptionist whose telephone number is (703) 308-1235.

If attempts to reach the examiner, patent analyst or Group receptionist are unsuccessful, the examiner's supervisor, Deborah Reynolds, can be reached on (703) 305-4051.

The official fax number for this Group is (703) 308-4242.

Michael C. Wilson

MICHAEL WILSON
PRIMARY EXAMINER

Form PTO -1449

SHEET 1 OF 1

INFORMATION DISCLOSURE CITATION

FORM PTO-1449

Atty. Docket No.: **R-10**	Serial No.: **10/005,168**
Inventor: **BRENNAN**	
Filing Date: **December 4, 2001**	Group Art Unit: **1632**

U.S. PATENT DOCUMENTS

EXAMINER'S INITIALS	REF.	PATENT NO.	DATE	NAME	CLASS	SUBCLASS	FILING DATE
				COPY OF PAPERS ORIGINALLY FILED			

FOREIGN PATENT DOCUMENTS

EXAMINER'S INITIALS	REF.	PATENT NO.	DATE	COUNTRY	CLASS	SUBCLASS	Translation Yes	Translation No

OTHER DOCUMENTS

EXAMINER'S INITIALS	REF.	(Including Author, Title, Date, Pertinent Pages, Etc.)
MM	AA	P. Powers et al., "LOCALIZATION OF THE GENE ENCODING THE α2/δ SUBUNIT (CACNL2A) OF THE HUMAN SKELETAL MUSCLE VOLTAGE-DEPENDENT Ca2+ CHANNEL TO CHROMOSOME 7q21-q22 BY SOMATIC CELL HYBRID ANALYSIS," Genomics, Vol. 19, 1994, pp. 192-193
MM	AB	D. Iles et al., "LOCALIZATION OF THE GENE ENCODING THE α2/δ-SUBUNITS OF THE L-TYPE VOLTAGE-DEPENDENT CALCIUM CHANNEL TO CHROMOSOME 7q AND ANALYSIS OF THE SEGREGATION OF FLANKING MARKERS IN MALIGNANT HYPERTHERMIA SUSCEPTIBLE FAMILIES," Human Molecular Genetics, Vol. 3, No. 6, April 15, 1994, pp. 969-975

EXAMINER: MM	DATE CONSIDERED: 10 9 03

EXAMINER: Initial if reference considered, whether or not citation is in conformance with MPEP 609; draw line through citation if not in conformity and not considered. Include copy of this form with next communication to applicant.

Notice of References Cited	Application/Control No. 10/005,168	Applicant(s)/Patent Under Reexamination BRENNAN, THOMAS J.	
	Examiner Michael C. Wilson	Art Unit 1632	Page 1 of 3

U.S. PATENT DOCUMENTS

*		Document Number Country Code-Number-Kind Code	Date MM-YYYY	Name	Classification
	A	US-			
	B	US-			
	C	US-			
	D	US-			
	E	US-			
	F	US-			
	G	US-			
	H	US-			
	I	US-			
	J	US-			
	K	US-			
	L	US-			
	M	US-			

FOREIGN PATENT DOCUMENTS

*		Document Number Country Code-Number-Kind Code	Date MM-YYYY	Country	Name	Classification
	N					
	O					
	P					
	Q					
	R					
	S					
	T					

NON-PATENT DOCUMENTS

*		Include as applicable: Author, Title Date, Publisher, Edition or Volume, Pertinent Pages)
	U	Barclay, Aug. 15, 2001, J. Neurosci., Vol. 21, No. 16. pg 6095-6104
	V	Brodbeck (March 8, 2002, J. Biol. Chem., Vol. 277. No. 10, pg 7684-7693
	W	Wagner, May 1995, Clin. and Experimental Hypertension, Vol. 17, pages 593-605
	X	Mullins 1996, J. Clin. Invest., Vol. 98, pages S37-S40

*A copy of this reference is not being furnished with this Office action. (See MPEP § 707.05(a).)
Dates in MM-YYYY format are publication dates. Classifications may be US or foreign.

Notice of References Cited	Application/Control No. 10/005,168	Applicant(s)/Patent Under Reexamination BRENNAN, THOMAS J.	
	Examiner Michael C. Wilson	Art Unit 1632	Page 2 of 3

U.S. PATENT DOCUMENTS

*		Document Number Country Code-Number-Kind Code	Date MM-YYYY	Name	Classification
	A	US-			
	B	US-			
	C	US-			
	D	US-			
	E	US-			
	F	US-			
	G	US-			
	H	US-			
	I	US-			
	J	US-			
	K	US-			
	L	US-			
	M	US-			

FOREIGN PATENT DOCUMENTS

*		Document Number Country Code-Number-Kind Code	Date MM-YYYY	Country	Name	Classification
	N					
	O					
	P					
	Q					
	R					
	S					
	T					

NON-PATENT DOCUMENTS

*		Include as applicable: Author, Title Date, Publisher, Edition or Volume, Pertinent Pages)
	U	Wall 1996, Theriogenology, Vol. 45, pg 57-68
	V	Mullins 1990, Nature, Vol. 344, pg 541-544
	W	Hammer 1990, Cell, Vol. 63, pg 1099-1112
	X	Mullins, 1989, EMBO, Vol. 8, pg 4065-4072

*A copy of this reference is not being furnished with this Office action. (See MPEP § 707.05(a).)
Dates in MM-YYYY format are publication dates. Classifications may be US or foreign.

Notice of References Cited	Application/Control No. 10/005,168	Applicant(s)/Patent Under Reexamination BRENNAN, THOMAS J.	
	Examiner Michael C. Wilson	Art Unit 1632	Page 3 of 3

U.S. PATENT DOCUMENTS

*		Document Number Country Code-Number-Kind Code	Date MM-YYYY	Name	Classification
	A	US-			
	B	US-			
	C	US-			
	D	US-			
	E	US-			
	F	US-			
	G	US-			
	H	US-			
	I	US-			
	J	US-			
	K	US-			
	L	US-			
	M	US-			

FOREIGN PATENT DOCUMENTS

*		Document Number Country Code-Number-Kind Code	Date MM-YYYY	Country	Name	Classification
	N					
	O					
	P					
	Q					
	R					
	S					
	T					

NON-PATENT DOCUMENTS

*		Include as applicable: Author, Title Date, Publisher, Edition or Volume, Pertinent Pages)
	U	Taurog, 1988, J. Immunol., Vol. 141, pg 4020-4023
	V	Snell, 1955, J. Hered. Vol. 46, pg 27-29
	W	
	X	

*A copy of this reference is not being furnished with this Office action. (See MPEP § 707.05(a).)
Dates in MM-YYYY format are publication dates. Classifications may be US or foreign.

The Journal of Neuroscience, August 15, 2001, 21(16):6095–6104

Ducky Mouse Phenotype of Epilepsy and Ataxia Is Associated with Mutations in the *Cacna2d2* Gene and Decreased Calcium Channel Current in Cerebellar Purkinje Cells

Jane Barclay,[1] Nuria Balaguero,[2] Marina Mione,[3] Susan L. Ackerman,[4] Verity A. Letts,[4] Jens Brodbeck,[2] Carles Canti,[2] Alon Meir,[2] Karen M. Page,[2] Kenro Kusumi,[5] Edward Perez-Reyes,[6] Eric S. Lander,[5] Wayne N. Frankel,[4] R. Mark Gardiner,[1] Annette C. Dolphin,[2] and Michele Rees[1]

[1]Department of Paediatrics and Child Health, Royal Free and University College Medical School, The Rayne Institute, London, WC1E 6JJ, United Kingdom, Departments of [2]Pharmacology and [3]Anatomy and Developmental Biology, University College London, London, WC1E 6BT, United Kingdom, [4]The Jackson Laboratory, Bar Harbor, Maine 04609, [5]Whitehead Institute for Biomedical Research, Cambridge, Massachusetts 02142, and [6]Department of Pharmacology, University of Virginia Health System, Charlottesville, Virginia 22908-0735

The mouse mutant ducky, a model for absence epilepsy, is characterized by spike-wave seizures and ataxia. The ducky gene was mapped previously to distal mouse chromosome 9. High-resolution genetic and physical mapping has resulted in the identification of the *Cacna2d2* gene encoding the $\alpha 2\delta 2$ voltage-dependent calcium channel subunit. Mutations in *Cacna2d2* were found to underlie the ducky phenotype in the original ducky (*du*) strain and in a newly identified strain (du^{2J}). Both mutations are predicted to result in loss of the full-length $\alpha 2\delta 2$ protein. Functional analysis shows that the $\alpha 2\delta 2$ subunit increases the maximum conductance of the $\alpha 1A/\beta 4$ channel combination when coexpressed *in vitro* in *Xenopus* oocytes. The Ca^{2+} channel current in acutely dissociated *du/du* cerebellar Purkinje cells was reduced, with no change in single-channel conductance. In contrast, no effect on Ca^{2+} channel current was seen in cerebellar granule cells, results consistent with the high level of expression of the *Cacna2d2* gene in Purkinje, but not granule, neurons. Our observations document the first mammalian $\alpha 2\delta$ mutation and complete the association of each of the major classes of voltage-dependent Ca^{2+} channel subunits with a phenotype of ataxia and epilepsy in the mouse.

Key words: epilepsy; ataxia; calcium channel; subunit; Purkinje cell; cerebellum; mouse mutant

Five spontaneous autosomal recessive mouse mutations impart a phenotype that includes epileptic seizures with features similar to those occurring in human idiopathic generalized epilepsy (IGE) (Puranam and McNamara, 1999). Tottering ($Cacna1a^{tg}$, $Cacna1a^{tg\text{-}la}$), slow-wave epilepsy ($Slc9a1^{swe}$), lethargic ($Cacnb4^{lh}$), stargazer ($Cacng2^{stg}$, $Cacng2^{stg\text{-}wag}$), and ducky (*du*) exhibit bilaterally synchronous spike-wave discharges (SWDs) on cortical electroencephalogram (EEG) recordings. These are accompanied by behavioral arrest and respond to the human anti-absence drug ethosuximide (Noebels et al., 1997). The electrophysiological hallmark of human absence epilepsy is 3 Hz SWDs. In mice, the frequency is usually 5–7 Hz (Noebels, 1991), except for those in $Slc9a1^{swe}$ (1–3 Hz) (Cox et al., 1997). Mutations in genes encoding voltage-dependent calcium channel (VDCC) subunits underlie three of these phenotypes: the genes encoding the $\alpha 1A$ (*Cacna1a*), $\beta 4$ (*Cacnb4*), and $\gamma 2$ (*Cacng2*) subunits are mutated in tottering (Fletcher et al., 1996), lethargic (Burgess et al., 1997), and stargazer (Letts et al., 1998) mice, respectively.

Voltage-dependent Ca^{2+} currents have been measured in all excitable cells and are implicated in many cellular processes (Berridge et al., 1998). They have been divided on the basis of kinetics and pharmacology into L-, N-, P/Q-, R-, and T-types (Catterall, 1998). Each VDCC is composed of a pore-forming $\alpha 1$ subunit that may be associated with an intracellular β, a membrane-spanning γ, and a membrane-anchored, but predominantly extracellular, $\alpha 2\delta$ subunit. The $\alpha 1$ subunit determines the main biophysical properties of the channel and is modulated by the other subunits (Walker and De Waard, 1998). Mammalian genes encoding 10 $\alpha 1$, four β, eight γ, and three $\alpha 2\delta$ subunits have been identified (for a comprehensive list, see Ertel et al., 2000; Burgess et al. 2001).

Homozygotes for the ducky (*du*) allele are characterized by an ataxic, wide-based gait and paroxysmal dyskinesia (Snell, 1955). They display reduced size and a failure to breed or survive beyond 35 d. Neuropathological studies revealed dysgenesis of selective regions of the CNS, including the cerebellum, medulla, and spinal cord (Meier, 1968). Axonal dystrophy and demyelination were also reported. Heterozygotes show no obvious phenotype. The *du* locus was localized to mouse chromosome 9 by linkage to the phenotypic markers dilute and short ear (Snell, 1955).

To identify and characterize the *du* locus, a positional cloning strategy was adopted. High-resolution genetic mapping identified

Received March 2, 2001; revised May 10, 2001; accepted June 1, 2001.

This work was supported by the Medical Research Council (UK), The Wellcome Trust, the Epilepsy Research Foundation, and National Institutes of Health Grants NS32801 (to V.A.L.) and NS31348 (to W.N.F.). We thank Dr. David Hosford and Randy Byers for generously sharing their expertise; Mick Keegan, Chantal Longo, Jo-Maree Courtney, and Eileen Sun for excellent technical assistance; the Human Genome Mapping Project Resource Centre for access to resources; and Hannah Mitchison and Anna-Elina Lehesjoki for useful comments.

N.B. and M.M. contributed equally to this work.

Correspondence should be addressed to Michele Rees, Department of Paediatrics and Child Health, Royal Free and University College Medical School, The Rayne Institute, 5 University Street, London, WC1E 6JJ, UK. E-mail: m.rees@ucl.ac.uk.

J. Barclay's present address: Novartis Institute for Medical Sciences, 5 Gower Place, London WC1E 6BS, UK.

 0270-6474/01/216095-10$15.00/0

the gene encoding the VDCC α2δ2 subunit as a positional and functional candidate. Mutations in this gene were identified in the original *du* strain and in a new allele, *du*^{2J}. This paper presents evidence that the gene underlying the ducky phenotype encodes the α2δ2 subunit and explores the effect of a mutation on Ca^{2+} channel function in *du/du* brain.

MATERIALS AND METHODS

Genetic and physical mapping

Mice were obtained from The Jackson Laboratory (Bar Harbor, ME). DNA was prepared from tail biopsies or liver samples by standard methods. Microsatellite markers were amplified as described previously (Dietrich et al., 1996). Recombinants were identified by agarose gel electrophoresis or PAGE or single-strand conformation polymorphism (*MDB1432*) analysis. Yeast artificial chromosome (YAC) clones were identified by PCR-based library screens (Haldi et al., 1996) or from a web-based database of clones (Nusbaum et al., 1999). Genomic clones were obtained from the Human Genome Mapping Project Resource Centre (Cambridge, UK).

Candidate gene analysis

Total RNA was prepared from frozen tissue using RNAzol B (Biogenesis, Sandown, NH) and used to prepare mRNA or cDNA using mRNA purification or First Strand cDNA synthesis kits (Amersham Pharmacia Biotech, Little Chalfont, UK). Northern blot analysis of 10 μg of cerebellar mRNA using Duralon UV nylon membrane and full-length *Cacna2d2* or human β actin as probes (Stratagene, La Jolla, CA) was performed using the suggested conditions of the manufacturer to optimize the identification of the wild-type 5.5 kb *Cacna2d2* transcript. This may have resulted in underestimation of the quantity of smaller transcripts (<2 kb). The full-length *Cacna2d2* cDNA was assembled using degenerate primers, reverse transcription (RT)-PCR, rapid amplification of cDNA ends (RACE), and sequencing. All primer sequences are available on request. RACE was performed using the 5′/3′ RACE kit (Roche Diagnostics, Hertfordshire, UK). Sequencing was performed on an ABI 373XL sequencer using TaqFS chemistry (PE Applied Biosystems, Foster City, CA). Genomic DNA was embedded in agarose and subjected to pulsed field gel electrophoresis (PFGE) on a Bio-Rad (Hercules, CA) clamped homogeneous electrical field electrophoresis system.

Electrode implantation and EEG measurements

Homozygous *du*^{2J} and control unaffected mice (8–12 weeks of age) were tested for spontaneous seizure activity. Mice were anesthetized with tribromoethanol (400 mg/kg, i.p.) and placed in a stereotaxic holder fitted with a mouse incisor bar. Burr holes were drilled (1 mm posterior to bregma, 1 mm lateral to midline) on both sides of the skull. Two Teflon-coated bipolar electrodes were implanted at 0.4–0.8 mm below the dura. Three screws were placed at the periphery of the skull to anchor the dental cap. Mice were allowed to recover for 2 d before EEG recordings were measured. The parameters for determining spike-wave discharges were described previously (Hosford et al., 1995).

In situ *hybridization and immunohistochemical analyses*

Mice [aged postnatal day 21 (P21) to P24] were terminally anesthetized by CO_2 inhalation and perfused with 4% paraformaldehyde. The brain was dissected into cold paraformaldehyde and then transferred through a sucrose gradient before embedding in OCT (Agar) and sectioning. Alternatively, the brain was removed without fixing and frozen in liquid nitrogen. Cryostat sections (10–15 μm) were cut and air dried onto positively charged slides (BDH Laboratory Supplies, Poole, UK).

cDNA fragments corresponding to α2δ2 [nucleotide (nt) 3705–4909], α2δ1 (nt 3521–3895), and α2δ3 (nt 2581–3602) were subcloned into pBluescript SK+. Sense and antisense RNA probes were prepared using T3 or T7 polymerase and digoxigenin (DIG) RNA labeling mix and purified using Quick spin columns (Roche Diagnostics). *In situ* hybridization was performed as described previously (Eisenstat et al., 1999).

Immunohistochemistry was performed on perfused tissue and isolated cells with a polyclonal calbindin D28K antibody (Chemicon, Harrow, UK) and on perfused tissue alone with a polyclonal calretinin antibody (Chemicon).

Heterologous expression of cDNAs

cDNAs encoding rabbit α1A (X57689), rat β4 (LO2315), and mouse α2δ2 (predominant brain splice variant that lacks exon 23 and 6 bp of exon 38, as described by Barclay and Rees, 2000) cDNAs, cloned into the pMT2 vector, were injected intranuclearly into *Xenopus* oocytes as described previously (Canti et al., 1999), except that 4 nl of cDNA mixture was injected at 1 μg/μl. Recordings were made using two-electrode voltage clamp as described previously (Canti et al., 1999).

Purkinje cell and granule cell preparation and I_{Ba} measurement

Purkinje neurons. Cells were dissociated from P4–P8 mice (Mintz et al., 1992) and plated onto concanavalin-A (2 μg/ml)-coated coverslips. Whole-cell I_{Ba} was recorded 1–4 hr later with 5 mM Ba^{2+} as described previously (Mintz et al., 1992). Purkinje cell (PC) identity was confirmed by positive calbindin immunostaining ($n > 70$).

Cerebellar granule cells. Granule cells (GCs) were isolated and cultured from P6–P8 mice, and whole-cell I_{Ba} was recorded as described previously using 10 mM Ba^{2+} (Pearson et al., 1995), except that the internal pipette solution contained (in mM): 100 HEPES, 30 EGTA, 0.57 $CaCl_2$, 2.25 $MgCl_2$, 3.68 ATP, and 0.1 GTP (Tris salt), pH 7.2 (320 mOsm).

Cells were used for analysis when the holding current at the holding potential was <20 pA for GCs and <50 pA for PCs. The holding current did not differ between genotypes. Leak current was subtracted using P/8 protocol. Individual *I–V* relationships were fitted with the modified Boltzmann equation $I = G_{max} * (V - V_{rev})/(1 + \exp[-(V - V_{50})/k])$, where G_{max} is the maximum conductance, V_{rev} is the reversal potential, k is the slope factor, and V_{50} is the voltage for 50% current activation.

Single-channel recording

All recordings were performed as described by Meir et al. (2000). Experiments were performed on cell-attached patches from PCs at room temperature (20–22°C). Recording pipettes were pulled from borosilicate tubes (World Precision Instruments, Sarasota, FL), coated with Sylgard (Sylgard 184; Dow Corning, Wiesbaden, Germany), and fire polished to form high-resistance pipettes (~10 MΩ with 100 mM $BaCl_2$). The bath solution was composed of (in mM): 135 K-aspartate, 1 $MgCl_2$, 5 EGTA, and 10 HEPES (titrated with KOH, pH 7.3). The patch pipettes were filled with a solution of the following composition (in mM): 100 $BaCl_2$, 10 tetraethylammonium (TEA)-Cl, 10 HEPES, and 200 nM TTX, titrated with TEA-OH to pH 7.4. Both solutions were adjusted to an osmolarity of 320 mOsm with sucrose. Data were sampled (Axopatch 200B and Digidata 1200 interface; Axon Instruments, Foster City, CA), at 5 kHz and filtered on-line at 1 kHz. Voltages were not corrected for liquid junction potential (Neher, 1995) measured to be −15 mV in these solutions.

Leak subtraction was performed by averaging segments of traces with no activity from the same voltage protocol in the same experiment and subtracting this average from each episode using pClamp6 (Axon Instruments). Event detection was performed using the half-amplitude threshold method. Single-channel amplitude was determined by either a Gaussian fit to the binned amplitude distributions or the mean amplitude in two experiments at +10 mV when there was a small number of events.

All results are presented as mean ± SEM, and statistical differences were determined by the Student's *t* test.

GenBank accession numbers

DNA and protein sequences described here have been deposited in GenBank under the following accession numbers: wild-type *Cacna2d2*, AF247139; *du* mutant transcript 1, AF247140; *du* mutant transcript 2, AF247141; and *du*^{2J} mutant transcript, AF247142.

RESULTS

Genetic and physical mapping of the *du* locus

Two genetic crosses were used to refine the location of *du* (Fig. 1*a*). Progeny representing 1460 meioses (564 backcross progeny and 448 intercross progeny) were typed with microsatellite markers 53.6–63.4 centimorgans (cM) from the centromere on mouse chromosome 9 (Dietrich et al., 1996). This region was assembled in overlapping yeast artificial chromosome (YAC) clones (Fig. 1*b*). Sequence tagged sites (STSs) to *Dag1* and *Lamb2* (Skynner

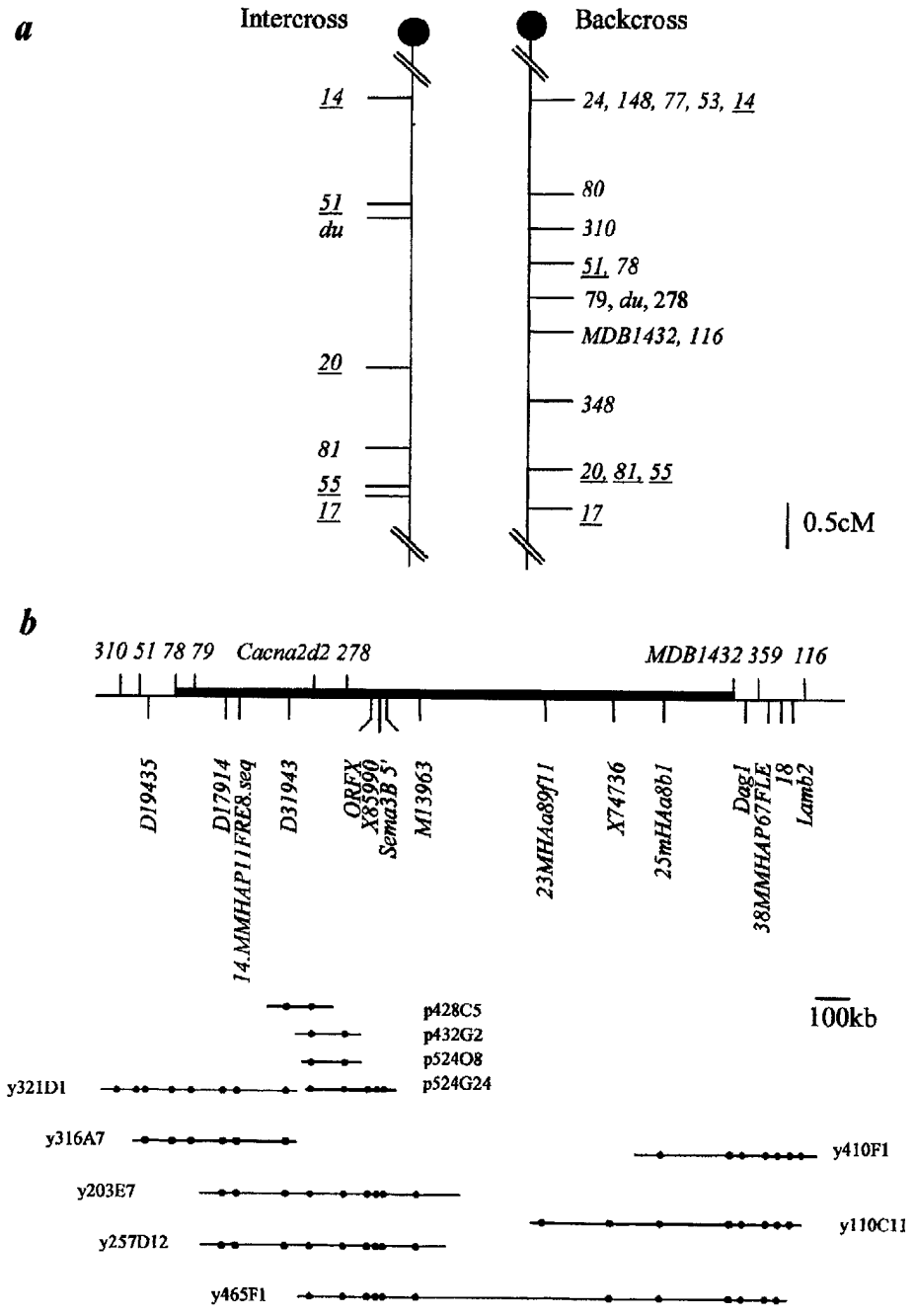

Figure 1. Genetic and physical maps define the *du* critical region. *a*, Genetic map around the *du* locus. The relation of the *du* gene to markers is shown to scale on partial chromosome linkage maps. Eight hundred ninety-six meioses of the (TKDU-+/*du* × STOCK *Dll3*^{pu} + *Tyr*$^{c\text{-}ch}$/+ *p Tyr*$^{c\text{-}ch}$) F1 intercross place *du* between *D9Mit51* and *D9Mit20* (2.9 ± 0.1 cM). Five hundred sixty-four meioses from an intersubspecific backcross [(TKDU-+/*du* × CAST/Ei) × TKDU-+/*du*] show that *D9Mit78* and *MDB1432* flank *du*, placing it in a 0.8 ± 0.3 cM interval. *D9Mit* prefixes have been removed from the markers for clarity. *Underlined* markers were typed in both crosses. *b*, Physical map of the *du* region. Markers ordered genetically are shown above the *horizontal line*, and those ordered on the physical map only are placed below. The region around *du* is indicated by a *filled bar*. A contig of YACs was assembled as illustrated. Library identification is prefixed with *y*. Four PAC clones are indicated and prefixed with *p*. Marker content in genomic clones is indicated by *filled circles* aligned with markers on the physical map. Gene symbols are as follows: *Sema3B*, *semaphorin3B*; *Dag1*, *dystroglycan1*; *Lamb2*, *laminin*β*2*.

et al., 1995) localized both genes distal to the *du* critical region (Fig. 1*b*). The human orthologs of these genes map to chromosome 3p21 (Skynner et al., 1995). The STS sequences *D31943*, *M13963*, and *X85990* demonstrated significant similarities with *CISH* (Uchida et al., 1997), *GNAT1* (Blatt et al., 1988), and *SEMA3B* (Sekido et al., 1996), respectively. These genes map to human 3p21.3, indicating that the *du* gene is in a region of conserved linkage with this region.

Cacna2d2 is a candidate gene for the *du* locus

Cacna2d2 was identified as a candidate gene for *du* as a direct result of the conservation of linkage of human chromosome 3p21.3 with this region of mouse chromosome 9. Human chromosome 3p21.3 is frequently deleted in small cell lung carcinoma and has been the target of positional cloning efforts. One transcript (human gene *CACNA2D2*; GenBank accession number AF042792) isolated from this region showed 55.6% homology with the α2δ1 VDCC subunit gene (Klugbauer et al., 1999; Gao et al., 2000). Two mouse expressed sequence tags (GenBank accession numbers AA000341 and AA008996) with 91 and 82% nucleotide identity to *CACNA2D2* were identified by Basic Local Alignment Search Tool analysis. This mouse sequence (gene *Cacna2d2*) was used to design a genomic PCR assay to test YACs

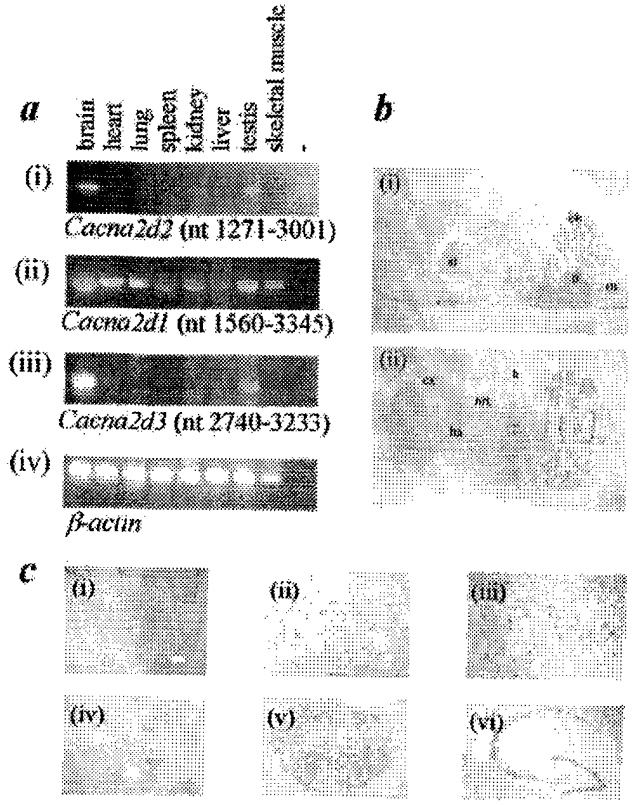

Figure 2. *Cacna2d2* is predominantly expressed in brain in a pattern distinct from *Cacna2d1* but similar to *Cacna2d3*. *a*, Expression of *Cacna2d2*, *Cacna2d1*, and *Cacna2d3* by RT-PCR of P28 +/+ mouse tissue RNA. β-Actin primers were used to allow comparisons of transcript levels. Negative control was no RNA. *i*, *Cacna2d2*-12F/14R; *ii*, *Cacna2d1*-1F/1R; *iii*, *Cacna2d3*-1F/1R; *iv*, β-actin. *b*, *In situ* hybridization analyses of whole-brain sections (P21 +/+) with a DIG-labeled antisense *Cacna2d2* RNA probe (nt 3705–4909). *i*, Sagittal section demonstrates the highest level of expression in cerebellum (*cb*), with some expression also in medulla (*m*), pons (*p*), and striatum (*st*). *ii*, The horizontal section shows expression in cortex (*cx*), nucleus reticularis thalami (*nrt*), habenula (*ha*), and hippocampus (*h*). *c*, Detailed examination of some of these areas by *in situ* hybridization with the same probe as above. Moderate expression is seen in medulla (*i*), and higher levels were seen in a subpopulation of cells of the striatum (*ii*) and cerebral cortex in a large proportion of cortical neurons throughout all layers (*iii*). Uniform expression is seen in nRT (*iv*), habenula (*v*), and hippocampus (*vi*). Scale bar: *Ci–Ciii*, 100 μ m; *Civ*, *Cv*, 50 μm.

from the *du* contig. Three positive clones (y203E7, y257D12, and y465F1) placed *Cacna2d2* between *D17914* and *M13963*, within the candidate interval (Fig. 1*b*). STS content mapping of four overlapping *Cacna2d2*-positive P1-artificial chromosomes (PACs) orientated the gene as 5′ to 3′ in a proximal to distal direction (Fig. 1*b*). An intragenic (CA)n repeat (α2δ2–43.21) was nonrecombinant with *du* in the backcross. Therefore, *Cacna2d2* was a good positional and functional candidate for *du*.

The 5.5 kb *Cacna2d2* cDNA (GenBank accession number AF247139) shared 91% nucleotide identity with *CACNA2D2*. The genomic structure of the *Cacna2d2* gene has been determined (see Fig. 3*d*) (Barclay and Rees, 2000). Overall, mouse α2δ2 shares 95% identity and 96.5% similarity with the human protein.

Cacna2d2 is predominantly expressed in mouse brain in a restricted pattern

The predominant *Cacna2d2* transcript is in brain, with lower levels in kidney and testis (Fig. 2*ai*), a pattern distinct from *Cacna2d1* (Fig. 2*aii*) but similar to *Cacna2d3* (Fig. 2*aiii*). By RT-PCR, no *Cacna2d2* expression was detected in lung at any age studied (1, 2, 6, and 20 months), a result confirmed using two additional sets of PCR primers (data not shown). Detailed *Cacna2d2* brain expression was studied by *in situ* hybridization. A *Cacna2d2* antisense RNA probe (exons 38–39) was hybridized to sections of P21 +/+ mouse brain. Analysis of whole-brain sagittal sections (Fig. 2*bi*) revealed the highest level of expression to be in the cerebellum, with moderate levels in medulla, pons, and striatum. Analysis of horizontal sections (Fig. 2*bii*) also shows expression in cortex, hippocampus, habenula, and nucleus reticularis thalami (nRT). Figure 2*c* shows higher-resolution images of medulla (*i*), striatum (*ii*), cerebral cortex (*iii*), nRT (*iv*), habenula (*v*), and hippocampus (*vi*). No signal was detected with a control sense probe (data not shown). Cerebellar expression is investigated further in Figure 5, demonstrating that the gene is highly expressed in PCs with only very low levels in the granule cell layer (GCL) (see Fig. 5*e*).

Cacna2d2 is mutated in *du/du* mice

No full-length *Cacna2d2* transcript was detected by RT-PCR in *du/du* mice. A failure of amplification between exon 1 and 4–39 implied disruption of the gene (Fig. 3*ai*, *top* and *middle panels*). Additional analysis identified two distinct mutant transcripts. 3′ RACE of *Cacna2d2* RNA in *du/du* identified a chimeric transcript (mutant transcript 1) composed of exons 1, 2, and 3 spliced to a novel sequence (X). RT-PCR using primers for *Cacna2d2* exon 1 and region X gave a *du*-specific product (Fig. 3*ai*, *bottom panel*). Mutant transcript 1 encodes the first 414 nucleotides of *Cacna2d2*, followed by 24 novel nucleotides and a stop codon. Amplification between exons 1 and 3 (Fig. 3*ai*, *top panel*) reveals a low level of mutant transcript 1 in *du/du* mice. A low level of mutant transcript 2 (exons 2–39) is also detected by RT-PCR in *du/du* brain (Fig. 3*aii*). Wild-type *Cacna2d2* (5.5 kb) and these mutant transcripts sized ~1.5 and 5 kb can be detected by Northern analysis of +/+ and *du/du* cerebellar mRNA, respectively (Fig. 3*b*).

The presence by RT-PCR of the two mutant transcripts in *du/du* mice suggested a duplication of exons 2 and 3, although additional bands were not detected by standard agarose gel electrophoresis and Southern blotting (data not shown). In contrast, PFGE and Southern blotting revealed a large genomic rearrangement (Fig. 3*c*). Exons 1 and 4–39 are present once per + and *du* chromosome. This is demonstrated by the presence of single 190 kb *Not*I hybridizing fragments with the probe corresponding to these exons (Fig. 3*ci*,*ciii*) in both genotypes. Exons 2–3 and region X are present once per + chromosome and twice per *du* chromosome, as indicated by the single (190 kb) and double (190 and 600 kb) *Not*I fragments (Fig. 3*cii*), respectively. This supports a genomic duplication of exons 2–3 and region X. The large size (>150 kb) of this duplication precludes its identification by conventional PCR and sequencing or Southern blotting because internal primer sites and restriction sites have been duplicated without disruption, preventing any distinction between original and duplicated exons. The wild-type position of region X as 3′ to the *Cacna2d2* gene was confirmed by PCR amplification of the PAC clones (Fig. 1*b*). In genomic DNA, the copy of region X common to +/+ and *du/du* contains two B2 repeat elements, and

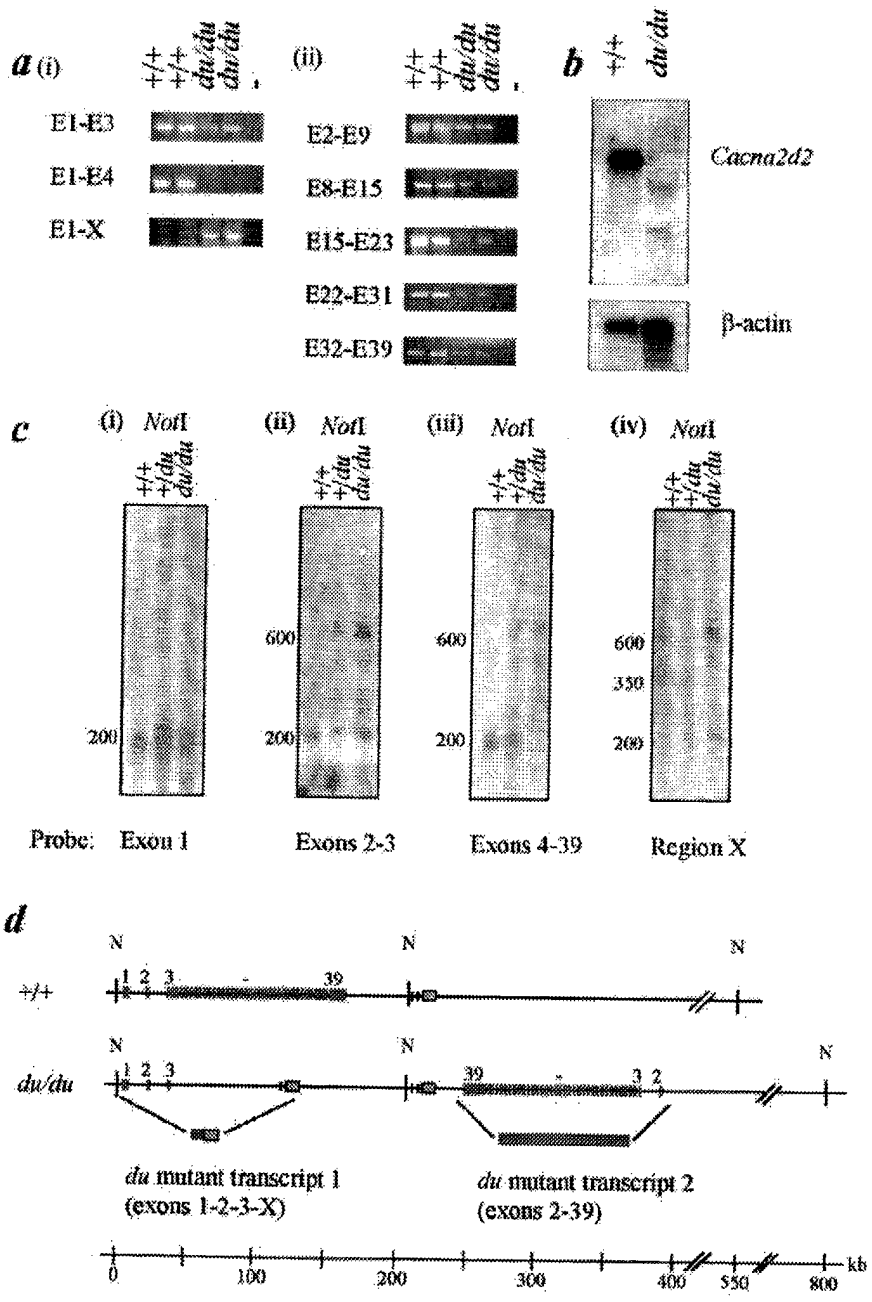

Figure 3. The *du* mutation is a genomic rearrangement involving the *Cacna2d2* gene. *a*, Two mutant transcripts can be identified by RT-PCR of total brain RNA from *du/du* mice. Two +/+, two *du/du* samples, and a negative control (no RNA) are shown per gel. *i*, *Top*, Normal size amplification product of exons 1–3 is shown in +/+ and *du/du* RNA, with reduced levels in the latter. *Middle*, Amplification between exons 1 and 4 does not produce a product in *du/du* RNA, suggesting disruption of the *Cacna2d2* gene in this region. *Bottom*, Amplification of the *du*-specific chimeric transcript of *Cacna2d2* exons 1, 2, and 3 and a novel sequence X. *ii*, Overlapping PCR fragments spanning exons 2–39 of *Cacna2d2* can be detected in +/+ and *du/du* RNA, with lower levels observed in *du/du* samples. *b*, Wild-type *Cacna2d2* transcript (5.5 kb) is absent from *du/du* brain by Northern analysis using cerebellar mRNA and full-length *Cacna2d2* as a probe. Low levels of two *du*-specific bands (~1.5 and 5 kb) are detected. The filter was rehybridized with β-actin as a control for RNA loading. *c*, PFGE shows duplication of *Cacna2d2* exons 2 and 3 and region X in *du/du* genomic DNA. Southern analysis of *Not*I-digested genomic DNA separated by PFGE from +/+, +/*du*, and *du/du* mice is shown. Blots were hybridized with *Cacna2d2* probes: *i*, exon 1; *ii*, exons 2–3; *iii*, exons 4–39; *iv*, region X. Sizes are in kilobases. *d*, A scale representation of the genomic region containing *Cacna2d2* (*red*) and region X (*blue*) in +/+ and *du/du* mice. *N*, *Not*I sites. The presence of one or two B2 repeats 5′ to region X is marked by a *vertical line*. The mutant transcripts 1 and 2 produced from each region in *du/du* are represented by *colored boxes*. The *Cacna2d2* gene is arranged 5′ to 3′ in +/+. In *du/du*, exons encoding mutant transcript 1 are shown in a 5′ to 3′ direction, and those encoding mutant transcript 2 are inverted and shown 3′ to 5′. The distance between exon 3 and region X is unknown but is >12 kb. The scale bar is in kilobases.

the *du*-specific copy contains a single B2 repeat (Fig. 3*d*). A plausible mutation mechanism, possibly mediated by the B2 repeats, is a head to tail duplication of *Cacna2d2* exons 2–39 and region X, followed by a deletion including exons 4–39 of the original *Cacna2d2*.

A second, distinct mutation of *Cacna2d2* in *du*^{2J}/*du*^{2J} mice

Recently, a spontaneous, autosomal recessive mouse mutant, with ataxia and paroxysmal dyskinesia, arose at The Jackson Laboratory. Breeding experiments established it as a novel ducky allele: *du*^{2J}. Cortical EEG recordings from *du*^{2J}/*du*^{2J} revealed infrequent bilateral SWDs of high amplitude (500 μV) and 5–7 Hz (Fig. 4*a*). These spontaneous discharges were accompanied by behavioral arrest. To determine whether these discharges were seizure related, an intraperitoneal injection of ethosuximide (100 mg/kg) was given, and the discharges were abolished.

Mutational analysis of *Cacna2d2* in *du*^{2J}/*du*^{2J} mice by RT-PCR and genomic sequencing revealed a 2 bp deletion (TG) within exon 9 (Fig. 4*b*) predicted to cause premature truncation of the protein (GenBank accession number AF247142). Sequence analysis of 45 subclones of the *du*^{2J}/*du*^{2J} RT-PCR product failed to detect any wild-type transcript (data not shown). Northern analysis of mRNA from *du*^{2J}/*du*^{2J} brain showed no difference in

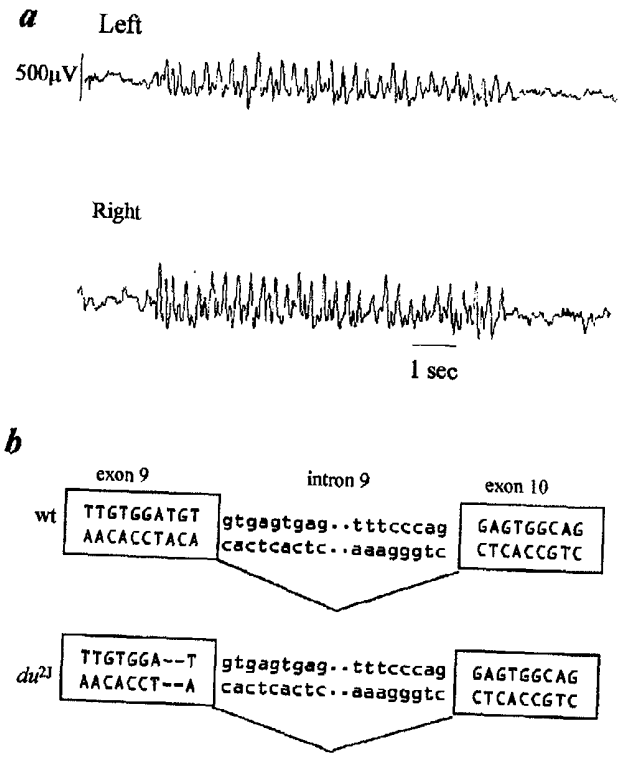

Figure 4. du^{2J}/du^{2J} mice show 5–7 Hz SWD on cortical EEG and a 2 bp deletion in *Cacna2d2*. *a*, Representative EEG recordings of seizures from homozygous du^{2J}/du^{2J} mice ($n = 8$). Low- and high-frequency filters were set at 0.3 and 35 Hz, respectively. Traces from cortical bipolar electrodes implanted in the left and right hemispheres are illustrated. These spike-wave discharges accompanied behavioral arrest. Control mice ($n = 2$) showed no abnormal activity (data not shown). *b*, Schematic representation of exons 9 and 10 and intron 9 of the *Cacna2d2* gene in +/+ and du^{2J}/du^{2J} genomic DNA.

Cacna2d2 transcription levels compared with wild type (data not shown), suggesting stability of the mutated transcript.

These observations suggest that *Cacna2d2* mutations in *du/du* and du^{2J}/du^{2J} mice underlie the ducky phenotype of ataxia, SWDs, and paroxysmal dyskinesia.

Immunohistochemistry of *du/du* Purkinje and granule cells reveals no cell loss

In view of the cerebellar pathology in *du/du* mice, we wanted to identify whether there was any loss of PCs or GCs that might be responsible for this. However, immunohistochemical investigations using calbindin as a PC marker (Fig. 5*a*,*b*) and calretinin as a GC marker (Fig. 5*c*,*d*) did not identify loss of cell bodies in *du/du* cerebella at P21 (Fig. 5*b*,*d*). Similar observations were made for du^{2J}/du^{2J} (data not shown).

Absence of full-length α2δ2 in *du/du* cerebellar Purkinje cells

In situ hybridization with a 3′ *Cacna2d2* anti-sense RNA probe (Fig. 5*e*,*f*) was used to demonstrate the presence of full-length *Cacna2d2* message in +/+ PCs (Fig. 5*e*) and its absence in *du/du* PCs (Fig. 5*f*).

The possibility of compensatory upregulation of *Cacna2d1* (Fig. 5*g*,*h*) and *Cacna2d3* (Fig. 5*i*,*j*) transcript levels in *du/du* cerebella was investigated by *in situ* hybridization with antisense RNA probes. No major differences were observed in their distribution in *du/du* compared with +/+ cerebellum, and in particular there was no compensatory expression of α2δ1 or α2δ3 mRNA in *du/du* PCs.

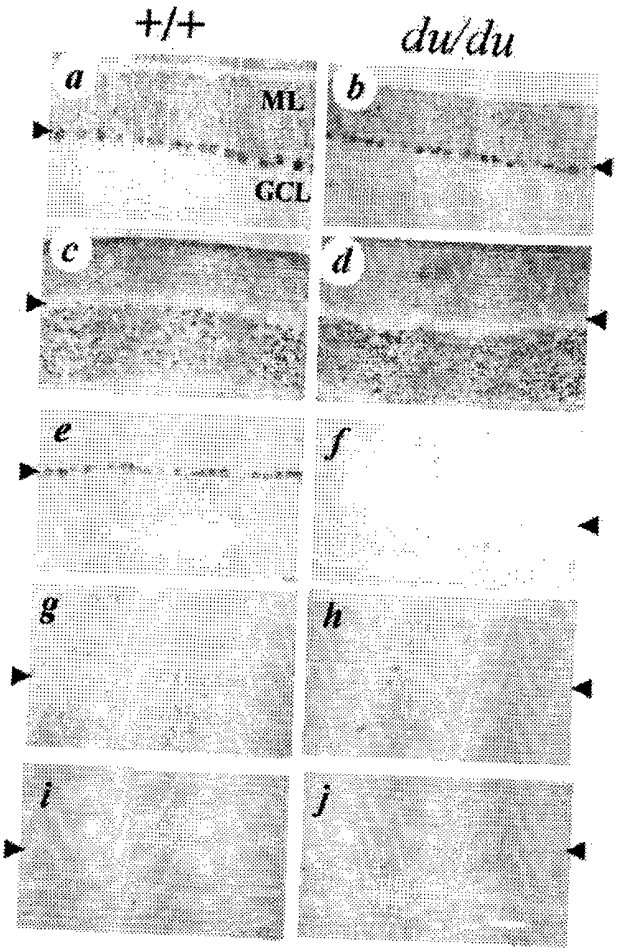

Figure 5. Analysis of *Cacna2d2*, *Cacna2d1*, and *Cacna2d3* expression in cerebellum of P21 +/+ and *du/du* mice. *a*, *b*, Immunohistochemical detection of calbindin showing no obvious differences in PC number in *du/du* (*b*) compared with +/+ (*a*) cerebellum. *c*, *d*, Calretinin immunostaining shows no difference in GC staining between +/+ (*c*) and *du/du* (*d*) cerebellum. *In situ* hybridization of +/+ and *du/du* sections with a 3′ *Cacna2d2* antisense RNA probe. Analyses were performed on +/+ (*e*) and *du/du* (*f*) sections. This probe does not detect any expression in the *du/du* PCs (*f*). *In situ* hybridization with *Cacna2d1* (*g*, *h*) and *Cacna2d3* (*i*, *j*) probes. (For *a–j*, $n = 3$ for each genotype and experiment.) For all three riboprobes used, no signal was detected on hybridization of control sense RNA to +/+ sections (results not shown). Scale bar: *a–j*, 100 μm. The PCL is indicated by an *arrowhead*, and the ML is *uppermost* in all sections. A small region of cerebellum is shown throughout for clarity.

Modulation of Ca^{2+} channel currents by α2δ2

The physiological function of the α2δ2 subunit encoded by the *Cacna2d2* gene was investigated using *in vitro* expression and electrophysiology. To mimic the composition of the predominant calcium channels in cerebellar Purkinje cells, we examined the effect of α2δ2 when coexpressed with α1A and β4 in *Xenopus* oocytes. Coexpression of α2δ2 induced a large enhancement of α1A current amplitude (Fig. 6*a*,*b*). For example, at 0 mV, the increase was from -0.55 ± 0.15 ($n = 14$) to -1.8 ± 0.27 μA ($n = 13$), and there was a small hyperpolarization of current activation,

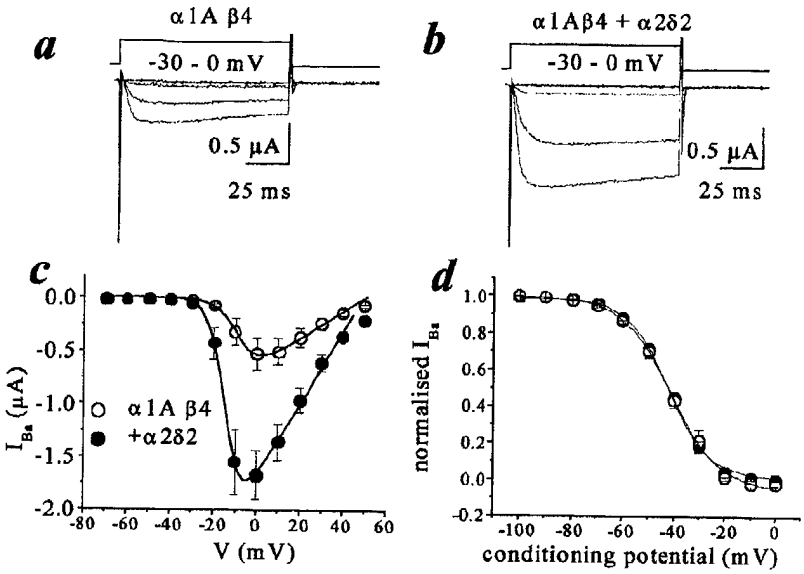

Figure 6. The effect of α2δ2 on α1A/β4 calcium channel currents expressed in *Xenopus* oocytes. *a*, *b*, Calcium channel currents recorded in 5 mM Ba^{2+} from *Xenopus* oocytes injected with either α1A/β4 (*a*) or α1A/α2δ2/β4 (*b*). For clarity, only the currents on the rising phase of the *I–V* relationship are shown. *c*, *I–V* relationship of α1A/β4 (○) and α1A/α2δ2/β4 (●) peak currents (n = 14 and 13, respectively). The mean *I–V* relationships were fitted with a combined Boltzmann and linear fit, as described in Materials and Methods. No significant differences were observed in the V_{rev} or k (results not shown). *d*, Steady-state inactivation of α1A/β4 (○) and α1A/α2δ2/β4 (●) currents (n = 14 and 13, respectively) were obtained by stepping to the conditioning potential for 25 sec, before measuring the current at the test potential of 0 mV. Individual data were fitted with a single Boltzmann equation of the form $I/I_{max} = 1/(1 + \exp[(V - V_{50})/k])$, where k is the slope factor and V_{50} is the voltage for 50% steady-state inactivation of the current. The $V_{50(inactivation)}$ was −41.73 ± 1.0 mV for α1A/β4 and −41.68 ± 1.1 mV for α1A/α2δ2/β4.

the voltage for 50% activation shifting from −6.4 ± 0.7 to −12.0 ± 1.4 mV ($p < 0.01$) (Fig. 6*c*). The maximum conductance was increased from 0.013 ± 0.003 to 0.036 ± 0.005 μS by coexpression of α2δ2. There was no effect of α2δ2 on steady-state inactivation of α1A/β4 currents (Fig. 6*d*).

Ca^{2+} channel currents in *du/du* Purkinje cells and granule cells

The effects of α2δ2 on the α1A/β4 current *in vitro* suggested that loss of wild-type α2δ2 may result in a reduction in Ca^{2+} current density. To test this, I_{Ba} was examined in acutely dissociated cerebellar PCs from P4–P8 mice. I_{Ba} density was clearly reduced in the PCs from *du/du* compared with +/+ and +/*du* mice (Fig. 7*a*,*b*). There was no effect on voltage dependence of activation (Fig. 7*a*) or on the kinetics of activation or inactivation (data not shown). Cell size, as determined by the capacitance, was not significantly different between the genotypes, being 14.9 ± 1.4, 15.1 ± 0.9, and 17.6 ± 1.7 pF in the +/+, +/*du*, and *du/du* PCs, respectively. To examine the basis for the reduction in the whole-cell I_{Ba} in *du/du* PCs, single P-type Ca^{2+} channels were examined in the cell-attached mode from +/+, +/*du*, and *du/du* PCs (Fig. 7*c*). There was no difference in the single-channel conductance or amplitude between the three genotypes (Fig. 7*d*). In cultured cerebellar GCs, taken from P6–P8 mice, there was no significant difference in I_{Ba} density at any potential (Fig. 7*e*,*f*) or in cell capacitance between the genotypes.

DISCUSSION

Our data provide strong evidence that the ducky phenotype is associated with mutations in the *Cacna2d2* gene. This is discussed together with a consideration of the normal expression pattern and function of the VDCC α2δ2 accessory subunit it encodes and how disruption of this function leads to the phenotypic features of ataxia and spike-wave seizures.

Cacna2d2 is disrupted in *du* and du^{2J} mice

These studies demonstrate that wild-type *Cacna2d2* transcript is absent from the brain of *du/du* and du^{2J}/du^{2J} mice. In *du/du* mice, a genomic rearrangement disrupts *Cacna2d2* and duplicates a nonfunctional open reading frame, region X, although the exact mechanism remains unclear. Mutant transcripts 1 and 2 are present at very low levels in *du/du* mice and, if translated, would encode proteins that are unlikely to function normally. The product of mutant transcript 1 would lack most of the α2 subunit and the δ subunit that includes the transmembrane domain, whereas that of mutant transcript 2 is unlikely to be trafficked correctly without a signal sequence. In du^{2J}/du^{2J} mice, a 2 bp deletion in exon 9 of *Cacna2d2* would result in a truncated protein lacking >800 amino acids, including the transmembrane domain. This is the first mammalian phenotype associated with disruption of an α2δ subunit gene and should allow the physiological roles of α2δ2 and the other α2δ subunits to be characterized further.

Cacna2d2 is predominantly expressed in mouse brain

Northern analysis of *CACNA2D2* in human tissue showed highest expression in heart, pancreas, and skeletal muscle and lower levels in kidney, liver, placenta, and brain (Klugbauer et al., 1999). A separate study reported highest expression in lung and testis and significant levels in brain, heart, and pancreas (Gao et al., 2000) and suggested that the pattern in the former study may reflect cross-hybridization of the probe with *CACNA2D1*. The expression pattern presented here corresponds more closely with the latter study, and the differences observed (particularly in lung) may be attributed to species differences and/or developmental differences. This is not unprecedented (Fougerousse et al., 2000).

In brain, *Cacna2d2* expression was highest in cerebellar PCs but was also detected in cerebral cortex, hippocampus, cerebellar GCs, nRT, habenula, pons, and medulla. The genes encoding the α2δ1, α2δ2, and α2δ3 subunits show generally distinct patterns of expression within the cerebellum. *Cacna2d1* is predominantly expressed in the GCL, *Cacna2d2* is predominant in the Purkinje cell layer (PCL), and *Cacna2d3* expression is detected in the molecular layer (ML) (Klugbauer et al., 1999; Hobom et al., 2000; present study). Most of the α1, β, and γ subunit genes share at least one region of expression with *Cacna2d2*, making it difficult to predict *in vivo* interactions based on expression profiles. However, the similarity of the ducky phenotype to that observed in mice with mutations in genes encoding the α1A and β4 subunits (Fletcher et al., 1996; Burgess et al., 1997) and their predominant

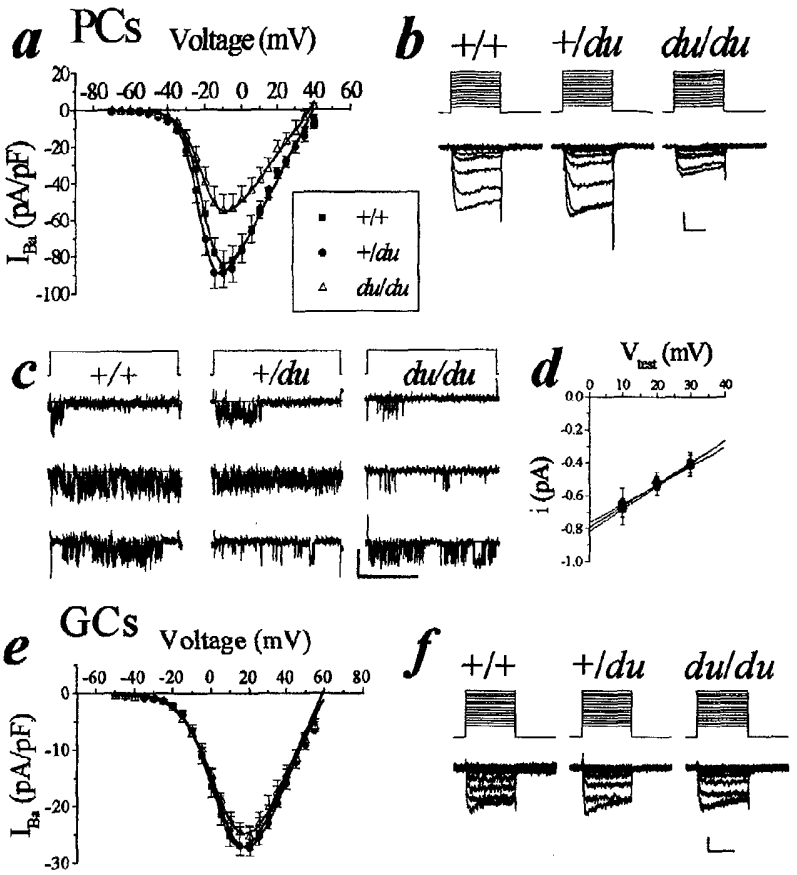

Figure 7. Calcium channel currents in cerebellar Purkinje cells and granule cells. *a*, *I–V* relationships in PCs from +/+ ($n = 19$), +/*du* ($n = 32$), and *du*/*du* ($n = 14$) mice. Genotypes as indicated in the figure. Cells were held at −80 mV. At −10 mV, the I_{Ba} density was −84.9 ± 8.2, −90.5 ± 7.8, and −54.2 ± 8.9 pA/pF in the +/+, +/*du*, and *du*/*du* PCs, respectively ($p < 0.05$ for *du*/*du* vs +/+; $p < 0.01$ for *du*/*du* vs +/*du*). There was no significant difference between the genotypes in the kinetics of activation or in the inactivation over 50 msec. The 10–90% rise times at −10 mV were 3.5 ± 0.2, 3.4 ± 0.2, and 3.9 ± 0.2 msec in +/+, +/*du*, and *du*/*du* PCs, respectively, and the respective percentage of inactivation in 50 msec was 13.6 ± 1.3, 16.4 ± 0.9, and 17.1 ± 2.0%. Calibration: 30 pA/pF, 20 msec. *b*, Example current traces from +/+, +/*du*, and *du*/*du* PCs. The currents were elicited by 50 msec voltage steps from −70 to −10 mV. I_{Ba} density is reduced in PCs from *du*/*du* mice compared with +/+ mice. *c*, Ca^{2+} channel activity in cell-attached patches from PCs of +/+ (*left*; two overlapping openings are evident, indicative of at least two channels active in the patch of membrane recorded), +/*du* (*middle*; two channels in patch), and *du*/*du* (*right*; single channel) mice. *Top*, The voltage protocol; holding potential, −70 mV; test potential, +20 mV, for 500 msec, delivered every 5 sec. Three representative current traces are shown for each cell; openings are *downward deflections*, and the *horizontal lines* that run through the *traces* represent the closed state. Calibration: 1 pA, 250 msec. *d*, Similar single-channel conductance for VDCCs in PCs of +/+, +/*du*, and *du*/*du* mice using the same symbols as in *a*. Single-channel amplitudes were measured at three different voltages and averaged for each population. $n = 3–4$, 4–5, and 2–6 patches for +/+, +/*du*, and *du*/*du*, respectively. The single-channel conductance was determined by fitting a linear function to the mean data and was 13.8, 11.4, and 13 pS, respectively. *e*, *I–V* relationships for GCs from +/+ ($n = 35$), +/*du* ($n = 18$), and *du*/*du* ($n = 23$) mice. Cells were held at −70 mV. The mean *I–V* relationships were fitted with a combined Boltzmann and linear fit. *f*, Example current traces from +/+, +/*du*, and *du*/*du* GCs. The currents shown were elicited by 100 msec depolarizing voltage steps from −50 to +15 mV. Calibration: 10 pA/pF, 50 msec.

PC expression pattern suggests that α2δ2 contributes to the P-type current.

α2δ2 interacts *in vitro* with the α1A/β4 combination

In vitro studies have shown that α2δ1 and α2δ3 subunits increase peak current amplitude and alter the kinetics of inactivation for a number of different α1 subunits (Walker and De Waard, 1998; Dolphin et al., 1999; Klugbauer et al., 1999). *In vitro* studies with human α2δ2 also demonstrate increased peak current amplitude for several α1 subunits (Gao et al., 2000). Our results show that mouse α2δ2 causes a 2.8-fold increase in maximum conductance for the α1A/β4 subunit combination when coexpressed in *Xenopus* oocytes.

Mechanism of the altered Ca^{2+} channel current in *du*/*du* PCs

The *in vitro* expression data suggested that disruption of α2δ2 expression in ducky mice may result in a decrease of the Ca^{2+} channel current in cells that express *Cacna2d2*. Electrophysiological recordings from isolated *du*/*du* PCs confirmed this hypothesis, with a 35% decrease in the peak P-type Ca^{2+} current density in *du*/*du* compared with +/+ PCs. This result has been confirmed recently by Ca^{2+} imaging experiments (J. Brodbeck and A. C. Dolphin, unpublished results). Furthermore, the comparable single P-type Ca^{2+} channel conductance in the two genotypes indicates that the reduction in I_{Ba} density reflects either a change in the number of functional channels or their open probability. The ducky mouse represents the first example of an accessory VDCC subunit mutant with a measurable effect in PCs. Recordings from α1A mutant mice PCs also revealed changes in the P-type Ca^{2+} current compared with that in wild-type PCs (Dove et al., 1998; Lorenzon et al., 1998; Wakamori et al., 1998; Jun et al., 1999). Similar studies performed on lethargic mice, however, showed no differences from wild type, potentially as a result of compensation by other β subunits (Burgess et al., 1999). The low levels of *Cacna2d1* and *Cacna2d3* transcripts in the PCs may preclude such compensation in PCs of *du*/*du* mice, and indeed no upregulation of these mRNAs was seen in *du*/*du* PCs. *In vitro* recordings from cultured *du*/*du* and +/+ GCs demonstrated no significant difference in the Ca^{2+} channel current, consistent with the lower expression levels of *Cacna2d2* in the GCL.

Calcium channel dysfunction and the ducky phenotype

It is likely that several features of the ducky phenotype, including the SWDs, ataxia, and paroxysmal dyskinesia, are attributable to loss of full-length functional α2δ2 in neurons of ducky mice. The occurrence of these traits in other mice with mutations in genes encoding VDCC subunits supports this hypothesis.

Homozygous *Cacna1a*^{tg}, *Cacnb4*^{lh} *Cacng2*^{stg}, *du*, and *du*^{2J} mice

all exhibit generalized bilaterally symmetrical SWDs with a frequency of 5–7Hz (Noebels and Sidman, 1979; Noebels et al., 1990; Hosford et al., 1992; present study). Evidence from animal models suggests that SWDs are generated by aberrant thalamocortical oscillations involving neocortical pyramidal neurons, thalamic relay neurons, and GABAergic neurons of the nRT (Snead, 1995). T-type Ca^{2+} currents underlie thalamic oscillations, and VDCCs have an essential role in presynaptic release of neurotransmitters, providing two potential mechanisms linking Ca^{2+} currents and thalamocortical circuits (Coulter, 1997). Reduction of excitatory but not inhibitory synaptic transmission in the thalamus of lethargic and tottering mice has been documented previously (Caddick et al., 1999), and it was proposed that a net enhanced GABAergic input in thalamocortical neurons may synchronize them into a burst firing mode. In contrast, hippocampal neurotransmitter release appears to be stabilized by a Ca^{2+} current compensatory mechanism in the same mice (Qian and Noebels, 2000). Additional work is required to elucidate the mechanism of SWD generation in ducky mice. However, the expression of *Cacna2d2* within the nRT and cortical pyramidal neurons suggests a similar mechanism may be involved.

An ataxic gait is first detectable between P10 and P21 in tottering, lethargic, stargazer, and ducky homozygotes (Snell, 1955; Green and Sidman, 1962; Dickie, 1964; Noebels et al., 1990). The high levels of expression of all the corresponding VDCC subunit genes in cerebellar neurons, particularly PCs, provides an obvious anatomical correlate with the presumed cerebellar dysfunction underlying the ataxia. PC loss has been documented in some, but not all, of these mutant strains; for example, it is observed in tg^{la} (Heckroth and Abbott, 1994). In *du/du* mice, no loss of PC somata was seen, but preliminary findings indicate major PC dendritic abnormalities (Brodbeck and Dolphin, unpublished results). The *du/du* PCs in which a reduced Ca^{2+} channel current was documented were obtained, for technical reasons, from ducky mice too young and developmentally immature to manifest an ataxic gait. However, it is reasonable to assume that the functional deficit is also present in older mice, and its presence before the overt phenotype is seen demonstrates that it is not merely a secondary effect. It is noteworthy that mutations in the human ortholog of the tottering gene *CACNA1A* are associated with ataxia and are also associated *in vitro* with a reduced whole-cell Ca^{2+} channel current (Hans et al., 1999).

There is one noticeable phenotypic difference between the *du/du* and du^{2J}/du^{2J} mice. Homozygous du^{2J} mice lack the characteristic "ducky" gait, potentially reflecting differences in the relative effects or stabilities of the mutant gene products. Additionally, the two mutations are maintained on different genetic backgrounds (*du* on TKDU and du^{2J} on C57BLKS/J), and this has an effect in other channelopathy phenotypes (Sprunger et al., 1999). Alternatively, these differences could result from involvement of other genes that are either disrupted or duplicated by the *du* rearrangement but unaltered in du^{2J}/du^{2J} mice. Several other genes lie within the *du* interval, including a semaphorin (Sekido et al., 1996).

These observations complete the association of mutations in all four main categories of VDCC subunits with a phenotype in mouse that includes SWDs and ataxia. A central role for disturbed neuronal calcium channel function can therefore be invoked. In the case of α2δ2, this is reinforced by the finding that a high-affinity binding site of the anti-epileptic drug gabapentin in brain has been identified as α2δ (Gee et al., 1996). In conclusion, these observations extend the occurrence of epileptogenic mutations to the last major category of genes encoding VDCC subunits and further strengthen the argument that such genes represent an important class of candidates for human IGEs.

REFERENCES

Barclay J, Rees M (2000) Genomic organisation of the mouse and human α2δ2 voltage dependent calcium channel subunit genes. Mamm Genome 11:1142–1144.

Berridge MJ, Bootman MD, Lipp P (1998) Calcium: a life and death signal. Nature 395:645–648.

Blatt C, Eversole-Cire P, Cohn VH, Zollman S, Fournier RE, Mohandas LT, Nesbitt M, Lugo T, Jones DT, Reed RR, Weiner LP, Sparkes RS, Simon MI (1988) Chromosomal localization of genes encoding guanine nucleotide-binding protein subunits in mouse and human. Proc Natl Acad Sci USA 85:7642–7646.

Burgess DL, Jones JM, Meisler MH, Noebels JL (1997) Mutation of the Ca^{2+} channel β subunit gene *Cchb4* is associated with ataxia and seizures in the lethargic (*lh*) mouse. Cell 88:385–392.

Burgess DL, Biddlecombe GH, McDonough SI, Diaz ME, Zilinski CA, Bean BP, Campbell KP, Noebels JL (1999) Beta subunit reshuffling modifies N- and P/Q-type Ca^{2+} channel subunit compositions in lethargic mouse brain. Mol Cell Neurosci 13:293–311.

Burgess DL, Gefrides LA, Foreman PJ, Noebels JL (2001) A cluster of three novel Ca^{2+} channel γ subunit genes on chromosome 19q13.4: evolution and expression profile of the γ subunit gene family. Genomics 71:339–350.

Caddick SJ, Wang C, Fletcher CF, Jenkins NA, Copeland NG, Hosford DA (1999) Excitatory but not inhibitory synaptic transmission if reduced in lethargic (*Cacnb4^{lh}*) and tottering (*Cacna1a^{tg}*) mouse thalami. J Neurophysiol 81:2066–2074.

Canti C, Page KM, Stephens GJ, Dolphin AC (1999) Identification of residues in the N terminus of α1B critical for inhibition of the voltage-dependent calcium channel by Gβγ. J Neurosci 19:6855–6864.

Catterall WA (1998) Structure and function of neuronal Ca^{2+} channels and their role in neurotransmitter release. Cell Calcium 24:307–323.

Coulter DA (1997) Thalamocortical anatomy and physiology. In: Epilepsy: a comprehensive textbook (Pedley JE, Pedley TA, eds), pp 341–351. Philadelphia: Lippincott-Raven.

Cox GA, Lutz CM, Yang C-L, Biemesderfer D, Bronson RT, Fu A, Aronson PS, Noebels JL, Frankel WN (1997) Sodium/hydrogen exchanger gene defect in slow-wave epilepsy mutant mice. Cell 91:139–148.

Dickie MM (1964) Lethargic (*lh*) mouse. Mouse News Lett 30:31.

Dietrich WF, Miller J, Steen R, Merchant MA, Damron-Boles D, Husain Z, Dredge R, Daly MJ, Ingalls KA, O'Connor TJ, Evans CA, DeAngelis MM, Levinson DM, Kruglyak L, Goodman N, Copeland NG, Jenkins NA, Hawkins TL, Stein L, Page DC, Lander ES (1996) A comprehensive genetic map of the mouse genome. Nature 380:149–152.

Dolphin AC, Wyatt CN, Richards J, Beattie RE, Craig P, Lee J-H, Cribbs LL, Volsen SG, Perez-Reyes E (1999) The effect of α2-δ and other accessory subunits on expression and properties of the calcium channel α1G. J Physiol (Lond) 519:35–45.

Dove LS, Abbott LC, Griffith WH (1998) Whole-cell and single-channel analysis of P-type calcium currents in cerebellar Purkinje cells of leaner mutant mice. J Neurosci 18:7687–7699.

Eisenstat DD, Liu JK, Mione M, Zhong W, Yu G, Anderson SA, Ghattas I, Puelles L, Rubenstein JL (1999) DLX-1, DLX-2, and DLX-5 expression define distinct stages of basal forebrain differentiation. J Comp Neurol 414:217–237.

Ertel EA, Campbell KP, Harpold MM, Hofmann F, Mori Y, Perez-Reyes E, Schwartz A, Snutch TP, Tanabe T, Birnbaumer L, Tsien RW, Catterall WA (2000) Nomenclature of voltage-gated calcium channels. Neuron 25:533–535.

Fletcher CF, Lutz CM, O'Sullivan TNJ, Hawkes R, Frankel WN, Copeland NG, Jenkins NA (1996) Absence epilepsy in tottering mutant mice is associated with calcium channel defects. Cell 87:606–617.

Fougerousse F, Bullen P, Herasse M, Lindsay S, Richard I, Wilson D, Suel L, Durand M, Robson S, Abitbol M, Beckmann JS, Strachan T (2000) Human–mouse differences in the embryonic expression patterns of developmental control genes and disease genes. Hum Mol Genet 9:165–173.

Gao B, Sekido Y, Maximov A, Saad M, Forgacs E, Latif F, Wei MH, Lerman M, Lee J-H, Perez-Reyes E, Besprozvanny I, Minna JD (2000) Functional properties of a new voltage-dependent calcium channel α2δ-2 auxiliary subunit gene (*CACNA2D2*). J Biol Chem 275:12237–12242.

Gee NS, Brown JP, Dissanayake VU, Offord J, Thurlow R, Woodruff GN (1996) The novel anticonvulsant drug, gabapentin (neurontin), binds to the α2δ subunit of a calcium channel. J Biol Chem 271:5768–5776.

Green MC, Sidman RL (1962) Tottering: a neuromuscular mutation in the mouse. J Hered 53:233–237.

Haldi M, Stickland C, Linm P, VanBerkel V, Chen X, Noya D, Korenberg J, Husain Z, Miller J, Lander E (1996) A comprehensive large-insert

yeast artificial chromosome library for physical mapping of the mouse genome. Mamm Genome 10:767–769.
Hans M, Luvisetto S, Williams ME, Spagnolo M, Urrtia A, Tottene A, Brust PF, Johnson EC, Harpold MM, Stauderman KA, Pietrobon D (1999) Functional consequences of mutations in the human α1A calcium channel subunit linked to familial hemiplegic migraine. J Neurosci 19:1610–1619.
Heckroth JA, Abbott LC (1994) Purkinje cell loss from alternating sagittal zones in the cerebellum of leaner mutant mice Brain Res 658:93–104.
Hobom M, Dai S, Marais E, Lacinova L, Hofmann F, Klugbauer N (2000) Neuronal distribution and functional characterization of the calcium channel α2δ2 subunit. Eur J Neurosci 12:1217–1226.
Hosford DA, Clark S, Cao Z, Wilson WA, Lin F-H, Morrisett RA, Huin A (1992) The role of $GABA_B$ receptor activation in absence seizures of lethargic (*lh/lh*) mice. Science 257:398–401.
Hosford DA, Lin F-H, Kraemer DL, Cao Z, Wang Y, Wilson JT (1995) Neural network of structures in which $GABA_B$ receptors regulate absence seizures in the lethargic (*lh/lh*) mouse model. J Neurosci 15:7367–7376.
Jun K, Piedras-Renteria ES, Smith SM, Wheeler DB, Lee SB, Lee TG, Chin H, Adams ME, Scheller RH, Tsien RW, Shin HS (1999) Ablation of P/Q-type Ca^{2+} channel currents, altered synaptic transmission, and progressive ataxia in mice lacking the alpha1A-subunit. Proc Natl Acad Sci USA 96:15245–15250.
Klugbauer N, Lacinova L, Marais E, Hobom M, Hofmann F (1999) Molecular diversity of the calcium channel α2δ subunit. J Neurosci 19:684–691.
Letts VA, Felix R, Biddlecombe GH, Arikkath J, Mahaffey CL, A V, Bartlett FS, Mori Y, Campbell KP, Frankel WN (1998) The mouse stargazer gene encodes a neuronal Ca^{2+}-channel γ subunit. Nat Genet 19:340–347.
Lorenzon NM, Lutz CM, Frankel WN, Beam KG (1998) Altered calcium channel currents in Purkinje cells of the neurological mutant mouse leaner. J Neurosci 18:4482–4489.
Meier H (1968) The neuropathology of ducky, a neurological mutation of the mouse. A pathological and preliminary histochemical study. Acta Neuropathol (Berl) 11:15–28.
Meir A, Bell DC, Stephens GJ, Page KM, Dolphin AC (2000) Calcium channel β subunit promotes voltage-dependent modulation of α1B by Gbγ. Biophys J 79:731–746.
Mintz IM, Adams ME, Bean BP (1992) P-type calcium channels in rat central and peripheral neurons. Neuron 9:85–95.
Neher E (1995) Voltage offsets in patch-clamp experiments. In: Single-channel recording (Sakmann B, Neher E, eds), pp 147–153. New York: Plenum.
Noebels JL (1991) Mutational analysis of spike-wave epilepsy phenotypes. In: Genetic strategies in epilepsy research (Anderson VE, Hauser WA, Leppik IE, Noebels JL, Rich SS, eds), pp 201–212. Amsterdam: Elsevier.
Noebels JL, Sidman RL (1979) Inherited epilepsy: spike-wave and focal motor seizures in the mutant mouse tottering. Science 204:1334–1336.
Noebels JL, Qiao X, Bronson RT, Spencer C, Davisson MT (1990) Stargazer: a new neurological mutant on chromosome 15 in the mouse with prolonged cortical seizures. Epilepsy Res 7:129–135.
Noebels JL, Fariello RG, Jobe PC, Lasley SM, Marescaux C (1997) Genetic models of generalized epilepsy. In: Epilepsy: a comprehensive textbook. (Pedley JE, Pedley TA, eds), pp 457–465. Philadelphia: Lippincott-Raven.
Nusbaum C, Slonim DK, Harris KL, Birren BW, Steen R, Stein LD, Miller J, Dietrich WF, Nahf R, Wang V, et al. (1999) A YAC-based physical map of the mouse genome. Nat Genet 22:388–393.
Pearson HA, Sutton KG, Scott RH, Dolphin AC (1995) Characterization of Ca^{2+} channel currents in cultured rat cerebellar granule neurones. J Physiol (Lond) 482:493–509.
Puranam HA, McNamara JO (1999) Seizure disorders in mutant mice: relevance to human epilepsies. Curr Opin Neurobiol 9:281–287.
Qian J, Noebels JL (2000) Presynaptic Ca^{2+} influx at a mouse central synapse with Ca^{2+} channel subunit mutations. J Neurosci 20:163–170.
Sekido Y, S B, Latif F, Chen JY, Duh FM, Wei MH, Albanesi JP, Lee CC, Lerman MI, Minna JD (1996) Human semaphorins A(V) and IV reside in the 3p21.3 small cell lung cancer deletion region and demonstrate distinct expression patterns. Proc Natl Acad Sci USA 93:4120–4125.
Skynner M, Gangadharan U, Coulton GR, Mason RM, Nikitopolou A, Brown SD, Blanco G (1995) Genetic mapping of the mouse neuromuscular mutation kyphoscoliosis. Genomics 25:207–213.
Snead OC (1995) Basic mechanisms of generalized absence seizures. Ann Neurol 37:146–157.
Snell GD (1955) Ducky, a new second chromosome mutation in the mouse. J Hered 46:27–29.
Sprunger LK, Escayg A, Tallaksen-Greene S, Albin RL, Meisler MH (1999) Dystonia associated with mutation of the neuronal sodium channel *Scn8a* and identification of the modifier locus *Scnm1* on mouse chromosome 3. Hum Mol Genet 8:471–479.
Uchida K, Yoshimura A, Inazawa J, Yanagisawa K, Osada H, Masuda A, Saito T, Takahashi T, Miyajima A (1997) Molecular cloning of *CISH*, chromosome assignment to 3p21.3, and analysis of expression in fetal and adult tissues. Cytogenet Cell Genet 78:209–212.
Wakamori M, Yamazaki K, Martsunodaira H, Teramoto T, Tanaka I, Niidomes T, Sawada K, Nishizawa Y, Sekiguchi N, Mori E, Mori Y, Imoto K (1998) Single tottering mutations responsible for the neuropathic phenotype of the P-type calcium channel. J Biol Chem 273:34857–34867.
Walker D, De Waard M (1998) Subunit interaction sites in voltage-dependent Ca^{2+} channels: role in channel function. Trends Neurosci 21:148–154.

THE JOURNAL OF BIOLOGICAL CHEMISTRY
Vol. 277, No. 10, Issue of March 8, pp. 7684–7693, 2002
Printed in U.S.A.

The Ducky Mutation in *Cacna2d2* Results in Altered Purkinje Cell Morphology and Is Associated with the Expression of a Truncated α2δ-2 Protein with Abnormal Function*

Received for publication, September 28, 2001, and in revised form, December 3, 2001
Published, JBC Papers in Press, December 26, 2001, DOI 10.1074/jbc.M109404200

Jens Brodbeck, Anthony Davies, Jo-Maree Courtney, Alon Meir‡, Nuria Balaguero, Carles Canti, Fraser J. Moss, Karen M. Page, Wendy S. Pratt, Steven P. Hunt§, Jane Barclay¶‖, Michele Rees¶, and Annette C. Dolphin**

From the Departments of Pharmacology and §Anatomy and Developmental Biology, University College London, Gower Street, London WC1E 6BT and ¶Department of Paediatrics and Child Health, Royal Free and University College Medical School, The Rayne Institute, 5 University Street, London WC1E 6JJ, United Kingdom

The mouse mutant ducky, a model for absence epilepsy, is characterized by spike-wave seizures and cerebellar ataxia. A mutation in *Cacna2d2*, the gene encoding the α2δ-2 voltage-dependent calcium channel accessory subunit, has been found to underlie the ducky phenotype. The α2δ-2 mRNA is strongly expressed in cerebellar Purkinje cells. We show that *du/du* mice have abnormalities in their Purkinje cell dendritic tree. The mutation in α2δ-2 results in the introduction of a premature stop codon and predicts the expression of a truncated protein encoded by the first three exons of *Cacna2d2*, followed by 8 novel amino acids. We show that both mRNA and protein corresponding to this predicted transcript are expressed in *du/du* cerebellum and present in Purkinje cells. Whereas the α2δ-2 subunit increased the peak current density of the $Ca_V2.1/\beta_4$ channel combination when co-expressed *in vitro*, co-expression with the truncated mutant α2δ-2 protein reduced current density, indicating that it may contribute to the *du* phenotype.

Voltage-gated Ca^{2+} (Ca_V)[1] channels have been divided functionally into L-, N-, P/Q-, R-, and T-types (1). Each Ca_V channel is composed of a pore-forming α_1 subunit, associated at least in the case of the Ca_V1 and -2 subfamilies with an intracellular β subunit responsible for trafficking (2) and a membrane-anchored, but predominantly extracellular, α2δ subunit, whose function is less well defined (2). $Ca_V1.1$ (α_1S) is also associated with a γ subunit (γ_1), and this may be true for other Ca_V channels (3), although the neuronal γ subunits may also subserve other functions (4). The α_1 subunit determines the main biophysical properties of the channel and is modulated by the other subunits (2). Mammalian genes encoding 10 α_1, 4 β, 8 γ, and 3 α2δ subunits have been identified (1, 5, 6).

A number of spontaneous autosomal recessive mutant mouse strains have now been identified, involving mutations in each of the four different subunits that together compose a voltage-dependent calcium channel. They all have a similar phenotype that includes cerebellar ataxia and spike-wave seizures. Tottering (*Cacna1a*^{tg}) has a point mutation in $Ca_V2.1$ (α_1A) (7), and a number of alleles of this mutant have now been identified, as summarized recently (8). Lethargic (*Cacnb4*^{lh}) represents a truncation mutation of the β_4 subunit (9). Stargazer (*Cacng2*^{stg}) has a truncation mutation in the γ_2 subunit (3), although its role as a calcium channel subunit remains controversial (4, 10, 11). Finally, the two ducky alleles (*Cacna2d2*^{du} and *Cacna2d2*^{du2J}) both predict truncation mutations in the α2δ-2 subunit (12).

Homozygotes for the ducky (*du*) allele are characterized by ataxia and paroxysmal dyskinesia (13). The cerebellum is reduced in size (14), but we have previously found no loss of Purkinje cell (PC) bodies at postnatal day (P) 21 (12). In this study we observed a reduction in calcium channel current in P21 PCs isolated from *du/du* compared with +/+ cerebella (12). The present study provides evidence that the *du* mutation results in the persistence of PCs with an immature and grossly abnormal morphology, including multiple primary dendrites and a reduction in the size of the PC dendritic tree. This is associated with loss of full-length α2δ-2 protein and expression of a truncated mutant α2δ-2 protein with aberrant function.

EXPERIMENTAL PROCEDURES

Construction of du-mut1 α_2—The *du* mutant 1 construct (*du*-mut1 α_2) was assembled by PCR (Platinum *Pfx* polymerase; Invitrogen) of *du/du* total brain cDNA using primers corresponding to the cDNA sequence (GenBank™ AF247140) containing engineered *Sma*I or *Spe*I restriction sites. The primer sequences are as follows: F, 5′- TTG(CCCGGG)GAACATGGCGGTGCCCGGCT-3′, and R, 5′- TCT(CAGGTC)AGAGTAACCAGAGACCAA-3′, with the recognition sites indicated in parentheses. The PCR product was digested with *Sma*I and *Spe*I and ligated into the corresponding sites of a modified pMT2 vector (Genetics Institute, Cambridge, MA). Insert sequence fidelity was determined by automated sequencing (PE Biosystems, Warrington, UK).

Genotyping—Mice were obtained from The Jackson Laboratory (Bar Harbor, ME), and a colony was established, as described previously (12). RNA was extracted from samples of mouse brain tissue using RNeasy Mini Kit and QIAshredder (Qiagen Ltd., Crawley, West Sussex, UK). RNA was reverse-transcribed using Moloney murine leukemia virus-reverse transcriptase (Promega, Southampton, UK) with 0.6 units·ml^{-1} RNasin Ribonuclease Inhibitor (Promega) and 25 ng·μl^{-1} Random Hexamers (Promega). PCRs were carried out with primers

* This work was supported by the Medical Research Council (UK), The Wellcome Trust, and Epilepsy Research Foundation. The costs of publication of this article were defrayed in part by the payment of page charges. This article must therefore be hereby marked "*advertisement*" in accordance with 18 U.S.C. Section 1734 solely to indicate this fact.

‡ Current address: Alomone Laboratories, Jerusalem 91042, Israel.
‖ Current address: Novartis Institute for Medical Sciences, 5 Gower Place, London WC1E 6BS, UK.
** To whom correspondence should be addressed: Dept. of Pharmacology, University College London, Gower Street, London WC1E 6BT, UK. Tel.: 44-20-7679-3054; Fax: 44-20-7813-2808; E-mail: a.dolphin@ucl.ac.uk.

[1] The abbreviations used are: Ca_V, voltage-gated Ca^{2+}; Ab, antibody; FL, first latency; ML, molecular layer; PBS, phosphate-buffered saline; PC, Purkinje cell; PCL, Purkinje cell layer; CHAPS, 3-[(3-cholamidopropyl)dimethylammonio]-1-propanesulfonic acid; DAPI, 4,6-diamidino-2-phenylindole; P, postnatal day; GFP, green fluorescent protein.

49F, 5′-ACGCCCGCTCTTGCTCTTGCT-3′, and 11R, 5′-CCTCCAAAAATCCGCATCAC-3′, which produce a 156-bp product from both the wild-type and *du* alleles of the *Cacna2d2* transcript. Primers 49F and 50R, 5′-TCAGCCTTGGCATCGTAGTA-3′, produce a 387-bp product from the wild-type allele only. Primers 20F, 5′-GCCGCATCTTGAATGGAAAC-3′, and 86R, 5′-CAGAGACCAATGAGACTGGA-3′, produce a 456-bp product from the *du* allele only.

DNA was extracted by incubating 2 mm of tail-snip tissue in 75 μl of 25 mM NaOH, 0.2 mM Na_2EDTA at 95 °C for 30 min followed by cooling to 4 °C and addition of 75 μl of 40 mM Tris-HCl. 5 μl of the resultant solution was amplified in the PCRs. Primers 98F, 5′-ACCTATCAGGCAAAAGGACG-3′, and 120R, 5′-AGGGATGGTGATTGGTTGGA-3′, produce a fragment of 541 bp from a region that is duplicated in the *du* allele. Digestion with *Bsp*HI results in two fragments of 286 and 273 bp from the *du* allele, whereas the wild-type allele remains uncut. Wild-type mice can be identified by the presence of a single band upon agarose gel electrophoresis. Heterozygous and *du*/*du* mice each show two bands and can by distinguished on the basis of their relative intensities.

Lucifer Yellow/Neurobiotin Injection and Quantification—P21-P26 mice were asphyxiated with CO_2, and the cerebella were sliced parasagitally at 400 μm in artificial cerebrospinal fluid (in mM: 125 NaCl, 25 $NaHCO_3$, 25 glucose, 2.5 KCl, 1.25 NaH_2PO_4, 2 $CaCl_2$, 1 $MgCl_2$, saturated with 95% O_2/5% CO_2 at 4 °C) using a vibratome (Campden Instruments, London, UK). Dendrites and somata of PCs were visualized by infrared differential interference contrast video microscopy (15). Glass microelectrodes (outer tip diameter 0.3 μm) were filled with an aqueous solution of 10% lucifer yellow lithium salt (Sigma) and 10% neurobiotin (Vector Laboratories Inc., Burlingame, CA), and backfilled with 1 M LiCl. Dye was injected iontophoretically into PC somata, by alternating the current repeatedly from −40 to +40 nA over 5 min. The tissue slices were then fixed for 1 h in 4% paraformaldehyde, stained for neurobiotin with Texas Red-coupled streptavidin (Molecular Probes, Eugene, OR, 25 μg·ml^{-1} for 1 h), and viewed by confocal microcopy.

Four cells of two genotypes (+/+ and *du*/*du*) were scanned using identical parameters. Selected fields were optically sectioned using 1-μm steps. The entire *z* series was projected as a single composite image by superimposition. The final image was thresholded to form a binary image for analysis by NIH Image J software version 1.62. Following formation of the skeleton, the dendritic tree was contained in a minimal rectangle, and the number of dendrites were counted crossing a horizontal and diagonal line. Branch points were determined from the soma to the end of the three longest dendrites for each cell.

Golgi-Cox Staining—P24 mice were asphyxiated with CO_2, and their brains were removed from the cranium, immediately immersed in 20 ml of fixative (34 mM $K_2Cr_2O_7$, 37 mM $HgCl_2$, and 23 mM K_2CrO_4), and left undisturbed for 12 weeks in the dark at 4 °C. Vibratome sections (100 μm) were developed for 20 min in a 5% Na_2SO_3 solution, before being mounted on microscope slides and coverslipped with Vectashield (Vector Laboratories). Slides were viewed on a Leica microscope using 64× magnification. Image sections were grabbed through an attached CCD camera, using Vision Explorer software (Alliance Vision, Mirmande, France), enabling the deconvolution and projection of different optical planes.

In Situ Hybridization and Immunohistochemistry—Mice (aged P21 to P24) were anesthetized by CO_2 inhalation or pentobarbitone injection (200 mg·kg^{-1}, intraperitoneal) and perfused intracardially with 4% paraformaldehyde in phosphate-buffered saline (PBS). The brain was placed in 4% paraformaldehyde at 4 °C for 3 h and then transferred into 30% sucrose overnight, before embedding in Cry-M-Bed (Bright Instrument Ltd., Huntingdon, UK) and sectioning. Alternatively, the brain was removed without fixation and frozen in liquid nitrogen. 10–25-μm cryostat sections were cut and air-dried onto positively charged slides (Merck).

A cDNA fragment corresponding to *Cacna2d2* 5′ (nucleotides 206–620, using the numbering system from GenBank™ accession number AF247139) was subcloned into pBluescript SK+ (Stratagene, La Jolla, CA). Sense and antisense RNA probes were prepared using T3 or T7 polymerase and digoxigenin RNA labeling mix and purified using Quickspin columns (Roche Molecular Biochemicals). *In situ* hybridization was carried out as described (16).

Two polyclonal antipeptide antibodies were raised in rabbits to amino acids 16–29 and 102–117 of α2δ-2. Neither of the peptides used as antigens showed any homology with other protein sequences in the data base. They were purified by affinity chromatography using the immobilized synthetic peptide and stored at 0.5 mg·ml^{-1} in PBS, pH 7.2, at −20 °C. For immunohistochemistry of α2δ-2, 25-μm sections were incubated overnight with primary antibody at 4 °C (1.25 μg·ml^{-1}). This was followed by a biotinylated anti-rabbit IgG secondary antibody (Sigma, 7.2 μg·ml^{-1}) and a Texas Red-streptavidin conjugate (2 μg·ml^{-1}). Some tissue sections or cells were also incubated for 1 min with the nuclear dye 4′,6-diamidino-2-phenylindole (DAPI, 300 nM, Molecular Probes). They were examined by laser scanning confocal microscopy, using 1-μm optical sections. For peptide controls the appropriately diluted antibody was incubated for 1 h at 37 °C with a 10× higher concentration (w/v) of the immunizing peptide, before applying it to sections.

Transfection of COS-7 Cells—Transfection was performed with GenePORTER transfection reagent (Gene Therapy Systems, San Diego, CA). Cells were plated onto coverslips or dishes, 2–3 h prior to transfection. The DNA and GenePORTER reagent (6 μg and 30 μl, respectively) were each diluted in 500 μl of serum-free medium, mixed, and applied to the cells. After 3.5 h, 1 ml of medium containing 20% serum was added to the cells, which were then incubated at 37 °C for 3–4 days. For electrophysiological recordings, cells were re-plated 1–6 h prior to use.

Immunocytochemistry on COS-7 Cells—The method used is essentially as described previously (17). Cells were fixed with 4% paraformaldehyde in PBS for 15 min at room temperature. For permeabilization, cells were incubated twice for 7 min in a 0.02% solution of Triton X-100 in Tris-buffered saline; otherwise, cells were washed twice with Tris-buffered saline for the same period. The primary antibodies were used at 1.25 μg·ml^{-1}. The biotinylated anti-rabbit IgG secondary antibody (7.2 μg·ml^{-1}) was then incubated for 2 h at 4 °C, followed by streptavidin-Texas Red (2 μg·ml^{-1}). Cells were then incubated for 1 min with DAPI (300 nM).

Preparation of Whole COS-7 Cell Lysates—COS-7 cells were transfected with either α2δ-2 or *du*-mut1 α_2 as described above. On day 4 post-transfection, the cells were resuspended in detergent-free Buffer A. Samples (2 mg of total protein) were then solubilized in Buffer A containing 1% CHAPS for immunoaffinity purification of α2δ-2 as described below.

Preparation of Cerebellar Tissue Homogenate—Cerebella, stored at −80 °C, were thawed in ice-cold Buffer A (10 mM HEPES, pH 7.4, 150 mM NaCl, 2 mM EDTA, and protease inhibitors (Complete EDTA-free, Roche Molecular Biochemicals, 1 tablet/50 ml buffer)), plus 150 mM sucrose. The tissue was homogenized, and the homogenate was centrifuged at 5000 × *g* for 10 min at 4 °C. The resultant supernatant was diluted 4 times with Buffer A, prior to detergent treatment. The protein concentration of samples was determined using either the bicinchoninic acid (BCA) assay (Perbio, Tattenhall, UK) in the presence of 0.5% SDS, or where the samples were in SDS-PAGE buffer, by a modified filter paper dye-binding assay (18).

Immunoaffinity Purification of α2δ-2 and du-mut1 α_2—Affinity-purified Ab(16–29) or Ab(102–117) (2 mg) was covalently coupled to a 1-ml column of Sepharose-NHS (Amersham Biosciences) according to manufacturer's instructions. The efficiency of coupling was assessed by SDS-PAGE. The columns were pre-washed with 200 mM glycine HCl, pH 2.4, and neutralized before first use to ensure complete removal of any residual unbound IgG. Control columns contained 2 mg of protein A-Sepharose-isolated IgG from the corresponding pre-immune rabbit sera. COS-7 cells transfected with either α2δ-2 or *du*-mut1 α_2 (2 mg of total protein) or cerebellar homogenate (+/+ or *du*/*du*, 6–20 mg of total protein) were solubilized in Buffer A (see above) containing 1% (w/v) CHAPS and placed on ice for 30 min following sonication 3 times for 10 s. The detergent extracts were cleared by centrifugation (48,000 × *g*, 20 min, 4 °C) and then applied to the relevant antibody or control IgG columns that had been pre-equilibrated with Buffer A containing 0.5% CHAPS. The lysates were recirculated through the columns using two opposing syringes for 60 min at 4 °C. Unbound material was washed from the columns in Buffer A containing 0.5% CHAPS and then Buffer A + 0.1% CHAPS. Bound proteins were eluted with 200 mM glycine HCl, pH 2.4, and then concentrated for SDS-PAGE and Western blot analysis by precipitation with 10% trichloroacetic acid followed by centrifugation (30,000 × *g*, 30 min, 4 °C). Samples of the precipitated proteins were separated on either 10 or 4–20% gradient gels under reducing conditions and then electrophoretically transferred to polyvinylidene difluoride membranes for immunodetection. The polyvinylidene difluoride membranes were blocked with 3% BSA for 3 h at 55 °C and incubated overnight with a 1:1000 dilution of either Ab(16–29) or Ab(102–117) followed by a 1:1000 dilution of goat anti-rabbit IgG-horseradish peroxidase conjugate (Bio-Rad) for 1 h at 20 °C and detected using ECL (Amersham Biosciences). The antibody and control IgG columns were neutralized and washed with 50 mM Tris, pH 7.4, 1 M NaCl, and 0.02% sodium azide and stored in PBS, pH 7.2, with 0.02% sodium azide at 4 °C.

Heterologous Expression of cDNAs and Electrophysiology—GenBank™ accession numbers of cDNAs are given in parentheses. Calcium channel expression in COS-7 cells was investigated by whole cell patch clamp recording, essentially as described previously (19), by transfection of rat Ca_V 2.1 (M64373) E1686R (20), in conjunction with rat β_4 (LO2315) and mouse α2δ-2 (AF247139, common brain splice variant, lacking exon 23 and 6 bp of exon 38 (21)) or *du*-mut1 α_2 (AF247140) cDNAs cloned into the pMT2 vector. The cDNA for green fluorescent protein (mut3 GFP) (22) was included in the transfection to identify transfected cells from which recordings were made. Transfection was performed as described above, using the ratios for α_1, β, α2δ, and GFP of 3:1:1:0.1. In the single channel experiments cDNA for β-adrenergic receptor kinase 1 (β-ARK1), Gβγ binding domain was included in the transfections, at the same concentration as the β subunit cDNA (23). For expression in *Xenopus* oocytes, cDNAs encoding rabbit Ca_V 2.1 (X57689), rat β_4 and mouse α2δ-2 or *du*-mut1 α_2 cDNAs were injected intranuclearly as described previously (24), except that 4 nl of the 1:1:1 ratio cDNA mixture was injected at 1 $\mu g \cdot \mu l^{-1}$. In control experiments where α2δ-2 was omitted, the ratio was made up with buffer. Recordings were made using two-electrode voltage clamp as described previously (24), using 10 mM Ba^{2+} as charge carrier. Individual I–V relationships were fitted with a modified Boltzmann Equation 1,

$$I = G_{max}(V - V_{rev})/(1 + \exp(-(V - V_{50})/k)) \quad \text{(Eq. 1)}$$

where G_{max} is the maximum conductance; V_{rev} is the reversal potential; k is the slope factor; and V_{50} is the voltage for 50% current activation.

Single Channel Recording and Analysis—All recordings were taken from cell-attached patches on GFP-positive cells at room temperature (20–22 °C). Recording pipettes were pulled from borosilicate tubes (World Precision Instruments, Inc., Sarasota, FL), coated with Sylgard (Sylgard 184, Corning Glass), and fire-polished to form high resistance pipettes (~10 megohms with 100 mM $BaCl_2$). The bath solution, designed to zero the resting membrane potential (25), was composed of (in mM) 135 potassium aspartate, 1 $MgCl_2$, 5 EGTA, and 10 HEPES (titrated with KOH, pH 7.3), and patch pipettes were filled with a solution of the following composition (in mM): 100 $BaCl_2$, 10 tetraethylammonium-Cl, 10 HEPES, 200 nM tetrodotoxin, titrated with tetraethylammonium-OH to pH 7.4. Both solutions were adjusted to an osmolarity of 320 mosmol with sucrose. Data were sampled (Axopatch 200B and Digidata 1200 interface, Axon Instruments, Foster City, CA) at 20 kHz and filtered on-line at 1–2 kHz. Voltages were not corrected for liquid junction potential (26), measured to be −15 mV in these solutions, in order to be able to compare the results to other published material. Leak subtraction was performed by averaging segments of traces with no activity from the same voltage protocol in the same experiment and subtracting this average from each episode using pClamp6 (Axon Instruments). Statistical analysis was performed using paired or unpaired Student's t test. For the single channel analysis, patches were only used in which three or fewer overlapping openings were detected. With an open probability of about 0.5 at +40 mV and at least 20 consecutive stimulations, the number of detectable multiple openings was considered to represent the number of channels active in these patches. Event detection was carried out using the half-amplitude threshold method. Single channel amplitude was determined by a Gaussian fit to the binned amplitude distributions. Mean open and closed times were determined as a single or double exponential fitted to open time distributions. Open time distributions were only collected in episodes or parts of episodes with no overlapping openings. For closed time distributions, we used either single channel patches or segments toward the end of episodes in which only one channel remains active and no further overlaps occur. Data are expressed as mean ± S.E. For steady-state inactivation, all the available patches were considered, and each was normalized to its peak current response during the prepulse to +40 mV. Latency to first opening was measured in 2-ms bins. First latency (FL) histograms from each experiment were divided by the number of episodes collected, and the plots were then accumulated and divided by the number of stimulations, to express the data as the FL probability (23, 27). Two- and three-channel patches were also corrected for the apparent number of channels in the patch, according to Equation 2,

$$FL_1 = 1 - (1 - FL_N)^{(1/N)} \quad \text{(Eq. 2)}$$

FL_1 and FL_N are the single channel and multichannel cumulative first latency functions, respectively, and N is the apparent number of channels.

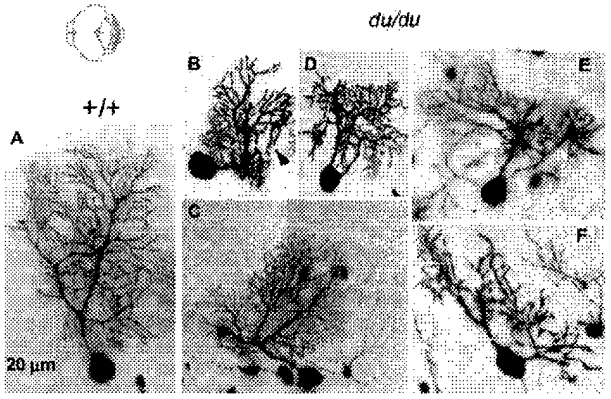

FIG. 1. **Comparison of +/+ and *du/du* PC morphology by Golgi impregnation.** Light micrographs showing individual Golgi-impregnated PCs of +/+ (*A*) and *du/du* (*B–F*) cerebellum. Parasagittal sections for both genotypes were taken from an identical region of the vermis (see *diagram top left*). *A*, typical +/+ PC with dendritic processes reaching the pial surface. *B–F*, *du/du* PCs were characterized by the absence of an apically oriented main dendrite. The cell in *B* also exhibits a weeping willow-like dendrite bending back toward the granule cell layer (*arrowhead*). The cells in *D–F* show multiple primary dendrites emerging from the perikaryon.

RESULTS

Comparison of Morphology of du/du and +/+ PCs—The *du/du* cerebellum exhibits normal foliation and laminar structure. There are no gaps in the PC layer, and their perikarya form a single row. The thickness of each layer is reduced in *du/du* compared with wild-type littermates as described previously (12). Two techniques were used to compare the morphology of cerebellar PCs between the different genotypes in more detail as follows: first, classical Golgi impregnation, and second, microinjection of PC somata with Lucifer Yellow and neurobiotin. Both methods revealed a changed PC cytoarchitecture in homozygous *du/du* cerebella at P21–26, which was the latest period in which morphology could be studied, given that the *du/du* mice die by P35. In the Golgi-impregnated cerebella, PCs were examined in detail in multiple cerebellar sections from one +/+ and six *du/du* mice. Atypical initial lateral extensions of the primary dendrite were seen in *du/du* but not in +/+ PCs (compare +/+ in Fig. 1*A* to *du/du* in Fig. 1, *B*, *C*, and *F*). The primary dendrites may then bend apically in a delayed targeting of the pial surface, which they frequently fail to reach (*e.g.* Fig. 1, *B* and *C*). Thickened tertiary branchlets were found to bend downwards in some *du/du* PCs, giving a "weeping willow" appearance (Fig. 1*B*, *closed arrowhead*). Additionally, PC somata are frequently multipolar, exhibiting up to three primary dendrites (Fig. 1, *D–F*), which, in the cells shown in Fig. 1, *E* and *F*, extend laterally rather than targeting the pial surface.

Similar results were obtained with the cell-filling technique, for which 4 +/+ and 4 *du/du* PCs were examined in detail. The *du/du* PCs displayed a dendritic arbor that was significantly less complex, reduced in size, and frequently did not reach the border of the molecular layer (compare the typical +/+ PC in Fig. 2*A* with three *du/du* PCs shown in Fig. 2*B*). Additionally, the shafts of the main and secondary dendritic branches of *du/du* PCs were often thickened (Fig. 2*B*). In one *du/du* PC, the dendrites drooped down toward the granule cell layer giving a weeping willow appearance (Fig. 2*B*, *top right panel*), similar to that seen in some of the Golgi-impregnated *du/du* PCs (Fig. 1*B*). Following formation of the skeleton of the dendritic trees (Fig. 2*C*), the numbers of dendrites were found to be reduced in *du/du* PCs (Fig. 2*D*, *left panel*), and the total length of the dendritic tree was also reduced (Fig. 2*D*, *center panel*). How-

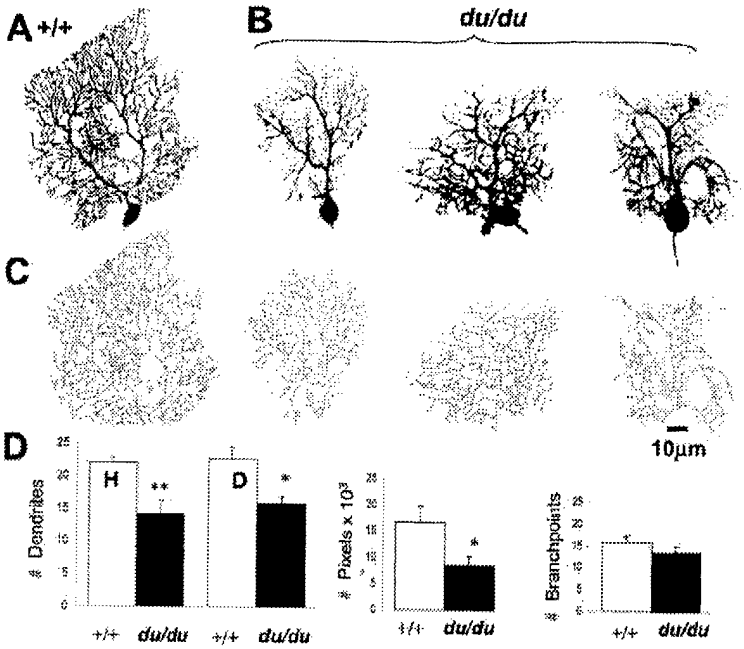

FIG. 2. **Comparison of +/+ and *du/du* PC morphology by cell filling.** Lucifer Yellow/neurobiotin injection of cerebellar PCs of +/+ (neurobiotin staining for one representative cell shown, as morphology of all +/+ PCs was similar) (*A*) and *du/du* (three cells shown, to illustrate variation in morphologies observed, the first imaged with neurobiotin staining, and the other two with lucifer yellow) (*B*). *C*, skeletonized dendritic tree of the cells, shown in *A* and *B*, for evaluation of arborization complexity, independent of dendritic width. This is quantified in *D*. *Left panel*, the number of dendrites per cell crossing a *horizontal* (*H*) and *diagonal* (*D*) *line*. *Center panel*, number of black pixels as indication of the whole area covered by skeletonized dendrites. *Right panel*, number of branch points. For all panels of *D*, $n = 4$ for both +/+ and *du/du* PCs. *Asterisks* indicate a statistically significant difference as follows: *, $p < 0.05$; **, $p < 0.01$, Student's *t* test.

ever, the number of branch points on the longest dendrites was unchanged (Fig. 2*D*, *right panel*).

The du 5′ Mutant Transcript Is Present and Translated in du/du Cerebellar PCs—We have shown previously, by *in situ* hybridization using a 3′ antisense probe, that no full-length transcript for *Cacna2d2* is present in *du/du* cerebellum, whereas a strong signal was obtained in +/+ cerebellar PCs (12). In the present study we performed *in situ* hybridization with a 5′ *Cacna2d2* antisense RNA probe to examine whether a truncated message was present in *du/du* PCs. This confirmed the presence of full-length transcript for *Cacna2d2* in +/+ PCs (Fig. 3*A*). The data would also not be inconsistent with the additional presence of transcript in small Bergmann glial cell bodies (Fig. 3*A*, *arrows*, see also Fig. 8). The results also demonstrate a low level of message hybridizing to the 5′ probe in *du/du* PCs (Fig. 3*B*, compared with Fig. 3*A*). This, together with the absence of full-length transcript in *du/du* PCs shown in our previous study (12), provides evidence for a low level of transcription of *du* mutant transcript 1 (12) in these cells.

We therefore generated an α2δ-2 antipeptide antibody utilizing an immunizing peptide corresponding to amino acids 102–117, with the intent of examining whether a mutant protein was expressed in *du/du* cerebellum. This sequence is near the N terminus of α2δ-2 and is also present in the predicted protein product of the *du* mutant transcript 1, termed *du*-mut1 α_2 (Fig. 4*A*). This antibody, called Ab(102–117), was first characterized against heterologously expressed α2δ-2. On Western blots of gels run under reducing conditions, α_2 is separated from the δ moiety to which it is disulfide-bonded under native conditions. Ab(102–117) specifically recognized the α_2 moiety of α2δ-2 (as a broad band at about 150 kDa) and not the α_2 moiety of α2δ-1 when both α2δ-1 and α2δ-2 were overexpressed in COS-7 cells (Fig. 4*B*). It also recognized an ~10-kDa protein product of the *du*-mut1 α_2 cDNA expressed in COS-7 cells (Fig. 4*B*). When Ab(102–117) was used to examine the immunocytochemical localization of α2δ-2 in these cells, the epitope was accessible in non-permeabilized cells, orienting it exofacially (Fig. 4*C*, *1st* and *2nd columns*, *upper panel*). Additional intracellular staining was observed when the cells were permeabilized (Fig. 4*C*, *1st* and *2nd columns*, *lower panel*). When *du*-mut1 α_2 was expressed, very little immunostaining was

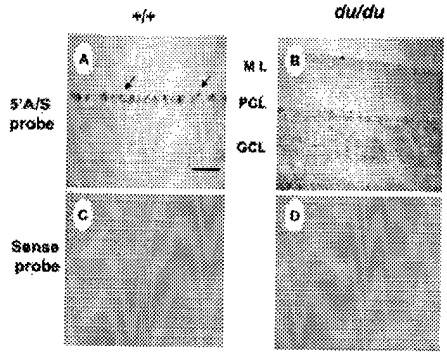

FIG. 3. **Analysis of *Cacna2d2* mutant transcript 1 expression in P21 +/+ and *du/du* cerebellum.** *In situ* hybridization of +/+ and *du/du* sections with 5′ *Cacna2d2* antisense (*A*/*S*) RNA probes designed to detect *du* mutant transcript 1 in *du/du* mice. This probe will also detect wild-type transcripts. Analyses were carried out on +/+ (*A*) and *du/du* sections (*B*). The *arrows* in *A* indicate the presence of a signal from smaller cell bodies, possibly Bergmann glial cells. No signal was detected on hybridization of control sense RNA to +/+ sections (*C* and *D*). *ML*, molecular layer; *PCL*, Purkinje cell layer; *GCL*, granule cell layer. *Scale bar*, 100 μm.

observed in non-permeabilized cells (Fig. 4*C*, *3rd column*, *upper panel*), although a large number of cells were present in the field (Fig. 4*C*, *4th column*, *upper panel*), whereas intense intracellular immunostaining, localized to intracellular organelles, was observed when the cells were permeabilized (Fig. 4*C*, *3rd* and *4th columns*, *lower panel*). The lack of staining with the anti-GFP antibody in non-permeabilized GFP-positive cells provides further evidence that the plasma membrane of the cells has not been permeabilized by fixation (Fig. 4*D*).

The predicted protein molecular mass of the entire *du*-mut1 α_2-truncated protein is 16 kDa, which is larger than the ~10-kDa band observed here. We therefore utilized another antipeptide antibody, generated against the epitope represented by amino acids 16–29, which is within the predicted signal sequence of α2δ-2, to further examine the processing of the *du*-mut1 α_2 protein. When *du*-mut1 α_2 was expressed in COS-7 cells, Ab(16–29) recognized a 16-kDa band in lysates of these cells (Fig. 5*A*, *lane 1*). No smaller molecular weight bands were

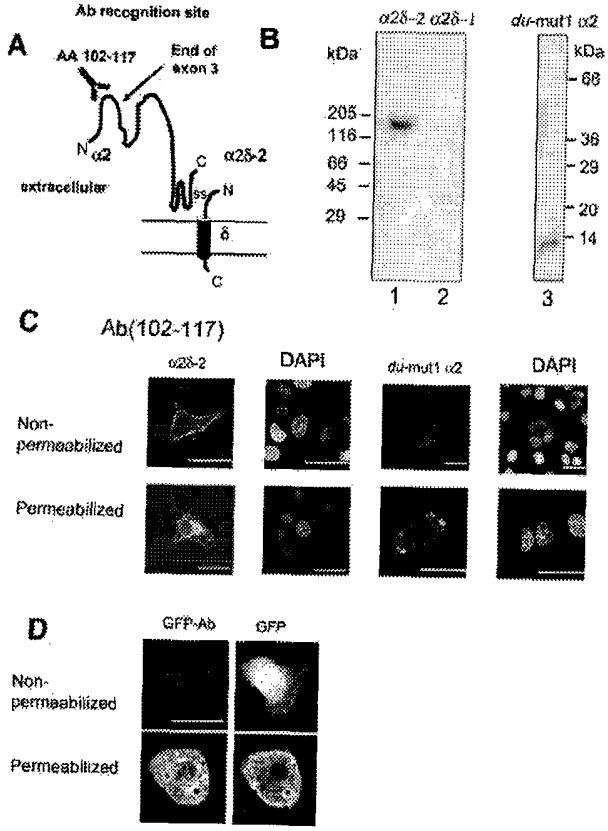

FIG. 4. **Specificity of Ab(102–117) and localization of α2δ-2 and *du*-mut1 α_2 in COS-7 cells.** *A*, schematic representation of α2δ-2 protein to show location of the Ab(102–117) binding site in relation to the end of exon 3. *B*, immunoblots to show the specificity of the anti-α 2δ-2 Ab(102–117), using lysates (20 μg of protein) from COS-7 cells overexpressing α 2δ-2 (*lane 1*, 150 kDa) or α2δ-1 as a control (*lane 2*) on 4–12% gradient SDS-PAGE gels, and *du*-mut1 α_2 (*lane 3*, ~10 kDa) on a 4–20% gel. The positions of the molecular mass markers are shown next to the blots. *C*, COS-7 cells transfected with cDNAs for GFP and α2δ-2 (*1st* and *2nd columns*) or *du*-mut1 α_2, (*3rd* and *4th columns*). Cells were either not permeabilized (*upper row*) or permeabilized with Triton X-100 (*lower row*). Immunostaining with Ab(102–117) is shown in the *1st* and *3rd columns*, and DAPI fluorescence to identify cell nuclei is shown in *2nd* and *4th columns*. For clarity, the GFP fluorescence is not shown. *D*, COS-7 cells transfected with cDNA for GFP alone. Cells were either not permeabilized (*upper row*) or permeabilized with Triton X-100 (*lower row*). GFP transfection was used as a control to show lack of immunostaining with anti-GFP Ab (*left column*) of this intracellular antigen in non-permeabilized cells. GFP fluorescence is shown in the *right column*. *Scale bar* (40 μm) applies to all sections.

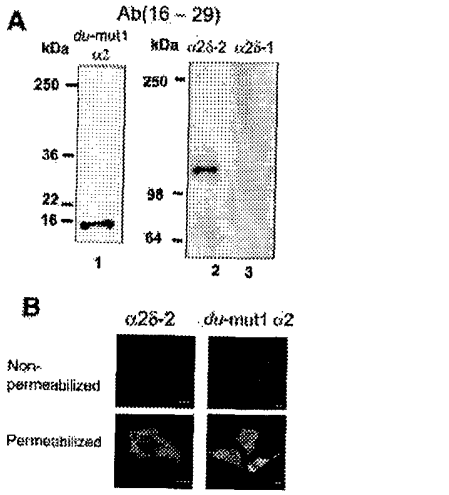

FIG. 5. **Specificity of Ab(16–29).** *A*, immunoblots to show the specificity of Ab(16–29), using lysates (20 μg of protein) from COS-7 cells overexpressing *du*-mut1 α_2 (*lane 1*, 16 kDa) on a 15% SDS-PAGE gel, or α2δ-2 (*lane 2*, 120 kDa), or α2δ-1 as a control (*lane 3*) on 4–12% gradient gels. The positions of the molecular mass markers are shown next to the blots. *B*, immunostaining using Ab(16–29) in COS-7 cells transfected cDNA for full-length α2δ-2 (*left panel*) or *du*-mut1 α_2 (*right panel*). Cells were either not permeabilized (*upper row*) or permeabilized with Triton X-100 (*lower row*), as described under "Experimental Procedures." *Scale bars*, 10 μm.

observed on this gel (but see Fig. 7). This suggested that the signal sequence of *du*-mut1 α_2 is at least partly uncleaved when it is expressed in COS-7 cells. Ab(16–29) also recognized a well defined 120-kDa protein when full-length α2δ-2 was expressed (Fig. 5*A*, *lane 2*) and no bands when α2δ-1 was expressed as a control (Fig. 5*A*, *lane 3*). This 120-kDa protein is likely to represent an immature form of α2δ-2 before cleavage of the signal sequence, which normally precedes glycosylation. The protein molecular mass of the α_2 moiety including the 6-kDa signal sequence is calculated to be 113 kDa. Unlike Ab(102–117), Ab(16–29) did not recognize a band of 150 kDa, indicating that, as expected, the signal sequence is cleaved from the mature glycosylated form of α2δ-2.

We then examined the immunolocalization of *du*-mut1 α_2 in COS-7 cells, using Ab(16–29). Immunostaining for this epitope was not observed at the plasma membrane in non-permeabilized cells expressing α2δ-2, indicating that the signal sequence is cleaved before insertion of α2δ-2 into the plasma membrane. Furthermore, this epitope was also generally not observed on the exofacial side of the plasma membrane when *du*-mut1 α_2 was expressed (Fig. 5*B*, non-permeabilized cells). Diffuse intracellular staining was observed when the cells were permeabilized, for both α2δ-2- and *du*-mut1 α_2-expressing cells (Fig. 5*B*).

Immunopurification of du-mut1 α_2 from du/du Cerebellum—The use of an Ab(102–117) immunoaffinity column allowed the isolation of a low abundance protein of ~10 kDa from *du/du* cerebellum (Fig. 6*A*, *lane 1*), which was detected using the same antibody. This protein is very similar in molecular weight to the *du*-mut1 α_2 protein isolated in the same way from lysates of COS-7 cells expressing *du*-mut1 α_2 (Fig. 6*A*, *lane 2*). If a protein product were produced from *du* mutant transcript 2 (GenBank™ accession number AF247141) in *du/du* cerebellum (12), its predicted molecular mass would be ~100 kDa. This would also be recognized by Ab(102–117), but no higher molecular weight immunoreactive bands were observed from 4 to 20% gradient gels of proteins isolated from *du/du* cerebellum (data not shown, $n = 2$). A broad band of protein of ~150 kDa, representing the α_2 moiety of α2δ-2, was isolated from +/+ cerebellum using the same immunoaffinity column and detected using the same antibody (Fig. 6*B*, *lane 1*). This protein was the same molecular weight as that isolated by the same antibody from COS-7 cells transfected with α2δ-2, with the broad band probably representing different glycosylation states (Fig. 6*B*, *lane 2*).

By using an Ab(16–29) immunoaffinity column, a protein of ~16 kDa was isolated from *du/du* cerebellum (Fig. 6*C*, *lane 1*). This protein is very similar in molecular weight to the *du*-mut1 α_2 protein isolated in the same way from COS-7 cells expressing *du*-mut1 α_2 (Fig. 6*C*, *lane 2*). Furthermore, a protein of about 120 kDa was isolated from +/+ cerebellum using the same immunoaffinity column (Fig. 6*D*, *lane 1*). This protein was the same molecular weight as that isolated by the same antibody from COS-7 cells transfected with α2δ-2 (Fig. 6*D*, *lane 2*).

The basis for the difference in molecular weight between the *du*-mut1 α_2 species recognized by the two antibodies was fur-

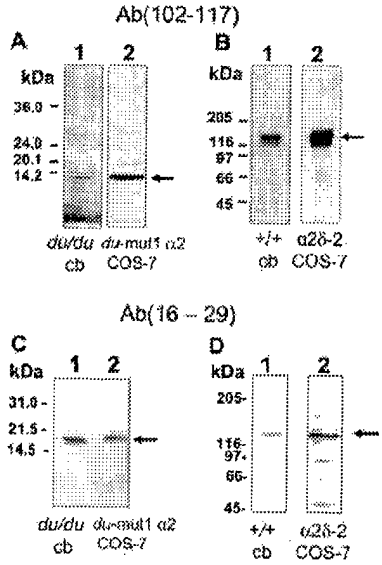

FIG. 6. **Immunopurification of *du*-mut1 α_2 from *du/du* cerebellum and the α_2 moiety of full-length α2δ-2 from +/+ cerebellum.** Immunoblot analysis of α2δ-2 proteins were immunocaptured from detergent-solubilized *du/du* or +/+ cerebellar membranes using column-immobilized peptide antibodies. Samples were separated on either 4–20% gradient gels (*A* and *B*), a 20% gel (*C*), or on a 7.5% gel (*D*). *Arrows* indicate the major protein bands detected. *A* and *C*, proteins from *du/du* cerebella (*lane 1*) or from COS-7 cells expressing *du*-mut1 α_2 (*lane 2*) isolated using Ab(102–117) and Ab(16–29), respectively. The respective apparent molecular mass values are ~10 and 16 kDa. *B* and *D*, proteins from +/+ cerebella (*lane 1*) or from COS-7 cells expressing full-length α2δ-2 (*lane 2*) isolated with Ab(102–117) and Ab(16–29), respectively. The respective apparent molecular mass values are 150 and 120 kDa.

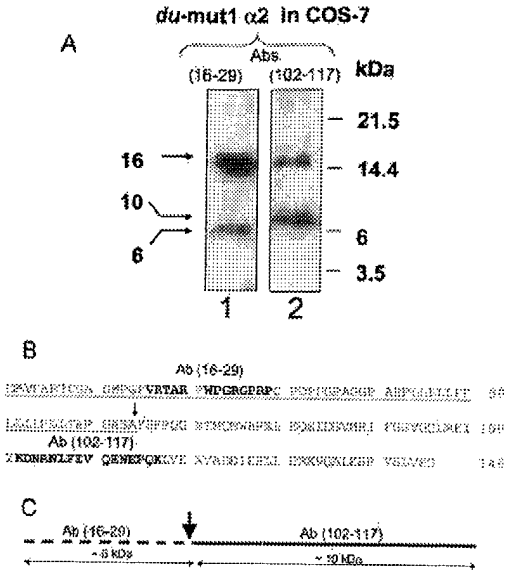

FIG. 7. **Processing of *du*-mut1 α_2.** *A*, immunoblot analysis of *du*-mut1 α_2 and fragments derived from cleavage of the signal peptide. Lysate (80 μg of protein) of COS-7 cells expressing *du*-mut1 α_2 was separated on a 10–20% gradient gel and probed with Ab(16–29) (*lane 1*) or Ab(102–117) (*lane 2*). A 16-kDa band is detected with both antibodies. Ab(16–29) also recognizes a band of 6 kDa, and Ab(102–117) recognizes a major band of ~10 kDa. *B*, amino acid sequence of *du*-mut1 α_2. The respective binding sites for Ab(16–29) and Ab(102–117) are shown in *bold*. The entire signal leader sequence is underlined with its predicted cleavage site marked by an *arrow* (40). *C* shows the calculated molecular mass values for *du*-mut1 α_2 (16 kDa) and the two proteolytic fragments as follows: *du*-mut1 α_2 following cleavage of the signal sequence (*solid line*, ~10 kDa) and the cleaved signal sequence (*dotted line*, ~6 kDa).

ther examined by PAGE of a larger amount (80 μg of protein) of COS-7 cell lysate expressing *du*-mut1 α_2, on a high percent gradient gel, followed by immunoblotting (Fig. 7*A*). A 16-kDa band was recognized by both antibodies, but the predominant band recognized by Ab(102–117) was ~10 kDa. This was not recognized by Ab(16–29), which recognized an additional 6-kDa band. The amino acid sequence of *du*-mut1 α_2 is shown in Fig. 7*B*, with the antibody recognition sites (*boldface letters*) and the predicted site of cleavage of the signal sequence (*arrow*). The predicted sizes of the peptides obtained before and after cleavage are 16 kDa for full-length *du*-mut1 α_2, 10 kDa for *du*-mut1 α_2 following cleavage of the signal sequence, and 6 kDa for the cleaved signal sequence (Fig. 7*C*), in agreement with the experimental results.

The immunolocalization of α2δ-2 in the cerebellum was subsequently examined using Ab(102–117). This antibody gave a pattern of immunostaining in the Purkinje cell layer (PCL) and molecular layer (ML) in sections of +/+ cerebellum, consistent with localization of α2δ-2 in PC bodies and dendrites (Fig. 8*A*, *left panel*). The staining was lost when the primary antibody was preincubated with the immunizing peptide or when the primary antibody was not used (Fig. 8*A*). In cerebellar sections from *du/du* mice, Ab(102–117) gave a low level of immunostaining (Fig. 8*A*, *right panel*), consistent with the presence of *du*-mut1 α_2 in *du/du* PCs. There was also some evidence for staining of Bergmann glia (Fig. 8*A*, *right panel* marked with *). We also used Ab(16–29) to determine where the uncleaved form of *du*-mut1 α_2 was expressed endogenously in *du/du* cerebellar sections. A low level of immunostaining was observed with this antibody in +/+ PCs, consistent with the presence of the immature 120-kDa form of α2δ-2, with the signal peptide still present, which is likely to be localized to the endoplasmic reticulum (Fig. 8*B*, *left panel*). Further evidence was obtained here for staining of Bergmann glia (Fig. 8*B*, *left panel*, *). In *du/du* cerebellum, we observed that immunostaining with this antibody was concentrated largely in the cell bodies of PCs (Fig. 8*B*, *right panel*). This is likely to represent the 16-kDa uncleaved *du*-mut1 α_2 species. The immunostaining was lost when the antibody was preincubated with the immunizing peptide (Fig. 8*B*). No differences were observed between +/+ and *du/du* PCs when Bergmann glia were visualized using an anti-glial fibrillary acidic protein antibody (results not shown).

Modulation of $Ca_V2.1$ Ca^{2+} Channel Currents by α2δ-2 and du-mut1 α_2—The possible pathological function of the *du*-mut1 α_2 protein encoded by the *Cacna2d2*^{du} gene was investigated using *in vitro* expression and electrophysiology. To mimic the PC complement of calcium channel subunits, the cDNAs corresponding to rat $Ca_V2.1$ and β_4 were transfected into COS-7 cells, with or without α2δ-2 or *du*-mut1 α_2 cDNA, and the resulting Ca_V currents (I_{Ba}) recorded. Co-expression of α2δ-2 increased $Ca_V2.1/\beta_4$ I_{Ba} currents, inducing a 2.9-fold enhancement of amplitude at 0 mV (Fig. 9*A*, and I-V relationships in Fig. 9*B*), with no significant shift in the voltage dependence of current activation (V_{50} for activation was -8.7 ± 0.7 mV (n = 28) for $Ca_V2.1/\beta_4$ and -10.7 ± 0.8 mV (n = 42) for $Ca_V2.1/\beta_4$/α2δ-2). There was no significant effect of α2δ-2 on the activation or inactivation of the $Ca_V2.1/\beta_4$ combination (Fig. 9*A* and results not shown).

In contrast, co-expression of *du*-mut1 α_2 induced a consistent reduction in $Ca_V2.1/\beta_4$ I_{Ba} amplitude throughout the voltage range (Fig. 9, *C* and *D*). This amounted to a 51% inhibition at 0 mV (Fig. 9*E*) and also resulted in a +5-mV shift in V_{50} for activation to -3.5 ± 1.1 mV (n = 12, $p < 0.01$ compared with $Ca_V2.1/\beta_4$). The mean current densities at 0 mV under the two

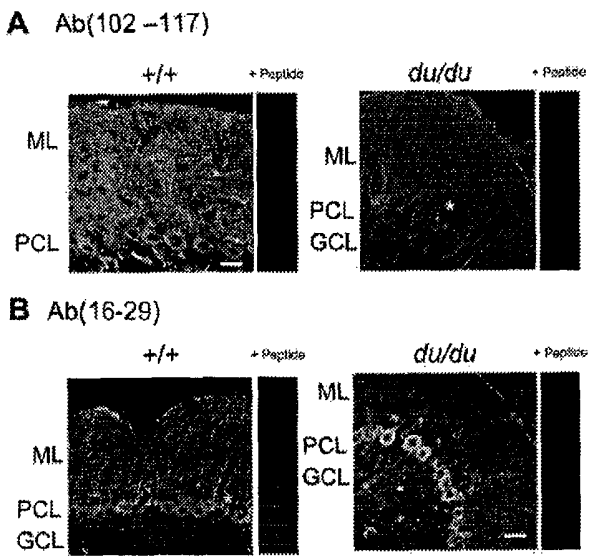

FIG. 8. **Immunohistochemistry in +/+ and *du/du* cerebellum.** *A*, Ab(102–117) detected the presence of α2δ-2 and *du*-mut1 α_2 protein in +/+ and *du/du* sections, respectively. The affinity of the antibody for α2δ-2 and *du*-mut1 α_2 may be different; therefore, relative intensities cannot be compared directly. Results are representative of four experiments. *B*, Ab(16–29) detected the presence of immature α2δ-2 in a +/+ cerebellar section (*left*) and *du*-mut1 α_2 protein in a *du/du* cerebellar section (*right*). Representative of three experiments. In both (*A* and *B*) the *calibration bar* is 30 μm. *ML*, molecular layer; *PCL*, Purkinje cell layer; *GCL*, granule cell layer. The label + peptide indicates that the primary antibody was preincubated with the immunizing peptide before application to the section. The * indicates examples of the presence of immunoreactivity in a smaller cell body and process, possibly a Bergmann glial cell.

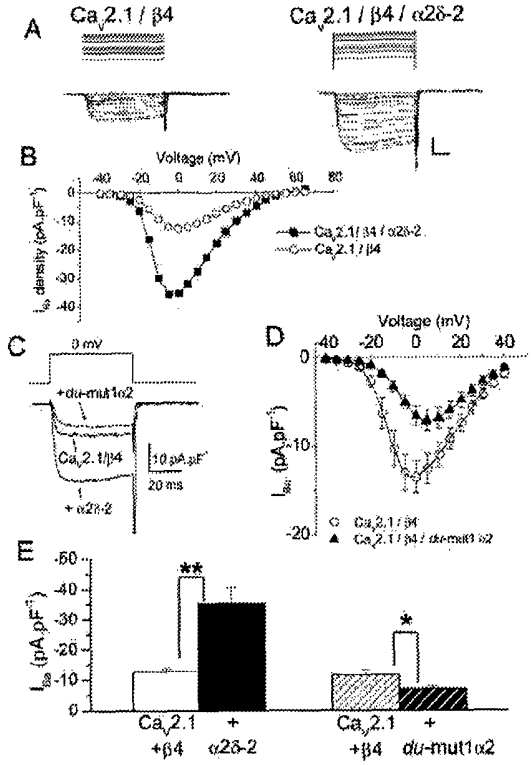

FIG. 9. **Enhancement of $Ca_V2.1/\beta_4$ currents by α2δ-2 and inhibition by *du*-mut1 α_2.** *A*, examples of I_{Ba} recorded from COS-7 cells transfected with $Ca_V2.1/\beta_4$/α2δ-2 or $Ca_V2.1/\beta_4$. The holding potential was −80 mV, and steps were to between −40 and +65 mV in 5-mV steps, delivered every 15 s. The charge carrier was 5 mM Ba^{2+}. The *scale bars* represent 10 pA·pF^{-1} and 10 ms. *B*, I–V relationships for $Ca_V2.1/\beta_4$ (○, n = 28) and $Ca_V2.1/\beta_4$/α2δ-2 (■, n = 42) peak I_{Ba} density in COS 7 cells. *C*, examples of the maximum I_{Ba} recorded at 0 mV from COS-7 cells transfected with $Ca_V2.1/\beta_4$, $Ca_V2.1/\beta_4$/α2δ-2, or $Ca_V2.1/\beta_4$/*du*-mut1 α_2, as in *A*. Co-expression of α2δ-2 induced a large enhancement of $Ca_V2.1/\beta_4$ I_{Ba}, whereas *du*-mut1 α_2 induced a reduction of $Ca_V2.1/\beta_4$ I_{Ba}. *D*, mean I–V relationships for $Ca_V2.1/\beta_4$ (○) and $Ca_V2.1/\beta$ 4/*du*-mut1 α_2 (▲) peak I_{Ba} density in COS-7 cells, fitted with a combined Boltzmann and linear function, as described under "Experimental Procedures." *E*, histogram of mean data, for the transfection conditions shown *below* the *bars*, from COS-7 cells. $Ca_V2.1/\beta_4$ (*open bar*, n = 13, controls for $Ca_V2.1/\beta_4$/α2δ-2 transfections); $Ca_V2.1/\beta_4$/α2δ-2 (*black bar*, n = 42); $Ca_V2.1/\beta_4$ (*open hatched bar*, n = 15, performed in parallel with $Ca_V2.1/\beta_4$/*du*-mut1 α_2 transfections) or $Ca_V2.1/\beta_4$/*du*-mut1 α_2 (*black hatched bar*, n = 12). Statistical significance of differences indicated given by *asterisks*: **, $p < 0.001$; *, $p < 0.05$ (Student's independent two tailed t test).

different conditions are compared in Fig. 9*E*. Similar results were obtained when these calcium channel subunits, in this case including rabbit Ca_V 2.1, were expressed in *Xenopus* oocytes (see Ref. 12 and data not shown).

Effect of α2δ-2 and du-mut1 α_2 on Single Ca^{2+} Channel Currents Formed by $Ca_V2.1$—We compared single channel parameters between cell-attached patches of COS-7 cells transfected with $Ca_V2.1/\beta_4$ cDNA, either without α2δ-2 (Fig. 10*A*) or co-expressed with either full-length α2δ-2 (Fig. 10*B*) or the *du*-mut1 α_2 (Fig. 10*C*). These experiments were performed in order to differentiate between a mechanism that involves changing the biophysical properties of Ca_V 2.1 channels and a mechanism that involves changing the trafficking or membrane expression levels of the Ca_V 2.1 channels, imposed by either α2δ-2 or *du*-mut1 α_2.

Once opened, Ca_V 2.1 channels showed an average single channel conductance of 9.9 ± 0.4 pS (n = 8) for $Ca_V2.1/\beta_4$, which was not significantly affected by co-expression of α2δ-2 (10.2 ± 0.6 pS, n = 8) or *du*-mut1 α_2 (8.8 ± 1.0 pS, n = 6) (Fig. 10*D*, *left*). This conductance is similar to that of P-type channels recorded from wild-type and *du/du* PCs under the same conditions (12). More detailed analysis demonstrated openings to three distinct amplitude levels, as has also been shown in native Purkinje cells (28), level 2 being the most prominent in our recordings (Fig. 10*D*, *middle* and *right*, see legend for conductance and amplitude values). Neither the conductance nor the amplitude of the three current levels was significantly affected by expression of α2δ-2 or *du*-mut1 α_2 (data not shown).

Neither α2δ-2 nor *du*-mut1 α_2 caused any significant change in mean open or closed times or in the pattern of voltage dependence of Ca_V 2.1 channels (Fig. 10*E*). We also examined the activation kinetics by measuring the latency to first opening of the channels in response to a square voltage pulse (Fig. 10*F*). Ca_V 2.1 channel activation was not influenced by the subunits examined (Fig. 10*F*, *left*), at any voltage (Fig. 10*F*, *right*). In addition, the voltage dependence of inactivation (Fig. 10*G*) was not influenced by either α2δ-2 or *du*-mut1 α_2.

Although the presence of α2δ-2 caused an ~3-fold increase in whole cell current amplitude, all the single channel parameters were indistinguishable between the three conditions. This implies that the basic active unit in the whole cell current (an individual channel) remains unchanged, and the modulation by α2δ-2 must involve an alteration in the number of active channels in the membrane.

DISCUSSION

PCs from du/du Mice Have a Reduced Dendritic Arbor—PC somata form a monolayer by 10 days postnatally in the mouse, and their dendrites reach the pial surface at day 20, coinciding with the completion of granule cell migration and concomitant parallel fiber production (29). The PC soma typically exhibits one primary dendrite, which emerges apically, and one axonal

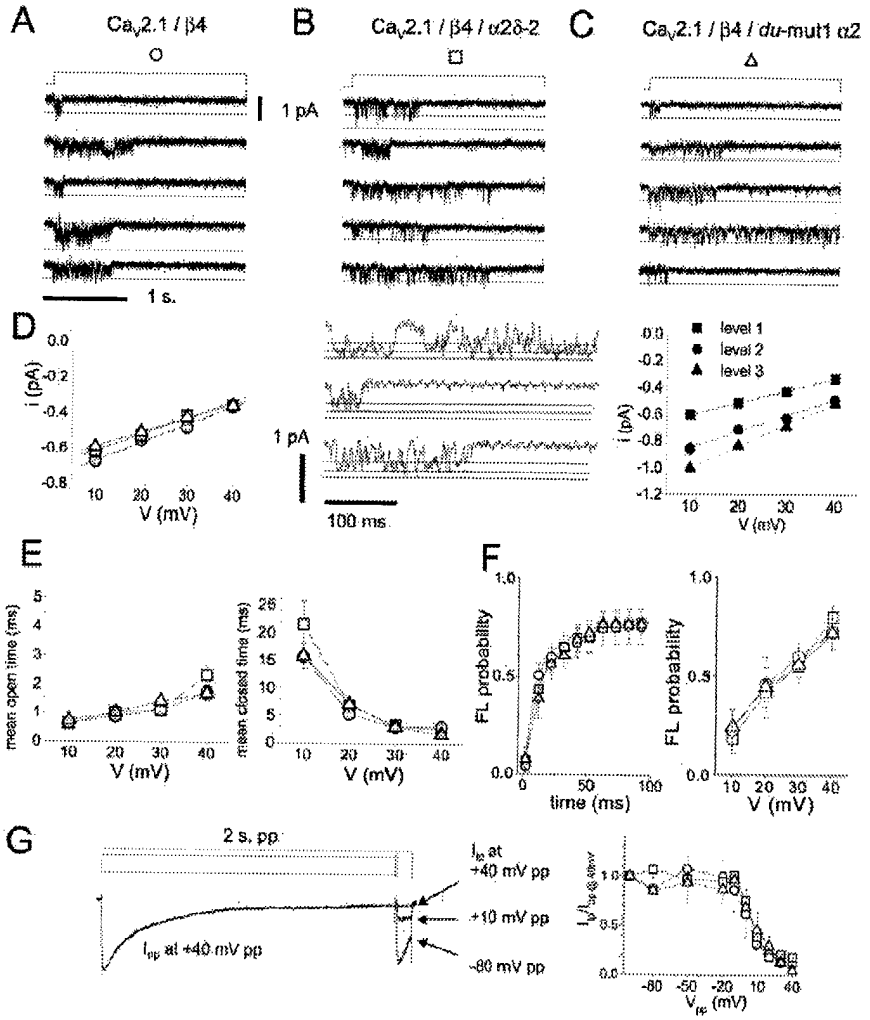

FIG. 10. **Comparison between the effect of α2δ-2 or *du*-mut1 α_2 on single channel parameters of Ca$_V$2.1.** *A*, single channel activity (maximum of two simultaneous overlapping openings) of Ca$_V$2.1/β_4 without the α2δ-2 auxiliary subunit. *Top*, the voltage protocol: holding potential −100 mV. A 2-s-long pulse, here to +30 mV, delivered every 10 s. *Bottom*, 5 representative traces of single channel activity. *Openings* are downward deflections, and a *continuous line* marks both the closed and open states, in traces with overlapping openings an additional *dashed line* marks the second level. *B*, single channel activity (maximum of two simultaneous overlapping openings) arising from Ca$_V$2.1/β_4 co-expressed with the α2δ-2 auxiliary subunit. Format as in *A*. *C*, single channel activity (maximum of two simultaneous overlapping openings) arising from Ca$_V$2.1/β_4 co-expressed with the *du*-mut1 α_2. Format as in *A*. *D*, *left*, average single channel conductance for the 3 conditions depicted in *A–C* (○, $n = 8$; □, $n = 8$; △, $n = 6$), respectively. Conductance was determined by linear fits to the data shown. See text for mean fit values. *Middle*, examples of single channel activity at +30 mV for Ca$_V$2.1/β_4 where more than one amplitude level was observed. *Continuous lines* mark the three amplitude levels, depicted by: ■, level 1; ●, level 2; ▲, level 3 on *right*. *Right*, single channel I–V plot to show the distinct conductances for data such as that shown. The single channel conductances for the three levels are 8.2 ± 1.2, 12.1 ± 1.05, and 16.2 ± 0.46 pS ($n = 6$), and the corresponding amplitudes at +30 mV are −0.43 ± 0.027, −0.63 ± 0.038, and −0.69 ± 0.033 pA. *E*, mean open (*left*) and closed (*right*) times were similar at all voltages examined, for the three conditions, respectively (○, $n = 8$; □, $n = 8$; △, $n = 6$). *F*, FL probability histogram, for the three conditions, respectively (○, $n = 8$; □, $n = 8$; △, $n = 5$). *Left*, mean (± S.E., shown every 10 ms for clarity) cumulative FL probability distributions at +30 mV, and *right*, FL probability at 20 ms for all voltages examined. *G*, steady-state inactivation of Ca$_V$ 2.1 ensemble currents from single and multichannel patches. *Left*, an example of inactivation experiment. *Top*, the voltage protocol, holding potential, −100 mV, followed by a 2 s. Prepulse (*pp*) to a potential (V_{pp}) between −80 and +40 mV, followed by a test pulse to +40 mV for 100 ms. *Bottom*, average ensemble currents (from the data as shown in *B* with a V_{pp} of +40 mV (*left*) and test pulse responses to V_{pp} of −80, +10, and +40 mV are superimposed. *Right*, all currents were normalized to the peak prepulse current at +40 mV and the ratio plotted as a function of V_{pp}. Data of the type shown in (*A–C*), respectively (○, $n = 11$; □, $n = 11$; △, $n = 4$).

process projecting in the opposite direction. The PC dendritic trees develop most dramatically between postnatal day 9 and 20, reaching 80% of their adult dimension in this period (30). PCs from *du/du* mice appear immature, reduced both in size and complexity, with multiple primary dendrites and small arbors that often terminate well below the pial surface. Thickened secondary and tertiary dendritic trunks are also present. The multipolar appearance of some of the *du/du* PCs may be a remnant of their immature stage (in which the normal resorption of all somatic filopodia fails to occur), with some of these processes continuing to develop into dendrites as found in weaver and staggerer mouse mutants (31).

Thus, although we have shown that PCs are not lost in *du/du* cerebella at P21 (12), we now find that the PC dendritic tree is reduced in size and shows other abnormalities, such as weeping willow dendrites and dendritic thickening. Similar abnormalities have been found in a number of the spontaneously occurring Ca$_V$ 2.1 mouse mutants (8), and some of these (in particular *tg^{la}*) also show PC loss in older mice (32). The mechanism of the altered PC morphology in *du/du* mice may result

either from the reduced PC calcium channel currents, which we observed in P5-P9 PCs, before the extensive growth of the dendritic arbor (12) or more directly from the loss of α2δ-2, with the possible additional consequences of expression of a truncated mutant α_2 protein. A number of the human genetic diseases involving $Ca_V2.1$, for example familial hemiplegic migraine (33), cerebellar ataxia, and PC degeneration are associated with mutations that have been shown to produce a reduction in $Ca_V2.1$ calcium currents *in vitro* (34). However, the mechanism whereby such molecular changes are translated into morphological and functional abnormalities remains to be determined.

A Truncated Mutant Protein Derived from the 5′ Mutant Transcript of Cacna2d2 Is Expressed in du Mice—The *in situ* hybridization study demonstrates that although wild-type *Cacna2d2* transcript is absent from the brain of *du/du* mice, because of the genomic rearrangement that disrupts *Cacna2d2* (12), a 5′ mutant transcript (*du* mutant transcript 1) is present in *du/du* PCs. This transcript is predicted to encode a protein (*du*-mut1 α_2) that lacks most of the α_2 subunit and the whole of the δ subunit, including its transmembrane domain. It is frequently the case that mRNA encoding mutant transcripts, where a frameshift or point mutation introduces one or more premature stop or nonsense codons, is unstable and subject to nonsense-mediated mRNA decay (35). Indeed, although a second mutant transcript 2, predicted to be formed from exons 2–39, was identified by reverse transcriptase-PCR and Northern blot in *du/du* mouse brain, it was not observed by *in situ* hybridization in *du/du* PCs (12). Furthermore, the 5′ *du* mutant transcript 1 appeared to be present at a low level in *du/du* brain (12). To determine whether this mutant transcript was translated, we used two α2δ-2 anti-peptide antibodies, which were raised against peptides within the *du*-mut1 α_2 sequence, Ab(16–29) and Ab(102–117).

It has been established, from studies with site-directed antipeptide antibodies, that the topology of the α2δ-1 subunit is such that the α_2 subunit, which has an N-terminal leader signal sequence, is entirely extracellular (36–38). The α_2 subunit is disulfide-bonded to a transmembrane δ subunit, and both subunits have been found to be involved in the interaction with the $Ca_V1.2$ subunit (38, 39). Now that two other α2δ subunit genes have been cloned, it is assumed that they have the same topology, and indeed, high homology is present between the N termini of α2δ-1 and α2δ-3, with the clear prediction of a cleaved signal peptide in both sequences. In contrast, although a putative signal peptide is found in α2δ-2, it is much longer. By using prediction analysis, it is found to have a potential cleavage site after position 64 (40) (Fig. 7*B*), whereas only 2% of eukaryotic signal peptides are longer than 35 residues (40). In particular, it has a longer sequence N-terminal to the putative hydrophobic signal sequence (~42 amino acids) than α2δ-1 or α2δ-3 (which are ~3 and 11 amino acids, respectively). Such "*n* regions" are found to be less than 25 amino acids in 80% of secreted or transmembrane proteins where they occur (41). Therefore, it remains unclear whether this signal sequence is cleaved efficiently, as cleavage is often delayed when the signal sequence is long (42). This results in extended transit times through the endoplasmic reticulum-Golgi apparatus, which may be required for highly glycosylated proteins (42). Such an explanation is likely to be the reason for our observation using Ab(16–29), of a 120-kDa immunolabeled protein when α2δ-2 was expressed in COS-7 cells. This is likely to represent the α_2 moiety of full-length α2δ-2 (predicted protein molecular mass of 113 kDa), which is immature in that it has an uncleaved signal peptide and, judging by the molecular weight, no added carbohydrate.

It appears that in the case of *du*-mut1 α_2 expressed in COS-7 cells, the truncated protein is processed such that the signal sequence remains at least in part uncleaved, because both Ab(16–29) and Ab(102–117) recognized a band of ~16 kDa, the predicted size for the uncleaved *du*-mut1 α_2, and Ab(16–29) also recognized a fainter band of about 6 kDa, which would represent the cleaved signal peptide. However, the predominant band recognized by Ab(102–117) but not Ab(16–29) was a ~10-kDa protein, which is therefore likely to represent *du*-mut1 α_2 with its signal peptide cleaved. This result corresponded exactly with the molecular weight of the native *du*-mut1 α_2 immunocaptured from *du/du* cerebellum by the same antibody, indicating that it is a stable *in vivo* species in these mice. This study also confirmed the previous indication (12) that *du* mutant transcript 2, which would be recognized by Ab(102–117), is not translated. A 16-kDa protein was immunocaptured by Ab(16–29) from *du/du* cerebellum, indicating that the signal sequence remains, in part, uncleaved from *du*-mut1 α_2. The reason that this species was not also immunocaptured by Ab(102–117) may indicate that Ab(102–117) is of lower affinity, as also suggested by the data in Fig. 8.

Immunolocalization of α2δ-2 and du-mut1 α_2 in Cerebellum—In cerebellar sections, we found, using Ab(102–117), that α2δ-2 is expressed in wild-type PC somata and also in the ML of the cerebellum, suggesting localization in PCs. It is also possible that some of the immunostaining arises from cerebellar afferents or from Bergmann glia, and this will be investigated in the future. In *du/du* cerebellum, a low level of immunostaining was observed with the same antibody. These results support the finding that *du*-mut1 α_2 is expressed in *du/du* cerebellum. Immunoreactivity in *du/du* cerebellar sections was also observed using Ab(16–29), where staining, presumably representing the uncleaved *du*-mut1 α_2, was concentrated in PC somata. In agreement with the expression study in COS-7 cells and the immunopurification data from cerebellum, this suggests that *du*-mut1 α_2 retains, in part, the putative signal sequence at its N terminus and does not appear to be secreted. When *du*-mut1 α_2 was expressed in COS-7 cells both Ab(16–29) and Ab(102–117) recognized an epitope that was only expressed intracellularly, indicating that *du*-mut1 α_2 is unlikely to be secreted or inserted into the plasma membrane as a transmembrane protein.

The Functional Interaction of the $Ca_V2.1/\beta_4$ Combination with α2δ-2—The similarity of the ducky phenotype to that observed in mice with mutations in genes encoding the $Ca_V2.1$ (7) and β_4 (9) subunits and their predominant PC expression pattern suggests that α2δ-2 contributes to the P-type current. This is reinforced by our finding that the currents formed by both rat and rabbit $Ca_V2.1$ co-expressed with β_4, which is the main PC β subunit, were strongly enhanced by α2δ-2, in two expression systems (COS-7 cells and *Xenopus* oocytes).

Previous *in vitro* studies have shown that α2δ-1, α2δ-2, and α2δ-3 subunits act to increase the maximum conductance of a number of expressed calcium channel α_1/β subunit combinations at the whole cell level (2, 43–46). However, this may be dependent to some extent on the specific combination of α_1 and β subunits expressed. Furthermore, the effects of α2δ subunits on kinetics and voltage dependence of activation are more minor (2, 44). We have also investigated this for the calcium channel subunit combinations used in the present study, and we show that α2δ-2 had no influence on voltage-dependent properties and had no effect on single channel conductance or other biophysical parameters of the $Ca_V2.1/\beta_4$ channels themselves. This implies that α2δ-2 probably has its main effect on the lifetime of the channel complex in the plasma membrane, either by enhancing trafficking or reducing turnover. In agree-

ment with this proposed mechanism, it has previously been found that α2δ-1 increased the amount of $Ca_V1.2$ protein expressed in *Xenopus* oocytes (47).

In contrast, the protein product of *du* mutant transcript 1, *du*-mut1 α_2, produced a consistent reduction in $Ca_V2.1/\beta_4$ currents in COS-7 cells. Thus, whereas loss of full-length α 2δ-2 is likely to be the most important contributing factor, the expression of the truncated *du*-mut1 α_2 may also contribute to the *du*/*du* phenotype, via an additional suppressive effect, possibly by interfering with the correct trafficking of α_1 subunits.

Acknowledgments—We thank Professor R. M. Gardiner for support and encouragement. We also thank Dr. Kevin Bittman, Dr. David Becker, and Dr. Marina Mione for generously sharing their expertise and Mick Keegan for excellent technical assistance.

REFERENCES

1. Catterall, W. A. (2000) *Annu. Rev. Cell Dev. Biol.* **16,** 521–555
2. Walker, D., and De Waard, M. (1998) *Trends Neurosci.* **21,** 148–154
3. Letts, V. A., Felix, R., Biddlecome, G. H., Arikkath, J., Mahaffey, C. L., Valenzuela, A., Bartlett, F. S., Mori, Y., Campbell, K. P., and Frankel, W. N. (1998) *Nat. Genet.* **19,** 340–347
4. Chen, L., Chetkovich, D. M., Petralia, R. S., Sweeney, N. T., Kawasaki, Y., Wenthold, R. J., Bredt, D. S., and Nicoll, R. A. (2000) *Nature* **408,** 936–943
5. Ertel, E. A., Campbell, K. P., Harpold, M. M., Hofmann, F., Mori, Y., Perez-Reyes, E., Schwartz, A., Snutch, T. P., Tanabe, T., Birnbaumer, L., Tsien, R. W., and Catterall, W. A. (2000) *Neuron* **25,** 533–535
6. Burgess, D. L., Gefrides, L. A., Foreman, P. J., and Noebels, J. L. (2001) *Genomics* **71,** 339–350
7. Fletcher, C. F., Lutz, C. M., O'Sullivan, T. N., Shaughnessy, J. D., Jr., Hawkes, R., Frankel, W. N., Copeland, N. G., and Jenkins, N. A. (1996) *Cell* **87,** 607–617
8. Zwingman, T. A., Neumann, P. E., Noebels, J. L., and Herrup, K. (2001) *J. Neurosci.* **21,** 1169–1178
9. Burgess, D. L., Jones, J. M., Meisler, M. H., and Noebels, J. L. (1997) *Cell* **88,** 385–392
10. Kang, M. G., Chen, C. C., Felix, R., Letts, V. A., Frankel, W. N., Mori, Y., and Campbell, K. P. (2001) *J. Biol. Chem.* **276,** 32917–32924
11. Sharp, A. H., Black, J. L., III, Dubel, S. J., Sundarraj, S., Shen, J. P., Yunker, A. M. R., Copeland, T. D., and McEnery, M. W. (2001) *Neuroscience* **105,** 599–617
12. Barclay, J., Balaguero, N., Mione, M., Ackerman, S. L., Letts, V. A., Brodbeck, J., Canti, C., Meir, A., Page, K. M., Kusumi, K., PerezReyes, E., Lander, E. S., Frankel, W. N., Gardiner, R. M., Dolphin, A. C., and Rees, M. (2001) *J. Neurosci.* **21,** 6095–6104
13. Snell, G. D. (1955) *J. Hered.* **46,** 27–29
14. Meier, H. (1968) *Acta Neuropathol. (Berl.)* **11,** 15–28
15. Stuart, G. J., Dodt, H. U., and Sakmann, B. (1993) *Pfluegers Arch. Eur. J. Physiol.* **423,** 511–518
16. Eisenstat, D. D., Liu, J. K., Mione, M., Zhong, W. M., Yu, G. Y., Anderson, S. A., Ghattas, I., Puelles, L., and Rubenstein, J. L. R. (1999) *J. Comp. Neurol.* **414,** 217–237
17. Brice, N. L., Berrow, N. S., Campbell, V., Page, K. M., Brickley, K., Tedder, I., and Dolphin, A. C. (1997) *Eur. J. Neurosci.* **9,** 749–759
18. Macart, M., and Gerbaut, L. (1982) *Clin. Chim. Acta* **122,** 93–101
19. Berrow, N. S., Brice, N. L., Tedder, I., Page, K., and Dolphin, A. C. (1997) *Eur. J. Neurosci.* **9,** 739–748
20. Hans, M., Urrutia, A., Deal, C., Brust, P. F., Stauderman, K., Ellis, S. B., Harpold, M. M., Johnson, E. C., and Williams, M. E. (1999) *Biophys. J.* **76,** 1384–1400
21. Barclay, J., and Rees, M. (2000) *Mamm. Genome* **11,** 1142–1144
22. Cormack, B. P., Valdivia, R. H., and Falkow, S. (1996) *Gene (Amst.)* **173,** 33–38
23. Meir, A., Bell, D. C., Stephens, G. J., Page, K. M., and Dolphin, A. C. (2000) *Biophys. J.* **79,** 731–746
24. Canti, C., Page, K. M., Stephens, G. J., and Dolphin, A. C. (1999) *J. Neurosci.* **19,** 6855–6864
25. Meir, A., and Dolphin, A. C. (1998) *Neuron* **20,** 341–351
26. Neher, E. (1995) in *Single-channel Recording* (Sakmann, B., and Neher, E., eds) pp. 147–153, Plenum Publishing Corp., New York
27. Imredy, J. P., and Yue, D. T. (1994) *Neuron* **12,** 1301–1318
28. Usowicz, M. M., Sugimori, M., Cherksey, B., and Llinas, R. (1992) *Neuron* **9,** 1185–1199
29. Fujita, S. (1967) *J. Cell Biol.* **32,** 272–288
30. Sadler, M., and Berry, M. (1984) *Proc. R. Soc. Lond. Ser. B Biol. Sci.* **221,** 349–367
31. Sotelo, C. (1975) *Adv. Neurol.* **12,** 335–351
32. Heckroth, J. A., and Abbott, L. C. (1994) *Brain Res.* **658,** 93–104
33. Ophoff, R. A., Terwindt, G. M., Vergouwe, M. N., van Eijk, R., Oefner, P. J., Hoffman, S. M., Lamerdin, J. E., Mohrenweiser, H. W., Bulman, D. E., Ferrari, M., Haan, J., Lindhout, D., van Ommen, G. J., Hofker, M. H., Ferrari, M. D., and Frants, R. R. (1996) *Cell* **87,** 543–552
34. Hans, M., Luvisetto, S., Williams, M. E., Spagnolo, M., Urrutia, A., Tottene, A., Brust, P. F., Johnson, E. C., Harpold, M. M., Stauderman, K. A., and Pietrobon, D. (1999) *J. Neurosci.* **19,** 1610–1619
35. Culbertson, M. R. (1999) *Trends Genet.* **15,** 74–80
36. Brickley, K., Campbell, V., Berrow, N., Leach, R., Norman, R. I., Wray, D., Dolphin, A. C., and Baldwin, S. (1995) *FEBS Lett.* **364,** 129–133
37. Gurnett, C. A., De Waard, M., and Campbell, K. P. (1996) *Neuron* **16,** 431–440
38. Gurnett, C. A., Felix, R., and Campbell, K. P. (1997) *J. Biol. Chem.* **272,** 18508–18512
39. Felix, R., Gurnett, C. A., De Waard, M., and Campbell, K. P. (1997) *J. Neurosci.* **17,** 6884–6891
40. Nielsen, H., Engelbrecht, J., Brunak, S., and vonHeijne, G. (1997) *Protein Eng.* **10,** 1–6
41. Martoglio, B., and Dobberstein, B. (1998) *Trends Cell Biol.* **8,** 410–415
42. Li, Y., Luo, L. Z., Thomas, D. Y., and Kang, C. Y. (1994) *Virology* **204,** 266–278
43. Mori, Y., Friedrich, T., Kim, M.-S., Mikami, A., Nakai, J., Ruth, P., Bosse, E., Hofmann, F., Flockerzi, V., Furuichi, T., Mikoshiba, K., Imoto, K., Tanabe, T., and Numa, S. (1991) *Nature* **350,** 398–402
44. Klugbauer, N., Lacinova, L., Marais, E., Hobom, M., and Hofmann, F. (1999) *J. Neurosci.* **19,** 684–691
45. Dolphin, A. C., Wyatt, C. N., Richards, J., Beattie, R. E., Craig, P., Lee, J.-H., Cribbs, L. L., Volsen, S. G., and Perez-Reyes, E. (1999) *J. Physiol. (Lond.)* **519,** 35–45
46. Hobom, M., Dai, S., Marais, E., Lacinova, L., Hofmann, F., and Klugbauer, N. (2000) *Eur. J. Neurosci.* **12,** 1217–1226
47. Shistik, E., Ivanina, T., Puri, T., Hosey, M., and Dascal, N. (1995) *J. Physiol. (Lond.)* **489,** 55–62

Genetic Engineering: Principles and methods. 1988 v.10 pp 221-246
Plenum press

THE USE OF TRANSGENIC ANIMAL TECHNIQUES FOR LIVESTOCK IMPROVEMENT

Reiner M. Strojek and Thomas E. Wagner

Edison Animal Biotechnology Center
Ohio University
Athens, Ohio 45701

INTRODUCTION

Breeding of livestock has always been characterized by selection of spontaneously occurring mutations which could be observed in the phenotype of the animals. This could be achieved even though the genetic and molecular mechanisms underlying those phenotypes were not understood. Depending on the generation intervals of the species involved, years to centuries were required to establish certain breeds in livestock fulfilling the needs of man. Still the ideal farm animals have not been found. As higher meat, egg or milk yields are obtained, higher susceptibilities towards environmental influences such as climate or food changes or stress are observed and disease resistance declines, especially when animals are kept in large numbers under industrial production conditions. Since the first successful gene transfer experiments into the germ line of mammals, namely mice, were reported in 1980 and 1981, many attempts have been made to use gene transfer techniques in livestock in order to improve the overall quality and productivity of farm animals.

Transgenic mice exhibiting the desired expression of the newly introduced gene and therefore showing an altered phenotype can now be produced routinely with different gene transfer techniques. Such mice are used in molecular biology research serving as genetically transformed, in vivo, models elucidating different kinds of scientific problems. In contrast, only little progress has been made in recent years in producing transgenic mammals of other species. The major drawbacks are inadequate regulation of expression of the foreign genes and therefore the desired phenotypical improvement has not been obtained so far.

In this chapter we will describe briefly the basic techniques involved and summarize the results which have been obtained until now, in respect to the production of transgenic mice and livestock in particular. The difficulties encountered in the application of

gene transfer techniques, which have been successfully used in mice, to farm animals, are discussed and their future implications for animal breeding are outlined.

PRODUCTION OF TRANSGENIC MICE

The term "transgenic" was introduced originally by Gordon and Ruddle (1) for mice which had integrated a foreign gene into all somatic tissues examined. This had been achieved by injecting these genes into the pronuclei of fertilized mouse ova. Since it became evident later (1a) that the offspring of these mice can inherit the foreign genes in a Mendelian fashion, the word transgenic is now commonly used to refer to a stable germline integration of foreign genes. At present three different approaches have been reported which succeed in the establishment of transgenic mouse lines. These methods include pronuclear injection of DNA, infection of embryonal stages with recombinant viral vectors and the production of germline chimeras which consist partially of totipotent, genetically transformed, cell lines.

Pronuclear Injection

Several groups (1a-4) established this method of gene transfer simultaneously showing that by using this technique integration of the introduced foreign gene into all somatic and also into the germ cells of the developing animal can be achieved. In order to achieve optimal results, approximately 1 pl of a DNA suspension containing 200 to 2000 linearized copies of the foreign gene is injected into either pronucleus of fertilized mouse eggs (5). After overnight cultivation cleaved eggs (50% to 75%) are transferred to the oviducts of foster mothers. Of these 10% to 25% usually develop to term and about 15% to 37% of the young born inherit the injected genes, which leads to an overall efficiency rate of 1% to 4% based on the total number of zygotes manipulated.

Provided the introduced genes are integrated into the genomic DNA before the zygote enters cleavage, all embryonal cells will contain the same integration site and copy number of the foreign gene. Integration after the first cleavage will give rise to chimeric animals, which consist of at least two genetically different cell populations. According to Wilkie et al. (6) the latter seems to be true in at least 30% of the mice born after microinjection of DNA.

Infection of Embryos by Viral Vectors

Infection of blastocysts by SV40 (7) was the first evidence that foreign genes could be integrated into the genome of embryo-

nal cells and lea
tissue. Jaenisch (
not only retained
was also transmitte
mice.

Viral infectio
prevented by the exi
be overcome by eith
two-cell to morula s
injection of virus p
procedure has been
the germline of mice
mosaic, as different
able number of embry

To transfer for
binant retroviral ve
interest. Since reco
competent, they re
gation. Stuhlmann et
fetuses with recombi
served subsequent i

fertiliz

Figure

nal cells and lead to their stable integration into somatic tissue. Jaenisch (8) also observed that the M-MuLV provirus was not only retained by somatic cells after embryonal infection but was also transmitted to the offspring of the resulting mature mice.

Viral infection of the preimplantation embryo is naturally prevented by the existence of the zona pellucida. This barrier can be overcome by either enzymatic digestion of the zona, so that two-cell to morula stages can be infected (9,10) or direct microinjection of virus particles into the blastocoele cavity (7). This procedure has been used successfully to introduce proviruses into the germline of mice. However, the resulting embryos generally are mosaic, as different integration events can take place in a variable number of embryonal cells (11).

To transfer foreign genes into the germline of mice, recombinant retroviral vectors can be used which contain the gene of interest. Since recombinant retroviruses generally are replication incompetent, they require the presence of helper virus for propagation. Stuhlmann et al. (12) have thus infected day-nine mouse fetuses with recombinant and helper virus simultaneously and observed subsequent integration and expression in the resulting

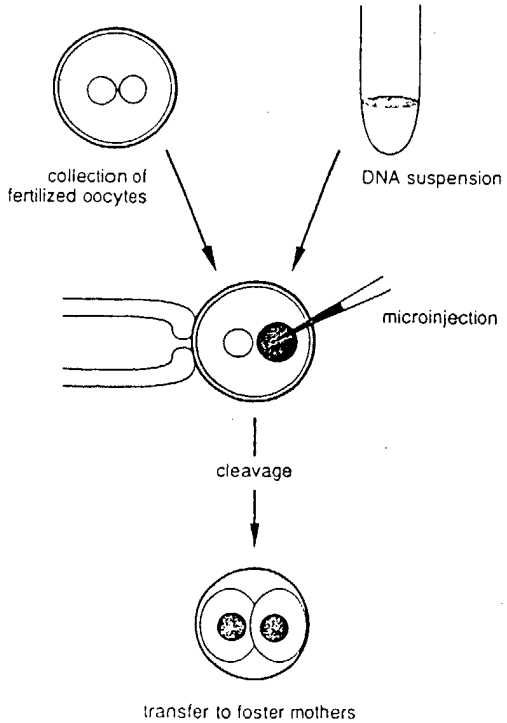

Figure 1. Pronuclear injection of DNA.

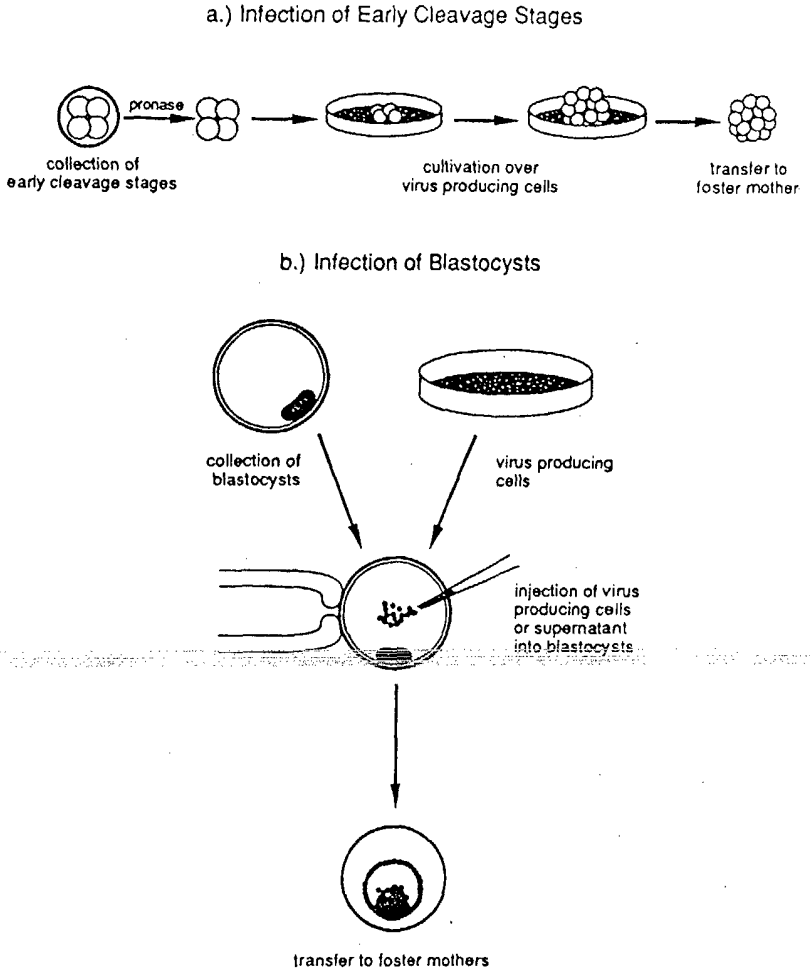

Figure 2. Infection of embryos with viral vectors.

offspring. However, their results suggested that the superinfection with helper virus in these mice had interfered with the spread of the recombinant virus and therefore limited the number of transformed somatic cells.

As separation of recombinant and helper virus yet cannot be achieved, an alternative propagation method using psi-2 cells (13) can be chosen if viremia from the helper virus is to be avoided in the resulting animals. Psi-2 cell lines have incorporated a retroviral genome which cannot be packaged into virus particles

itself because of a
all the information
virus with an intact
yield of recombinant
is not accompanied by

Van der Putten
infected pre-implanta
tion-incompetent retr
denuded 8-cell stage
hours and subsequentl
one animal which had
ing the foreign gene
Rubenstein et al. (10
os over psi-2 cells
transfer, of which on

Pro

Chimeras can be
by injecting embryona
ure that results in t
two or more genetical
embryonal cell lines,
erations, are genetic
era formation, this
transgenic animals, p
ticipate in the forma

The first embryo
of murine embryonal
these cells appeared
ency to lose their
therefore lose their
germline. Also the de
EC-cell derived chime
with embryonal stem E
vitro attached mouse
passages. After micr
blastocysts, Bradley
of 70%; about 50% of
which 20% also showed
gregated 8-cell-stage
birth rates of 36%, 2
use of genetically tr
sion of the transfe
chimeric animals. Ro
cells, which had been
fection, and selecte
blastocysts. Out of
chimeric, of which tw

itself because of a mutation in its psi region, but it delivers all the information needed for the propagation of recombinant virus with an intact psi region to the cell. Consequently, the yield of recombinant virus will be lower in these cell lines, but is not accompanied by the production of helper virus.

Van der Putten et al. (14) and Rubenstein et al. (10) have infected pre-implantation mouse embryos with recombinant replication-incompetent retrovirus without the use of helper virus. 197 denuded 8-cell stages cultivated over psi-2 monolayers for 16 hours and subsequently transferred to foster mothers gave rise to one animal which had incorporated the recombinant provirus including the foreign gene and transmitted it to its offspring (14). Rubenstein et al. (10) co-cultivated 278 4-cell-stage mouse embryos over psi-2 cells and obtained 76 (30%) live fetuses after transfer, of which one contained the recombinant provirus.

Production of Germline Chimeras

Chimeras can be produced either by aggregating two embryos or by injecting embryonal cells into expanded blastocysts, a procedure that results in the formation of individuals which consist of two or more genetically different cell lines (15). When totipotent embryonal cell lines, which can be grown in culture for many generations, are genetically transformed before being used for chimera formation, this technique offers another route of producing transgenic animals, provided that the transformed cells will participate in the formation of germ cells.

The first embryonal cell line used for this purpose consisted of murine embryonal teratocarcinoma (EC-) cells (16). However, these cells appeared to have the disadvantage of showing a tendency to lose their euploidy during in vitro cultivation and therefore lose their totipotency, especially to contribute to the germline. Also the development of abnormal fetuses was observed in EC-cell derived chimeras (17). More stable results can be obtained with embryonal stem ES-cells (18), which can be isolated from *in vitro* attached mouse blastocysts and grown in culture for many passages. After microinjection of ES-cells into expanded mouse blastocysts, Bradley et al. (19) obtained an average birth rate of 70%; about 50% of the young born proved to be chimeric, of which 20% also showed germline chimerism. Stewart et al. (20) aggregated 8-cell-stage mouse embryos with ES-cells and received birth rates of 36%, 20% of the pups being chimeric. The successful use of genetically transformed ES-cells (20,21) led to the expression of the transferred genes within somatic tissues of the chimeric animals. Robertson et al. (21) injected 10 to 12 ES-cells, which had been repeatedly exposed to psi-2 cells for transfection, and selected for transformation, into expanded mouse blastocysts. Out of 21 mice born after transfer 20 proved to be chimeric, of which two were reported to have transgenic offspring.

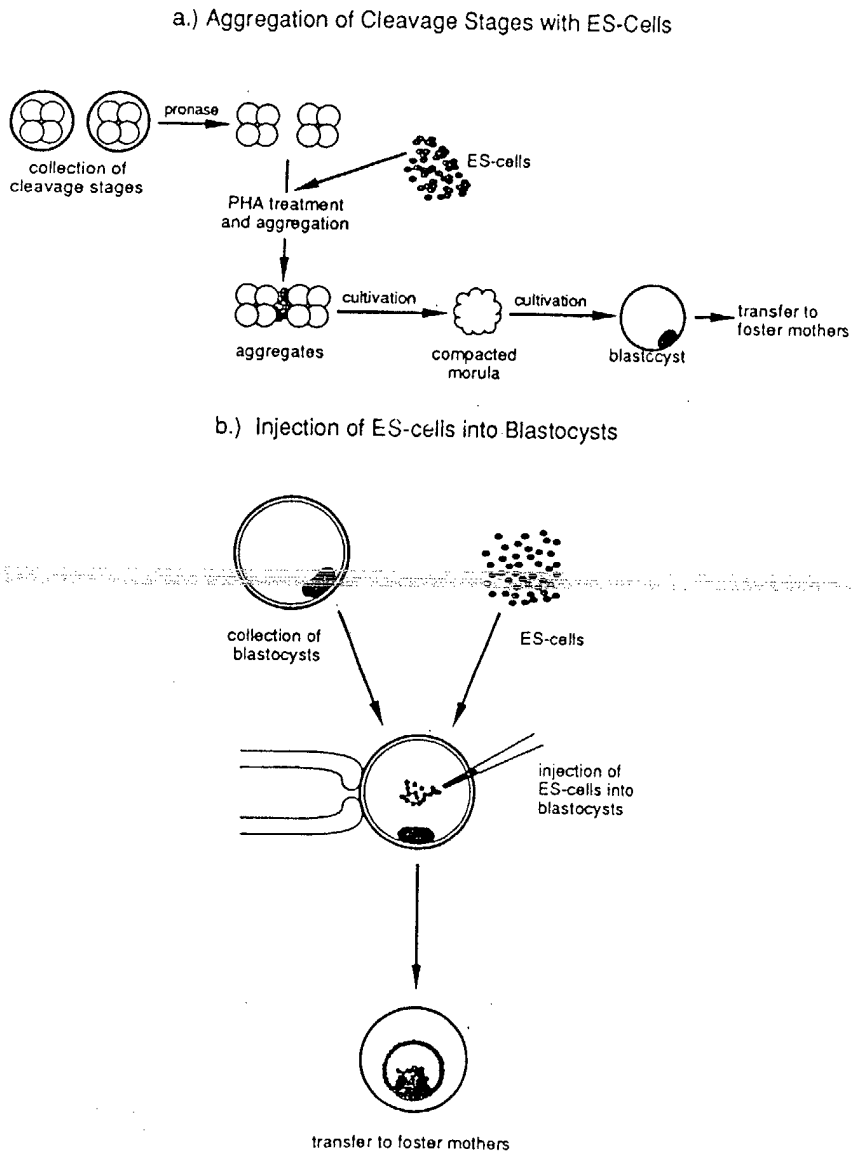

Figure 3. Production of chimeras with transformed totipotent cells.

According to Evans
achieved by this meth

A very critical
animals is the succe
are several methods
of these cells with
equipment and skill
method, which is comp
formants (frequency
bers of totipotent ce

One alternative
efficiently is the
Rubenstein et al. (25
ed recombinant retrov
had incorporated the
of the virus in thes
mediated transformati
on the infectivity an
as on the time of exp

If retroviral
reason, microinjectio
onal cells offers a t
gene transfer with a

Genomic Integrat

The integration
mammalian genome is u
to be an entirely ran
lines have shown that
precipitates), transg
high molecular weight
sociated with chromo
transformation proces
tegration during the
servations (23,28-31)
within the nucleus, u
ing including ligatio
of nuclear enzymes f
genome has also been
Israel (32), who fo
synchronized mammalia
periments were perfo
cycle.

In DNA-mediated
malian cells, as well
nuclei or pronuclei,
This pattern consists
gration sites per cel

According to Evans (22) 20% to 30% germline chimerism can be achieved by this method.

A very critical step in this approach of producing transgenic animals is the successful transformation of the ES-cells. There are several methods of introducing foreign genes into the genomes of these cells with variable degrees of efficiency and technical equipment and skill required. The calcium-phosphate-precipitation method, which is comparatively simple, yields only very few transformants (frequency 10^{-6} to 10^{-7}), but can be used if large numbers of totipotent cells are available (23,24,24a).

One alternative method of transforming EC- or ES-cells more efficiently is the use of recombinant retroviruses (20,21,25). Rubenstein et al. (25) infected EC-cells with psi-2 cell propagated recombinant retrovirus and demonstrated that 1 of 250 EC-cells had incorporated the retrovirus without any further multiplication of the virus in these cells. The efficiency of this retrovirus-mediated transformation method can be further increased depending on the infectivity and the titer of the recombinant virus as well as on the time of exposure (21).

If retroviral infection cannot be established for some reason, microinjection of DNA into the nuclei of totipotent embryonal cells offers a third most effective but cumbersome method of gene transfer with a frequency of 10^{-2} to 1 (24).

Genomic Integration of Foreign DNA in Transgenic Mice

The integration of foreign DNA introduced physically into the mammalian genome is up to now not clearly understood and appears to be an entirely random process. Experiments with mammalian cell lines have shown that after DNA transfections (calcium phosphate precipitates), transgenomes can be found within the nucleus, i.e., high molecular weight structures containing DNA, which are not associated with chromosomes (26). The stability of the genetic transformation process depends on its subsequent chromosomal integration during the following cell cycles (27). A number of observations (23,28-31) have shown clearly that foreign DNA, once within the nucleus, undergoes rather complex biochemical processing including ligation and recombination reactions. The importance of nuclear enzymes for the integration of foreign DNA into the genome has also been indicated by the experiments of Giulotto and Israel (32), who found that the transformation efficiency in synchronized mammalian cells was significantly higher when the experiments were performed during the early S-phase of the cell cycle.

In DNA-mediated gene transfer experiments with somatic mammalian cells, as well as after microinjection of foreign DNA into nuclei or pronuclei, the same integration pattern can be found. This pattern consists of only a single, rarely, two (33,34), integration sites per cell and the integration of one to 400 copies

(35) per site in a concatamer structure, i.e., a head-to-tail arrangement of the foreign gene copies.

Smithies et al. (36) have shown that homologous recombination can be used to target the integration site of foreign genes into endogenous gene loci of somatic mammalian cells. Until now homologous recombination of foreign DNA with endogenous genes has not been reported in transgenic mice. It may well be that this is due to the very low frequency of such events (10^{-9} in somatic cells), which makes it rather improbable to occur in only a few thousand microinjection experiments.

Usually intact gene copies are found to be integrated into the genomes of transgenic mice showing the expected restriction patterns in a Southern blot (1). It has been reported (1,3,37-44) that occasionally partially deleted or recombined foreign genes were integrated into some transgenic mice. Moreover, in established transgenic mouse lines instability of the transgenes is sometimes observed. This is expressed either in a reduction of the number of integrated exogenous gene copies (45) which Gordon (35) explains by their possible recombination and subsequent excision from the chromosomal structure, or in a change of their restriction patterns (47,48). The latter can be found within different generations (40,48) or even in ontogenetic development (47), indicating that structural alterations of the integrated foreign genes can occur during replication and meiosis.

Recent reports (44,49) suggest that alterations of the foreign genes introduced into the genomes are generated by extensive rearrangements of endogenous sequences flanking the integration sites. Tarantul et al. (44) hypothesized that repeated endogenous sequences, which are often associated with genome rearrangements, may be involved in the integration process of foreign DNA.

The biological gene delivery system by retroviral vectors differs from the physical procedures, since the virus itself induces mechanisms which lead to the integration of a biologically functioning provirus. It is important to emphasize that therefore this system also has its limitations, as these biological mechanisms regulating the expression of proviral genes may well interfere with the expression of the enclosed foreign gene and its regulation. This will be discussed later.

Foreign genes enclosed within a retroviral vector integrate as a single copy per integration site (8,9). Depending on the infectivity and the titer of the virus, multiple integration sites (up to 26) per cell can be obtained in ES-cells and, therefore, in transgenic mice (21). Although the instability of recombinant retroviral genomes in somatic and ES-cells (20) and also partial instability of M-MuLV in two provirus containing mouse strains (11) have been reported, no such evidence has been found so far within transgenic mice established by the use of replication deficient recombinant retroviral vectors. However, the comparatively small number of mice obtained so far by this method does not exclude the possibility of such events to occur.

Expression of Forei

Expression of
first detected by E
living mice and th
Although several tra
by these authors, o
foreign gene. Lack
integration into in
supported by Palmit
(51), who observed
transgenic mouse lin
patterns (54) or ab
(51). Furthermore, i
mRNA produced in
correlated with the
observation which
integration site in
in expression was als
molecules transcribed

Additionally, o
in the regulative m
foreign genes. The
foreign genes had be
rived sequences (5,37
karyotic sequences on

The work of Pa
clearly that the exp
stimulated when these
exemplified by the m
human growth hormone
ectopically in a var
Mt-I promotor, which
tion and growth rate
al. (56) have found
Mt-I-rGH fusion gene
fected by the integra
structs, which incluc
ride other inhibitory
importance of the int

Since then, tran
velopment of fusion g
for tissue specific
terns. Although eukar
remains unclear in ma
ment of cell specifi
cis-acting elements h
pression in transgeni
examples in which ge
and strictly directed

i.e., a head-to-tail

nologous recombination
of foreign genes into
lls. Until now homo-
ogenous genes has not
l be that this is due
$^{-9}$ in somatic cells),
n only a few thousand

:o be integrated into
expected restriction
reported (1,3,37-44)
mbined foreign genes
reover, in establish-
transgenes is some-
a reduction of the
45) which Gordon (35)
subsequent excision
ige of their restric-
ind within different
velopment (47), indi-
egrated foreign genes

erations of the for-
nerated by extensive
cing the integration
repeated endogenous
enome rearrangements,
foreign DNA.
y retroviral vectors
the virus itself in-
on of a biologically
asize that therefore
se biological mecha-
enes may well inter-
oreign gene and its

ral vector integrate
Depending on the in-
e integration sites
s and, therefore, in
y of recombinant re-
and also partial in-
g mouse strains (11)
found so far within
eplication deficient
comparatively small
does not exclude the

Expression of Foreign Genes and its Regulation in Transgenic Mice

Expression of foreign genes after pronuclear injection was first detected by E.F. Wagner et al. (3) in fetuses and (2) in living mice and their offspring by T.E. Wagner et al. (1a). Although several transgenic fetuses or living young were analyzed by these authors, only a few showed detectable expression of the foreign gene. Lack of expression was then explained by gene integration into inappropriate genomic sites, a theory that was supported by Palmiter, Chen and Brinster (54) and Lacy et al. (51), who observed that varying expression of foreign genes in transgenic mouse lines was accompanied by different methylation patterns (54) or abnormal chromosomal positions of these genes (51). Furthermore, it was pointed out that the amount of foreign mRNA produced in expressing transgenic mouse lines was not correlated with the copy number of the integrated gene (52), an observation which also indicated a possible role of the integration site in expression of transgenes. Recently, variance in expression was also discussed as a relative instability of mRNA molecules transcribed from the foreign gene construct (53).

Additionally, other factors have become known to be involved in the regulative mechanisms which determine the expression of foreign genes. The expression rate was drastically reduced when foreign genes had been integrated together with plasmid vector derived sequences (5,37,40), suggesting an inhibitory effect of prokaryotic sequences on foreign gene expression in transgenic mice.

The work of Palmiter and colleagues (52,54,55) has shown clearly that the expression of exogenous structural genes can be stimulated when these are fused to certain cis-acting factors, as exemplified by the mouse metallothionein (Mt-I) promoter. Rat or human growth hormone genes fused to this promoter were expressed ectopically in a variety of tissues under the regulation of the Mt-I promotor, which led to a striking increase in hormone production and growth rate of the transgenic mice. Moreover, Swanson et al. (56) have found in their experiments that expression of a Mt-I-rGH fusion gene in separate transgenic mouse lines was unaffected by the integration site, suggesting that certain gene constructs, which include appropriate cis-acting factors, can override other inhibitory environmental effects, thus decreasing the importance of the integration site to a certain extent.

Since then, transgenic research has mainly focused on the development of fusion genes which contain the information necessary for tissue specific and developmentally regulated expression patterns. Although eukaryotic gene regulation, especially in mammals, remains unclear in many respects, in particular when the involvement of cell specific trans-acting factors is considered, some cis-acting elements have been found to provide tissue specific expression in transgenic mice when fused to structural genes. Some examples in which gene expression was developmentally regulated and strictly directed into promoter specific tissues are listed in

Table 1

Promoter Specific Expression of Foreign Genes in Transgenic Mice

Promoter	Structural gene	Reference
elastase I (rat)	elastase I (rat)	57
elastase I (rat)	growth hormone (human)	58
myosin-L-chain (rat)	myosin-L-chain (rat)	39
beta-globin (human)	beta-globin (human)	59
beta-globin (mouse)	beta-globin (human)	60
insulin II (rat)	SV40 T antigen	61
alpha-A-crystallin (mouse)	CAT (prokaryotic)	62
alpha-I-collagen (mouse)	CAT (prokaryotic)	43
insulin (human)	insulin (human)	63 64
skeletal muscle actin (rat)	epsilon-globin (human)	40
whey acidic protein (mouse)	Ha-ras oncogene (human)	53
delta-crystallin (chicken)	delta-crystallin (chicken)	65
alpha-I-antitrypsin (human)	alpha-I-antitrypsin (human)	66
pancreatic amylase (mouse)	pancreatic amylase (mouse)	67

Table 1.

In some cases t
in transgenic mice v
metals (52,54,55), a
chicken transferrin
by glucose (64), the
and whey acidic pro
hormones (53). Thes
gene constructs cont
after integration ir
monal controlled exp
tigators (33,56,70,7
promoter fusion gene
pendent on the promo
particular gene cons
found, suggesting in
ision genes.

Expression of f
pensate, to some ext
transgenic mice (41
application of gene

When recombinar
complicated by mech
provirus. Jaenisch e
viral genomes to be
pre-implantation mou
observed in EC-cells
M-MuLV provirus in t
can occur during emb
vated at all or at
this finding by prov
in each substrain.
was found to be co
virus after integrat
is the cause of the
(78).

Linney et al. (
that retroviral expr
appropriate function
LTR. The existence
which interact with
When foreign genes i
are transferred to
expression block car
are placed in the
partially deleted

nes in Transgenic Mice

Reference
57
58
39
59
60
61
62
43
63
64
40
53
65
66
67

Table 1.

In some cases the inducibility of expression of foreign genes in transgenic mice was reported, as for Mt-I fusion genes by heavy metals (52,54,55), a mouse MHC-II-antigen by interferon (68), the chicken transferrin gene by estrogens (69), the human insulin gene by glucose (64), the mouse pancreatic amylase gene by insulin (67) and whey acidic protein (WAP)-promoter fusion genes by lactogenic hormones (53). These results demonstrate that certain genes or gene constructs contain sufficient cis-acting information so that, after integration into the mouse genome, tissue specific and hormonal controlled expression can be obtained. However, other investigators (33,56,70,71) have shown that expression patterns of Mt-I promoter fusion genes in transgenic mice were not exclusively dependent on the promoter sequence itself, but that depending on the particular gene construct used, different expression patterns were found, suggesting internal cis-acting regions within the different fusion genes.

Expression of foreign genes can be regulated in order to compensate, to some extent, for certain endogenous insufficiencies in transgenic mice (41,72-74). These results indicate the possible application of gene transfer for germline gene therapy in animals.

When recombinant retroviral vectors are used, expression is complicated by mechanisms which regulate the expression of the provirus. Jaenisch et al. (9) have found the expression of retroviral genomes to be blocked when infection had occurred during pre-implantation mouse development, a phenomenon which also was observed in EC-cells (75). In some mouse substrains containing the M-MuLV provirus in their germline, activation of the viral genome can occur during embryogenesis, whereas in others it is not activated at all or at different times (11). The authors explained this finding by proviral integration into different genomic sites in each substrain. Later the expression block in embryonic cells was found to be correlated with de-novo methylation of the provirus after integration (75-77), but it has been doubted that this is the cause of the expression block but rather its consequence (78).

Linney et al. (79) and Gorman et al. (80) presented evidence that retroviral expression in EC-cells is impaired because of inappropriate functioning of cis-acting sequences within the M-MuLV LTR. The existence of trans-acting factors in embryonal cells which interact with these sequences has been postulated (80,81). When foreign genes introduced into recombinant retroviral vectors are transferred to mouse embryos or EC/ES-cells, the described expression block can be overcome when strong internal promoters are placed in the vector construct (10,20,25) or the LTR is partially deleted and replaced by other enhancers (14).

USE OF TRANSGENIC MICE IN BIOLOGICAL RESEARCH

Transgenic mice offer the unique possibility to study the developmental control of expression of introduced gene copies. The transferred and monitored genes can either be naturally occurring sequences or recombinant gene constructs. Since expression studies in vitro with eukaryotic cell lines are only of limited value in explaining the natural mechanisms involved in gene expression, many questions can only be answered after gene transfer into intact developing organisms. For example, transgenic mice have been successfully used to approach different problems in oncology. The c-myc oncogene was shown to be carcinogenic in mice when fused to a viral promoter (82,83) or immunoglobulin enhancers (84,85). Quaife et al. (86) induced pancreatic neoplasia in transgenic mice by fusion of the activated c-ras oncogene to regulatory elements of the rat elastase-I gene, whereas the c-myc gene was not capable of transforming pancreatic cells under these conditions, demonstrating the tumorigenic ability of the activated cellular oncogene. Palmiter et al. (86a) found that a single viral protein, namely the T antigen of SV40, was able to transform choriod plexus epithelia into malignant tumor cells. Sinn et al. (34) presented evidence for the synergistic tumorigenic action of the two oncogenes v-Ha-ras and c-myc when transgenic mice derived from different lines each containing one of these oncogenes fused to a MMTV-promoter were mated and their offspring analyzed.

Since it was shown that subunits of immunoglobulin genes can be introduced into transgenic mice (87) and their subsequent expression in B-cells was observed (88), several authors (42,89-95) have concentrated on transgenic mice, investigating the maturation of B-lymphocytes as a rearrangement process of immunoglobulin genes. Their observations lead to the confirmation and specification of the "allelic exclusion" theory (89).

Genes coding for a variety of different cell surface antigents have been introduced into transgenic mice and their functional expression reported (68,96-100), resulting in a better understanding of the function of these antigens. Other investigators (101-103) have used transgenic mice to investigate the mechanisms of hepatitis B virus surface antigen expression, uncovering interesting aspects of the pathogenesis of hepatitis B. Small and collaborators (104,105) established transgenic mice containing early regions of human papova viruses which resembled the pathological findings in humans and thus provide suitable animal models for the study of these diseases.

Work with transgenic mice containing different forms of beta globin genes (106,107) has revealed interesting information on the developmental regulation of beta globin synthesis. Recently, the use of transgenes as an autosomal DNA marker has served to elucidate the meaning and the mechanism of parental imprinting in transgenic mice (108,109).

Insertional mutagenesis during gene integration can also be

used to establish ce
specified recessive
alpha-1(I) collagen lo
mice has been establi
into the germline (4
lines were establishec
the DHRF locus of EK
mutagenesis these cell
to transgenic animals
genesis by insertion
interest can be used
netic diseases in man.

ATTEMPTS

Up to the present
116), sheep (114,117),
reported. Attempts to
(120-122) have not so

The main purpose
growth hormone genes
line of livestock in
mals (113-115,117,119
interferon genes have
ter procedure aiming
tion and therefore i
(120,121). A fusion ge
moter and the marker
nome in order to study
nisms in more detail
clear or nuclear (tw
formed. In chicken inf
achieved by injection
facilitate pronuclear
had to be centrifuged
the ooplasmic granula
scopic visualization
ing of pronuclei as
give satisfying result

Birth rates after
to foster mothers are
tion rates varied in t
24% (115) and 41% (116
injection during the
ever, these were asso
transferred gene so t
had integrated struct
blot hybridization. A
rabbits containing Mt-

used to establish certain transgenic mouse lines which contain specified recessive mutations as shown for a mutation in the alpha-1(I) collagen locus (110). A dominant mutation in transgenic mice has been established by introduction of a mutated DHFR gene into the germline (46). Other DHFR deficient transgenic mouse lines were established with the use of retroviral insertions into the DHRF locus of EK-cells (111,112). After random insertional mutagenesis these cells were selected in HAT medium and gave rise to transgenic animals via the chimeric route. Thus induced mutagenesis by insertion of exogenous DNA into certain gene loci of interest can be used to establish animal models for certain genetic diseases in man.

ATTEMPTS TO PRODUCE TRANSGENIC LIVESTOCK

Up to the present the production of transgenic rabbits (113-116), sheep (114,117), pigs (113,114) and chicken (118) has been reported. Attempts to produce transgenic goats (119) and cattle (120-122) have not so far been successful.

The main purpose of these experiments was the introduction of growth hormone genes fused to the Mt-I promoter into the germline of livestock in order to increase the growth rate of the animals (113-115,117,119,122). Viral TK genes or simian alpha-interferon genes have been injected into cattle embryos, the latter procedure aiming at the amplification of interferon production and therefore increased disease resistance in the animals (120,121). A fusion gene consisting of the rabbit uteroglobin promoter and the marker gene CAT was introduced into the rabbit genome in order to study the uteroglobin-specific expression mechanisms in more detail (116). In all the mammalian species pronuclear or nuclear (two-cell stage embryos) injection was performed. In chicken infection of recombinant and helper virus was achieved by injection of virus into the yolk of fertile eggs. To facilitate pronuclear or nuclear injections in pigs and cattle ova had to be centrifuged prior to microinjection in order to remove the ooplasmic granula which otherwise interfere with the microscopic visualization of the nucleus (114,120). Fluorescent staining of pronuclei as an alternative (123) has not been found to give satisfying results (114).

Birth rates after micromanipulation and transfer of rabbit ova to foster mothers are consistently 9.5% to 12% (113-116). Integration rates varied in this species between 5.5% (113), 12.8% (114), 24% (115) and 41% (116). The latter results were explained by gene injection during the DNA replication phase of the pronuclei; however, these were associated with a high mutation frequency of the transferred gene so that at least 60% of the transgenic rabbits had integrated structurally altered genes as shown by Southern-blot hybridization. Although several transgenic breeding lines of rabbits containing Mt-hGH fusion genes have been established, none

of these is consistently expressing the foreign gene or showing increased growth rates (124).

The production of one single transgenic lamb after manipulation of 1032 (114) and 436 (117) sheep ova, respectively, has been reported. One lamb had integrated a structurally altered gene (114) and neither one showed any expression of the foreign gene. Recently, the birth of 2 Mt-I-bGH transgenic and 9 Mt-I-hGHRF transgenic lambs has been reported (124). One of these expressed the bovine growth hormone gene and two expressed the gene for the human GH-releasing factor, but none of them showed increased growth.

Transgenic pigs have been produced with the use of growth hormone genes fused to the Mt-I promoter (113,114). Birth rates varied between 5.5% (113) and 9% (114). Brem et al. (113) reported 1 piglet out of 15 born to be transgenic, whereas Hammer et al. (114) obtained 20 transgenic piglets with an integration rate of 10.4%. Six transgenic pig lines have been established containing Mt-I-hGH fusion genes of which only one is expressing the foreign gene (124). These pigs show detectable amounts of hGH (human growth hormone) in their serum but do not grow significantly larger than controls. However, the average backfat of these pigs is less as compared to controls at a body weight of 90 kg indicating some effect of the exogenous GH on body composition (124).

Fabricant et al. (119) transferred 153 goat ova which had been injected with Mt-I-rGH (rat growth hormone) genes to 27 recipients. Of these 20 returned to heat and two aborted their pregnancies; the remaining recipients gave birth to 9 young of which 5 were stillborn. None of the remaining 4 kids which were analyzed proved to be transgenic.

Gene transfer experiments on cattle ova were first described by Lohse et al. (120) who injected about 1000 copies of the plasmid pMK containing the HSV-TK gene into pronuclei of centrifuged cattle oocytes. After in vitro culture for 24 hr about 30% of the manipulated embryos showed expression of the HSV-TK gene. Loskutoff et al. (121) injected HSV-TK or simian alpha-interferon genes into pronuclei or nuclei of bovine one-or two-cell stage embryos. After transfer of 81 manipulated embryos to 24 recipients 3 pregnancies were diagnosed. McEvoy et al. (122) transferred Mt-I-rGH genes or a modification of this gene carrying bovine papilloma virus enhancers to bovine one or two-cell stage embryos. Subsequent transfer of 47 manipulated ova to 17 recipients resulted in at least 4 pregnancies. The birth of transgenic calves has not yet been reported.

Transgenic chicken lines were obtained by retroviral infection of embryos (118). Out of 37 viremic males tested 9 were mosaic according to the integration of provirus into the germline. The frequencies of provirus transmission to their offspring varied between 1% and 11%. Animals from the F-1 generation transmitted the gene in a Mendelian fashion to the F-2 generation. These experiments aimed at the establishment of a suitable gene delivery sys-

tem into the germli
recombinant retrovir
genes (118).

Factors Limiting

In summarizing t
that gene transfer ir
the intended phenotyp
However, results from
will be possible as
conditions can be ac
stock appear to be n

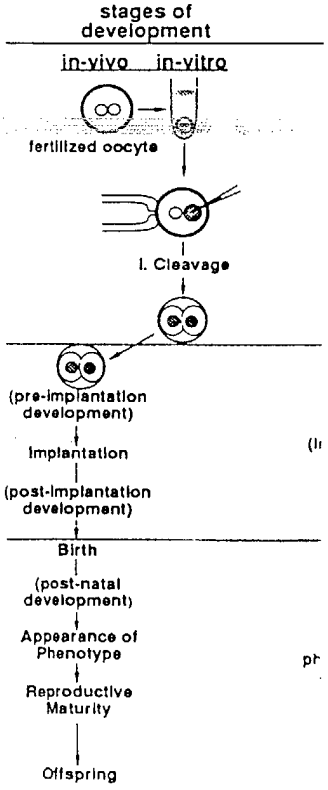

Figure 4. Steps i
(pronuclear injection

eign gene or showing

lamb after manipula-
spectively, has been
urally altered gene
of the foreign gene.
ic and 9 Mt-I-hGHRF
e of these expressed
sed the gene for the
em showed increased

e use of growth hor-
3,114). Birth rates
t al. (113) reported
ereas Hammer et al.
integration rate of
tablished containing
pressing the foreign
unts of hGH (human
significantly larg-
at of these pigs is
of 90 kg indicating
ition (124).
ova which had been
genes to 27 recipi-
orted their pregnan-
9 young of which 5
which were analyzed

ere first described
copies of the plas-
clei of centrifuged
hr about 30% of the
the HSV-TK gene.
an alpha-interferon
e-or two-cell stage
os to 24 recipients
22) transferred Mt-
rying bovine papil-
stage embryos. Sub-
recipients resulted
enic calves has not

retroviral infection
ed 9 were mosaic ac-
germline. The fre-
ffspring varied be-
ion transmitted the
tion. These experi-
gene delivery sys-

tem into the germline of chicken and will be continued with recombinant retroviral vectors which include foreign functional genes (118).

Factors Limiting the Production of Transgenic Livestock

In summarizing the results mentioned above, it can be said that gene transfer into the germline of livestock is possible but the intended phenotypic improvement has not been obtained so far. However, results from transgenic mouse work suggest that this also will be possible as soon as more information on species-specific conditions can be acquired. Thus further experiments with livestock appear to be necessary. Unfortunately, production of trans-

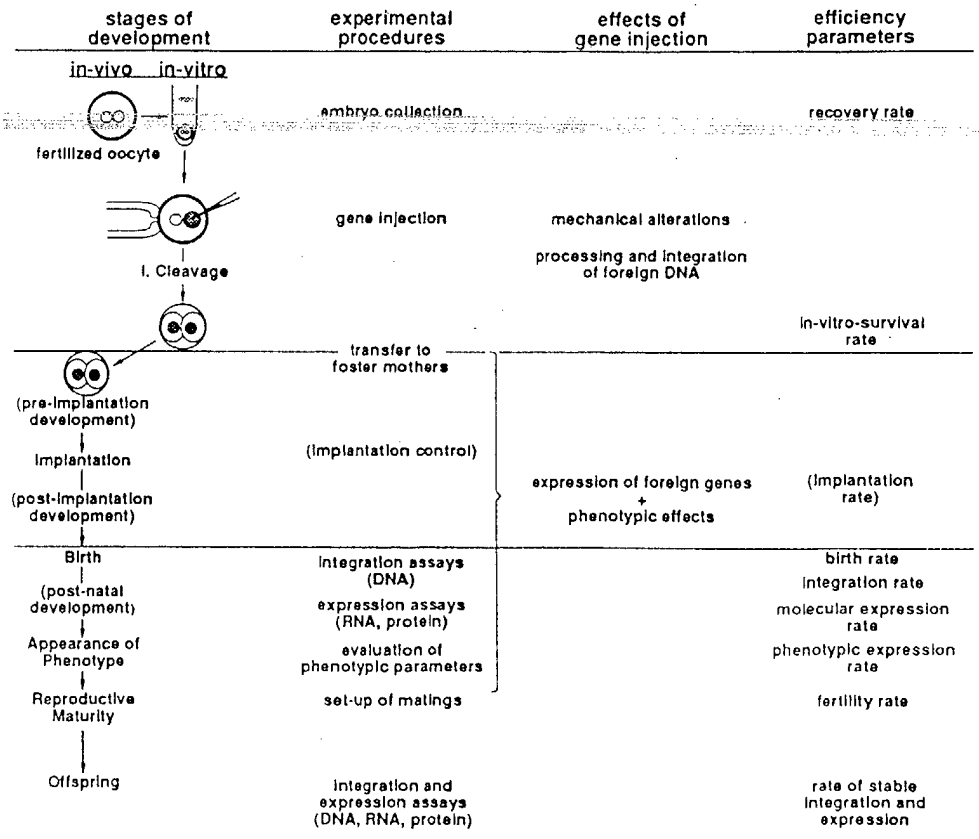

Figure 4. Steps in the production of transgenic animals (pronuclear injection method).

genic livestock is facing two major obstacles: first, very high costs for farm animal husbandry combined with long generation intervals restrict research in this field and second, a relatively small amount of scientific knowledge of farm animals is available as compared to the mouse as the major laboratory animal. How can these obstacles be overcome?

Successful gene transfer to the germline of farm animals requires the collaboration of three major branches of science. These branches are animal physiology, molecular biology and embryology. The latter provides the techniques for introducing foreign genes into the germline of the animals and therefore influences the efficiency rates of gene transfer. Molecular biology contributes the genes and monitors the molecular effects on the genome. An underestimated aspect in this field of research is the necessary participation of animal physiology which provides insight into the regulative mechanisms and phenotypic effects of functional proteins in different species. In order to analyze the current limitations of gene transfer to livestock the different steps of these experiments have to be considered (see Figure 4). Efficiency can be determined at different levels, each referring to the competence of the different scientific branches named above. First, the overall efficiency of the production of transgenic animals (transgenic animals/manipulated oocytes), second the expression efficiency and third, the efficiency of phenotypic improvement can be analyzed.

Considering the costs of livestock husbandry, it is obvious that the efficiencies should be as high as possible. From the data shown above it can be concluded that the maximal overall efficiency in producing transgenic animals is approximately 4% in mice (33,71), 3% in rabbits, (116) 1% in pigs (114) and 0.2% in sheep (117). In order to produce transgenic farm animals for research purposes this efficiency has to be increased drastically considering the expenses involved but until now hardly any attention has been paid to transgenic production efficiencies and little is known about the limiting factors. Overall efficiency is influenced by two components, the ratio of manipulated oocyte development to live young and the integration frequency of the foreign gene. Survival rates have been determined at different stages of *in vitro* or *in utero* development and after birth. *In vitro* cultivation results show that about 10% (1a) to 50% (2) of the manipulated mouse oocytes are lost at the one-cell stage. As these losses are directly due to mechanical alterations of oocyte structures, the varying results indicate the importance of technical skill required in these experiments. However, species-specific differences in mechanical susceptibility of oocytes exist; mouse oocytes, for example, are much more fragile than rabbit oocytes (unpublished observations). When pronuclear injections are performed in rabbit oocytes about 5% to 10% undergo lysis within a period of one hr and 83% cleave to two-cell stages (controls 100%) within 24 hr of *in vitro* cultivation (116). *In*

vitro cultivation expe
to gene transfer to mo
ment to the morula stag
different DNA concentr
jection of buffer alon
to the injection of 5,
copies were injected a
was noticed. Strojek
embryos derived from
showed a significant
blastocysts (75%) as c
(125) investigated sev
developmental potentia
after transfer to she
injected ova to 32-cel
tion for four hours a
transferred ova). Ad
did not lead to furthe
of Tris/HCl buffer was
tion of gene suspensio
stages *in vivo*. These
suspension buffer as
exhibit toxic effects
birth rates (young b
usually found in a l
mice are produced. In
obtained after transfe
ed observations). Thus
insufficiencies are re
injection but that the
developmental potentia
tion is supported by
into rabbit oocytes,
and post-implantationa
in two independent se
bility of the animals
rabbits (115,116,124)
vations consistently
gene injection on the
pre- and post-implant
rates. These effects
alterations alone.

Low integration
gene transfer to live
integration frequency
trations were used (5
ity of the manipulate
limited to approximat
unknown whether integ
is higher in pre-impl

cles: first, very high
with long generation
id second, a relatively
m animals is available
ratory animal. How can

line of farm animals
branches of science.
olecular biology and
iques for introducing
animals and therefore
transfer. Molecular
the molecular effects
this field of research
siology which provides
phenotypic effects of
order to analyze the
vestock the different
dered (see Figure 4).
evels, each referring
tific branches named
the production of
anipulated oocytes),
i, the efficiency of

andry, it is obvious
ssible. From the data
the maximal overall
s approximately 4% in
gs (114) and 0.2% in
ic farm animals for
increased drastically
ntil now hardly any
tion efficiencies and
Overall efficiency is
f manipulated oocyte
on frequency of the
ermined at different
and after birth. In
% (1a) to 50% (2) of
ie one-cell stage. As
alterations of oocyte
importance of tech-
. However, species-
tibility of oocytes
h more fragile than
hen pronuclear injec-
t 5% to 10% undergo
ve to two-cell stages
ultivation (116). In

vitro cultivation experiments over a period of 4 days subsequent to gene transfer to mouse ova resulted in a decrease of development to the morula stage of at least 20% (5). In these experiments different DNA concentrations were used. It was shown that the injection of buffer alone did not increase the survival as compared to the injection of 5, 53 or 520 gene copies. But when 5,300 gene copies were injected a further reduction of the development of 35% was noticed. Strojek (116) reported that two-cell stage rabbit embryos derived from ova injected with 2000 to 4000 gene copies showed a significant reduction in the in vitro development to blastocysts (75%) as compared to controls (89%). Rexroad and Wall (125) investigated several factors which can interfere with the developmental potential of injected sheep ova. They found that after transfer to sheep oviducts, in vivo development of non-injected ova to 32-cell stages was impaired by in vitro cultivation for four hours alone (65% as opposed to 89% in immediately transferred ova). Additional microscopic inspection for 30 min did not lead to further impairment of the survival, but injection of Tris/HCl buffer was detrimental (42% survival). After injection of gene suspension only 19% of the ova developed to 32-cell stages in vivo. These consistent results indicate that the gene suspension buffer as well as the foreign genes themselves can exhibit toxic effects on the developing embryos. Furthermore, birth rates (young born/eggs transferred) of 10% to 30% are usually found in a large number of experiments when transgenic mice are produced. In contrast, birth rates of 50% to 60% can be obtained after transfer of unmanipulated mouse oocytes (unpublished observations). Thus it can be concluded that not only technical insufficiencies are responsible for these low results after gene injection but that they rather reflect a further reduction in the developmental potential of the manipulated oocytes. This assumption is supported by the observation that after gene injection into rabbit oocytes, implantation was low (30% of non-injected) and post-implantational resorption rates exceptionally high (50%) in two independent sets of experiments (116). Additionally, viability of the animals born appears to be reduced in mice (90,97), rabbits (115,116,124) and pigs (124,126). These independent observations consistently suggest deleterious effects of pronuclear gene injection on the viability of embryos which lead to impaired pre- and post-implantational as well as post-natal development rates. These effects probably cannot be explained by mechanical alterations alone.

Low integration frequencies also limit the efficiency of gene transfer to livestock by pronuclear injection. In mice the integration frequency was increased to 37% if higher DNA concentrations were used (5). But this was associated with lower viability of the manipulated embryos, so that the overall efficiency was limited to approximately 6% (d-13 fetuses analyzed). It is still unknown whether integration frequency of foreign genes initially is higher in pre-implantation embryos and is reduced subsequent to

integration by contra-selection; however, at maximum 24% of the rabbits born (115) and 10.4% of the born piglets (114) have integrated foreign gene copies. Strojek (116) has attempted to increase this rate by restricting the time of gene injection to the pronuclear DNA replication phase, referring to results of Giulotto and Israel (32) who had worked with synchronized somatic cells. As a result gene integration was found to be highly increased (integration rate 41%), but this was accompanied by a high frequency of mutation of the integrated foreign gene. These findings were considered to be related to species-specific activities of pronuclear enzymes, as rabbits show much faster pronuclear development than mice, for example, in which similar observations have been reported only rarely (see section Genomic Integration of Foreign DNA in Transgenic Mice).

It can be assumed that genetic and species-specific conditions can cause different limitations of gene integration efficiency, an assumption that is supported by the fact that in sheep integration frequency is comparatively low (114,117) and also by the observation that integration frequency varies considerably between different mouse strains (5) and somatic cell lines of different species (127). Therefore, the major limitations of gene transfer efficiency into the germline of animals appear to arise from deleterious effects of the injected gene suspension on the viability of the manipulated embryos and from low integration frequencies. As both phenomena are as yet poorly understood, considerable improvement in the efficiency of this gene transfer method appears to be rather unlikely in the near future. It would, therefore, be of great advantage if genetically pre-selected totipotent cells could be used to produce germline chimeras which contain the desired genetic make-up in their germ cells, including intact and stably integrated foreign gene copies. This procedure has been shown to be highly efficient in mice (21) and experiments are under way in our laboratory to establish this technique in pigs and cattle.

As far as expression of the integrated foreign genes is concerned, it has been shown in mice that a high degree of appropriate expression can be achieved when certain cis-acting elements are contained in the foreign gene construct, so that approximately 90% to 100% of the Mt-I-GH transgenic mice express the foreign gene (52,55). In pigs this expression frequency is 50% and in rabbits 25% although the same Mt-I-hGH fusion genes have been transferred (114). It should be emphasized that results taken from one species such as the mouse can be considered to apply to other species only to a limited extent. This appears also to be true for results from molecular biology, as cis-acting elements obviously are controlled differently by varying trans-acting factors in genomes of different species. Therefore, transgenic mouse work alone is only of limited value when problems arising in the production of transgenic livestock are to be solved, particularly when there is a necessity of finding cis-acting factors which are suitable

for appropriate gene e

The production of
rabbits and pigs has r
increased growth rates
not understood. Thus,
lation and functional
products in livestock
the inefficiency of f
transgenic pigs is due
receptors on the targe
onset of GH expressio
with different promote
after birth are under
answer this question.

Future

The many advantag
been discussed extensi
provement of productiv
sistance in farm ani
which has been possib
can possibly cause res
tain species-specific
diseases such as infec
in pigs are especiall
viruses is highly inef
all disease resistanc
specific resistance f
could be achieved via

Current work
which have integrated
growth rate and theref
could also be used t
lactation-specific pro
paid to the fact that
been bred during the
lection methods are bi
require more than one
parameters as fertilit
stance, in dairy cattl
high productivity par
has been observed, but

It should be empl
the molecular genetics
tion necessary not
but also to contra-se
healthy performance.
potent cell lines of

maximum 24% of the
piglets (114) have
6) has attempted to
of gene injection to
rring to results of
synchronized somatic
and to be highly in-
accompanied by a high
gn gene. These find-
-specific activities
aster pronuclear de-
similar observations
nomic Integration of

cies-specific condi-
e integration effi-
e fact that in sheep
14,117) and also by
ies considerably be-
cell lines of dif-
limitations of gene
als appear to arise
e suspension on the
low integration fre-
understood, consid-
gene transfer method
re. It would, there-
-selected totipotent
as which contain the
including intact and
procedure has been
and experiments are
s technique in pigs

reign genes is con-
gh degree of appro-
cis-acting elements
o that approximately
express the foreign
y is 50% and in rab-
ies have been trans-
sults taken from one
to apply to other
also to be true for
elements obviously
ting factors in ge-
nic mouse work alone
g in the production
icularly when there
which are suitable

for appropriate gene expression in a given species.

The production of foreign growth hormone (GH) in transgenic rabbits and pigs has not shown any phenotypic effects in terms of increased growth rates thus far (124). The reasons for this are not understood. Thus, further studies on the developmental regulation and functional effect of endogenous as well as foreign gene products in livestock species are required. It might well be that the inefficiency of foreign GH produced continuously in Mt-I-GH transgenic pigs is due to refractoriness of corresponding hormone receptors on the target cells caused by the unphysiological early onset of GH expression during embryonic development. Experiments with different promoters which lead to regulated expression only after birth are under way in our laboratory and will enable us to answer this question.

Future Impact on Livestock Production

The many advantages of transgenic livestock production have been discussed extensively elsewhere (128,129). These include improvement of productivity as well as the transfer of disease resistance in farm animals. Alteration of cell surface antigens which has been possible in transgenic mice (96,97), for example, can possibly cause resistance of transgenic animals towards certain species-specific viruses. Herpes virus infections, causing diseases such as infectious bovine rhinotracheitis or pseudorabies in pigs are especially challenging as immunization against these viruses is highly ineffective under field conditions. Also, overall disease resistance could be increased if stimulation of unspecific resistance factors such as interferon, for example, could be achieved via gene transfer.

Current work is mainly concentrating on farm animals which have integrated foreign GH fusion genes to increase their growth rate and therefore their productivity. In cattle this gene could also be used to increase milk production when fused to lactation-specific promotors. In this context attention should be paid to the fact that highly productive farm animals which have been bred during the last centuries with mainly phenotypical selection methods are biochemically extremely balanced organisms and require more than one gene for high productivity, especially when parameters as fertility and longevity are also desired, as for instance, in dairy cattle. Generally, a negative correlation between high productivity parameters and overall health of farm animals has been observed, but there are individual exceptions.

It should be emphasized that further progress in research of the molecular genetics of farm animals will provide the information necessary not only to introduce new genes into the genome but also to contra-select for certain genes which interfere with healthy performance. This could even be done *in vitro* if totipotent cell lines of livestock were available, thus transferring

directed mutation and subsequent selection mainly to in vitro systems in order to establish phenotypically healthy and highly productive livestock breeds.

Since the work in mice has shown that far more is possible today in respect to genotype alteration than had been assumed five years ago, there is a high probability that the production of genetically improved livestock by gene transfer and in vitro selection will also be feasible. However, a large amount of scientific research needs to be done in livestock species requiring the cooperation of embryologists, molecular biologists and animal physiologists before this can be achieved.

REFERENCES

1 Gordon, J.W. and Ruddle, F.H. (1981) Science 214, 1244-1246.

1a Wagner, T.E., Hoppe, P.C., Jollick, J.D., Scholl, D.R., Hodinka, R.L. and Gault, J.B. (1981) Proc. Nat. Acad. Sci. U.S.A. 78, 6376-6380.

2 Gordon, J.W., Scangos, G.A., Plotkin, D.J., Barbosa, J.A. and Ruddle, F.H. (1980) Proc. Nat. Acad. Sci. U.S.A. 77, 7380-7384.

3 Wagner, E.F., Stewart, T.A. and Mintz, B. (1981) Proc. Nat. Acad. Sci. U.S.A. 78, 5016-5020.

4 Costantini, F. and Lacy, E. (1981) Nature 294, 92-94.

5 Brinster, R.L., Chen, H.Y., Trumbauer, M.E., Yagle, M.K. and Palmiter, R.D. (1985) Proc. Nat. Acad. Sci. U.S.A. 82, 4438-4442.

6 Wilkie, T.M., Brinster, R.L. and Palmiter, R.D. (1986) Dev. Biol. 118, 9-18.

7 Jaenisch, R. and Mintz, B. (1974) Proc. Nat. Acad. Sci. U.S.A. 71, 1250-1254.

8 Jaenisch, R. (1976) Proc. Nat. Acad. Sci. U.S.A. 73, 1260-1264.

9 Jaenisch, R., Fan, H. and Croker, B. (1975) Proc. Nat. Acad. Sci. U.S.A. 72, 4008-4012.

10 Rubenstein, J.L.R., Nicolas, J.-F., and Jacob, F. (1986) Proc. Nat. Acad. Sci. U.S.A. 83, 366-368.

11 Jaenisch, R., Jahner, D., Nobis, P., Simon, I., Lohler, J., Harbers, K. and Grotkopp, D. (1981) Cell 24, 519-529.

12 Stuhlmann, H., Cone, R., Mulligan, R.C. and Jaenisch, P. (1984) Proc. Nat. Acad. Sci. U.S.A. 81, 7151-7155.

13 Mann, R., Mulligan, R.C. and Baltimore, D. (1983) Cell 33, 153-159.

14 van der Putten, H., Botteri, F.M., Miller, A.D., Rosenfeld, M.G., Fan, H., Evans, R.M. and Verma, I.M. (1985) Proc. Nat. Acad. Sci. U.S.A. 82, 6148-6152.

15 McLaren,A. (1976) Mammalian Chimeras, Cambridge University Press, England.

16 Watanabe, T., Dev Acad. Sci. U.S.A.

17 Rossant, J. and M 70, 99-112.

18 Evans, M.J. and Ka

19 Bradley, A., Ev E. (1984) Nature 3

20 Stewart, C.L., Va 3701-3709.

21 Robertson, E., Br Nature 323, 445-44

22 Evans, M.J. (1987) Placid, NY.

23 Pellicer, A., Rob Lowy, Roberts, J.I (1980) Science 209

24 Lovell-Badge, R.H. Stem Cells - A P 153-182, IRL Press

24a Lovell-Badge, R.H Evans, M.J. and Ch Quant. Biol. 50, 7

25 Rubenstein, J.L. R Nat. Acad. Sci. U.

26 Perucho, M., Hanah 317.

27 Scangos, G., and R

28 Robins, D.M., Ripl 29-39.

29 Miller, C.K. and T

30 Small, J.A. and Sc

31 Kucherlapati, R.S. Smithies, O. (19 3153-3157.

32 Giulotto, E. and Commun. 118, 310-3

33 Low, M.J., Hamme Palmiter, R.D. and

34 Sinn, E., Muller, and Leder, P. (198

35 Gordon, J.W. (1986

36 Smithies, O., Greg Kucherlapati, R.S.

37 McKnight, G.S., H R.L. (1983) Cell 3

38 Ross, S.R. and So U.S.A. 82, 5880-58

39 Shani, M. (1985) N

40 Shani, M. (1986) M

mainly to in vitro sys-
ealthy and highly pro-

far more is possible
had been assumed five
the production of ge-
er and in vitro selec-
e amount of scientific
es requiring the coop-
ts and animal physiol-

ence 214, 1244-1246.
J.D., Scholl, D.R.,
roc. Nat. Acad. Sci.

J., Barbosa, J.A. and
d. Sci. U.S.A. 77,

B. (1981) Proc. Nat.

294, 92-94.
M.E., Yagle, M.K. and
id. Sci. U.S.A. 82,

er, R.D. (1986) Dev.

roc. Nat. Acad. Sci.

Sci. U.S.A. 73, 1260-

975) Proc. Nat. Acad.

and Jacob, F. (1986)

lmon, I., Lohler, J.,
24, 519-529.
C. and Jaenisch, P.
151-7155.
, D. (1983) Cell 33,

ler, A.D., Rosenfeld,
M. (1985) Proc. Nat.

Cambridge University

16 Watanabe, T., Dewey, M.J. and Mintz, B. (1978) Proc. Nat. Acad. Sci. U.S.A. 75, 5113-5117.
17 Rossant, J. and McBurney, M.W (1982) J. Embryol. Exp. Morph. 70, 99-112.
18 Evans, M.J. and Kaufman, M.H. (1981) Nature 292, 154-156.
19 Bradley, A., Evans, M., Kaufman, M.H. and Robertson, E. (1984) Nature 309, 255-256.
20 Stewart, C.L., Vanek, M. and Wagner, E.F. (1985) Embo J. 4, 3701-3709.
21 Robertson, E., Bradley A., Kuehn, M. and Evans, M. (1986) Nature 323, 445-448.
22 Evans, M.J. (1987) 3rd Internat. Symp. Cell. Endocrinol., Lake Placid, NY.
23 Pellicer, A., Robins, D., Wold, B., Sweet, R., Jackson, J., Lowy, Roberts, J.M., Sim, G.K., Silverstein, S. and Axel, R. (1980) Science 209, 1414-1427.
24 Lovell-Badge, R.H. (1987) in Teratocarcinomas and Embryonic Stem Cells - A Practical Approach (Robertson, E.J., ed., 153-182, IRL Press, Oxford.
24a Lovell-Badge, R.H., Bygrave A.E., Bradley, A., Robertson, E., Evans, M.J. and Cheah, K.S.E. (1985) Cold Spring Harbor Symp. Quant. Biol. 50, 707-711.
25 Rubenstein, J.L. R,Nicholas, J.-F. and Jacob, F. (1984) Proc. Nat. Acad. Sci. U.S.A. 81, 7137-7140.
26 Perucho, M., Hanahan, D. and Wigler, M. (1980) Cell 22, 309-317.
27 Scangos, G., and Ruddle, F.H. (1981) Gene 14, 1-10.
28 Robins, D.M., Ripley, S., Henderson, A.S. and Axel R. Cell 23, 29-39.
29 Miller, C.K. and Temin, H.M. (1983) Science 220, 606-609.
30 Small, J.A. and Scangos, G. (1983) Science 219, 174-176.
31 Kucherlapati, R.S., Eves, E.M., Song, K.-Y., Morse, B.S. and Smithies, O. (1984) Proc. Nat. Acad. Sci. U.S.A. 81, 3153-3157.
32 Giulotto, E. and Israel, N. (1984) Biochem. Biophys.Res. Commun. 118, 310-316.
33 Low, M.J., Hammer, R.E., Goodman, R.H. Habener, J.F., Palmiter, R.D. and Brinster, R.L. (1985) Cell 41, 211-219.
34 Sinn, E., Muller, W., Pattengale, P., Tepler, I., Wallace, R. and Leder, P. (1987) Cell 49, 465-475.
35 Gordon, J.W. (1986) (Mt. Sinai J. Med. 53, 223-231.
36 Smithies, O., Gregg, R.G., Boggs, S., S. Kotalewski, M.A. and Kucherlapati, R.S. (1985) Nature 317, 230-234.
37 McKnight, G.S., Hammer, R.E., Kuenzel, E.A. and Brinster, R.L. (1983) Cell 34, 335-341.
38 Ross, S.R. and Solter, D. Proc. (1985) Proc. Nat. Acad. Sci. U.S.A. 82, 5880-5884.
39 Shani, M. (1985) Nature 314, 283-286.
40 Shani, M. (1986) Mol. Cell. Biol. 6, 2624-2631.

41 Yamamura, K.-I., Kikutani, H., Folson, V., Clayton, L.K., Kimoto, M., Akira, S., Kashiwamura, S.-I., Tonegawa, S. and Radamitsu, K. (1985) Nature 316, 67-69.
42 Yamamura, K.-I., Kudo, A., Ebihara, T., Kamino, K., Araki, K., Kumahara, Y. and Watanabe, T. (1986) Proc. Nat. Acad. Sci. U.S.A. 83, 2152-2156.
43 Khillan, J.S., Schmidt, A., Overbeek, P.A., Crombrugghe, B. de and Westphal, H. (1986) Proc. Nat. Acad. Sci. U.S.A. 83, 725-729.
44 Tarantul, V.Z., Kucheriavy, V.V., Makarova, I.V., Baranov, Yu.N., Begetova, I.V., Andreerva, L.E. and Gazaryan, K.G. (1986) Mol. Gen. Genet. 203, 305-311.
45 Palmiter, R.D., Wilkie, T.M., Chen, H.W. and Brinster, R.L. (1984) Cell 36, 869-877.
46 Gordon, J.W. (1986) Mol. Cell. Biol. 6, 2158-2167.
47 Gordon, J.W. (1983) J. Exp. Zool. 228, 313-324.
48 van der Putten, H., Botteri, F. and Ilmensee, K. (1984) Mol. Gen. Genet. 198, 128-138.
49 Covarrubias, L., Nishida, Y. and Mintz, B. (1986) Proc. Nat. Acad. Sci. U.S.A. 83, 6020-6024.
50 Joyner, A. and Bernstein, A. (1983) Mol. Cell. Biol. 3, 2180-2190.
51 Lacy, E., Roberts, S., Evans, E.P., Burtenshaw, M.D. and Constantini, F.D. (1983) Cell 34, 343-358.
52 Palmiter, R.D., Norstedt, G., Gelinas, R.E., Hammer, R.E. and Brinster, R.L. (1983) Science 222, 809-814.
53 Andres, A.-C., Schonenberger, C.-A., Groner, B., Hennighausen, L., LeMeur, M. and Gerlinger, P. (1987) Proc. Nat. Acad. Sci. U.S.A. 84, 1299-1303.
54 Palmiter, R.D., Chen, H.Y. and Brinster, R.L. (1982) Cell 29, 701-710.
55 Palmiter, R.D., Brinster, R.L., Hammer, R.E., Trumbauer, M.E., Rosenfeld, M.G., Birnberg, N.C. and Evans, R.M. (1982) Nature 300, 611-615.
56 Swanson, L.W., Simmons, D.M., Arriza, J., Hammer, R., Brinster, R., Rosenfeld, M.G. and Evans, R.M. (1985) Nature 317, 363-366.
57 Swift, G.H., Hammer, R.E., MacDonald, R.J. and Brinster, R.L. (1984) Cell 38, 639-646.
58 Ornitz, D.M., Palmiter, R.D., Hammer, R.E., Brinster, R.L., Swift, G.H. and MacDonald, R.J. (1985) Nature 313, 600-602.
59 Townes, T.M., Lingrel, J.B., Chen, H.Y., Brinster, R.L. and Palmiter, R.D. (1985) Embo J. 4, 1715-1723.
60 Chada, K., Magram, J., Raphael, K., Radice, G., Lacy, E. and Constantini, F. (1985) Nature 314, 377-380.
61 Hanahan, D. (1975) Nature 315, 115-122.
62 Overbeek, P.A., Chepelinsky, A.B., Khillan, J.S.,Piatigorsky, J. and Westphal, H. (1985) Proc. Nat. Acad. Sci. U.S.A 82, 7815-7819.

63 Bucchini, D., Rip
Lorès, P., Monthic
R. and Jami, J.
2511-2515.
64 Selden, R.F., Skć
and Goodman, H.M.
65 Kondoh, H., Katoh,
M., Kimura, S., Ka
Y. and Okada, T.S.
66 Sifers, R.N., Ca
Bullock, D.W. and
1459-1475.
67 Osborn, L., Rosen
(1987) Mol. Cell.
68 Pinkert, C.A.,
Palmiter, R.D., F
J. 4, 2225-2230.
69 Hammer, R.E., Idze
S. (1986) Mol. Cel
70 Low, M.J., Lecha
Habener, J.F., Ma
231, 1002-1004.
71 Stout, J.T., Che
Brinster, R.L. (19
72 Hammer, R.E., Pal
311, 65-67.
73 LeMeur, M., Gerli
Nature 316, 38-42.
74 Readhead, C., P
Saavedra, R.A.,
703-712.
75 Stewart, C.L., St
(1982) Proc. Nat.
76 Jähner, D., Stuh
Löhler, J., Simor
623-628.
77 Jähner, D. and Jae
78 Gautsch, J.W. and
79 Linney, E., Davis
(1984) Nature 308,
80 Gorman, C.M., Ri
519-526.
81 Niwa, O., Yokota,
32, 1105-1113.
82 Stewart, T.A., Pa
627-637.
83 Leder, A. Patteng
P. (1986) Cell 45,

V., Clayton, L.K.,
., Tonegawa, S. and

ımino, K., Araki, K.,
oc. Nat. Acad. Sci.

, Crombrugghe, B. de
d. Sci. U.S.A. 83,

ova, I.V., Baranov,
and Gazaryan, K.G.

and Brinster, R.L.

58-2167.
-324.
nsee, K. (1984) Mol.

). (1986) Proc. Nat.

ol. Cell. Biol. 3,

ırtenshaw, M.D. and

E., Hammer, R.E. and

, Groner, B.,
er, P. (1987) Proc.

t.L. (1982) Cell 29,

E., Trumbauer, M.E.,
, R.M. (1982) Nature

J., Hammer, R.,
R.M. (1985) Nature

and Brinster, R.L.

E., Brinster, R.L.,
ure 313, 600-602.
Brinster, R.L. and

e, G., Lacy, E. and

n, J.S.,Piatigorsky,
Nat. Acad. Sci.

63 Bucchini, D., Ripoche, M.A., Stinnakre, M.-G. Desbois, P., Lorès, P., Monthioux, E., Absil, J., Lepesant, J.-A., Pictet, R. and Jami, J. (1986) Proc. Nat. Acad. Sci. U.S.A. 83, 2511-2515.

64 Selden, R.F., Skóskiewicz, M.J., Howie, K.B., Russell, P.S. and Goodman, H.M. (1986) Nature 321, 525-528.

65 Kondoh, H., Katoh, K., Takahashi, Y., Fujisawa, H., Yokoyama, M., Kimura, S., Katsuki, M., Saito, M., Nomura, T., Hiramoto, Y. and Okada, T.S. (1987) Dev. Biol. 120, 177-185.

66 Sifers, R.N., Carlson, J.A., Clift, S.M., DeMayo, F.J., Bullock, D.W. and Woo, S.L.C. (1987) Nucl. Acids Res. 15, 1459-1475.

67 Osborn, L., Rosenberg, M.P., Keller, S.A. and Meisler, M.H. (1987) Mol. Cell. Biol. 7, 326-334.

68 Pinkert, C.A., Widera, G., Cowing, E., Heber-Katz, E., Palmiter, R.D., Flavell, R.A. and Brinster, R.L. (1985) Embo J. 4, 2225-2230.

69 Hammer, R.E., Idzerda, R.L., Brinster, R.L. and McKnight, G. S. (1986) Mol. Cell. Biol. 6, 1010-1014.

70 Low, M.J., Lechan, R.M., Hammer, R.E., Brinster, R.L., Habener, J.F., Mandel, G. and Goodman, R.H. (1986) Science 231, 1002-1004.

71 Stout, J.T., Chen, H.Y., Brennand, J., Caskey, C.T. and Brinster, R.L. (1985) Nature 317, 250-252.

72 Hammer, R.E., Palmiter, R.D. and Brinster, R.L. (1984) Nature 311, 65-67.

73 LeMeur, M., Gerlinger, P., Benoist, C. and Mathis, D. (1985) Nature 316, 38-42.

74 Readhead, C., Popka, B., Takahashi, N., Shine, H.D., Saavedra, R.A., Sidman, R.L. and L. Hood (1987) Cell 48, 703-712.

75 Stewart, C.L., Stuhlmann, H., Jahner, D. and Jaenisch, R. (1982) Proc. Nat. Acad. Sci. U.S.A. 79, 4098-4102

76 Jähner, D., Stuhlmann, H., Stewart, C.L., Harbers, K., Löhler, J., Simon, I. and Jaenisch, R. (1982) Nature 298, 623-628.

77 Jähner, D. and Jaenisch, R. (1985) Nature 315, 594-597.

78 Gautsch, J.W. and Wilson, M.C. (1983) Nature 301, 32-37.

79 Linney, E., Davis, B., Overhauser, J., Chao, E. and Fan, H. (1984) Nature 308, 470-472.

80 Gorman, C.M., Rigby, P.W.J. and Lane, D.P. (1985) Cell, 42, 519-526.

81 Niwa, O., Yokota, Y., Ishida, H. and Sugahara, T. (1983) Cell 32, 1105-1113.

82 Stewart, T.A., Pattengale, P.K. and Leder, P. (1984) Cell 38, 627-637.

83 Leder, A. Pattengale, P.K., Kuo, A., Stewart, T.A. and Leder, P. (1986) Cell 45, 485-495.

84 Adams, J.M., Harris, Pinkert, C.A., Corcoran, L.M., Alexander, W.S., Cory, S., Palmiter, R.D. and Brinster, R.L. (1985) Nature 318, 533-538.
85 Langdon, W.Y., Harris, A.W., Cory, S. and Adams, J.M. (1986) Cell 47, 11-18.
86 Quaife, C.J., Pinkert, C.A., Ornitz, D.M., Palmiter, R.D. and Brinster, R.L. (1987) Cell 48, 1023-1034.
86a Palmiter, R.D., Chen, H.Y., Messing, A. and Brinster, R.L. (1985) Nature 316, 457-460.
87 Brinster, R.L., Chen, H.Y., Trumbauer, M.E., Yagle, M.K. and Palmiter, R.D. (1983) Nature 306, 332-336.
88 Storb, U., O'Brien, R.L., McMullen, M.D., Gollahon, K.A. and Brinster, R.L. (1984) Nature 310, 238-241.
89 Ritchie, Brinster, R.L. and Storb, U. (1984) Nature 312, 517-520.
90 Grosschedl, R., Weaver, D., Baltimore, D. and Costantini, F. (1984) Cell 38, 647-658.
91 Rusconi, S. and Koehler, G. (1985) Nature 314, 330-334.
92 Weaver, D., Costantini, F., Imanishi-Kari, T. and Baltimore, D. (1985) Cell 42, 117-127.
93 Weaver, D., Reis, M.H., Albanese, C., Costantini, F., Baltimore, D. and Imanishi-Kari, Cell 45, 247-259.
94 Storb, U., Pinkert, T. (1986) C., Arp, B., Engler, P., Gollahon, K., Manz, J., Brady, W. and Brinster, R.L. (1986) J. Exp. Med. 164, 627-641.
95 O'Brien, R.L., Brinster, R.L. and Storb, U. (19326, 405-411.
96 Frels, W.I., Bluestone, J.A., Hodes, R.J., Capecchi, (1987) Nature 326, M.R. and Singer, D.S. (1985) Science 228, 577-580.
97 Bieberich, Co., Scangos, G., Tanaka, K. and Jay, G. (1986) Mol. Cell. Biol. 6, 1339-1342.
98 Flood, P.M., Benoist, C., Mathis, D. and Murphy, D.B. (1986) Proc. Nat. Acad. Sci. U.S.A. 83, 8308-8312.
99 Isobe, K.-I., Kollias, G., Kolsto, A.-B. and Grosfeld, F. (1986) J. Immunol., 137, 137, 2089-2092.
I00 Kollias, G., Spanopoulou, E., Groveld, F., Ritter, M., Beech, J. and Morris, R. (1987) Proc. Nat. Acad. Sci. U.S.A. 84, 1492-1496.
101 Babinet, C., Farza, H. and Morello, D. (1985) Science 230, 1160-1163.
102 Chisari, F.V., Pinkert, C.A., Milich, DFilippi, P., McLachlan, A., Palmiter, R.D. and Brinster, R.L. (1985) Science 230, 1157-1160.
103 Farza, H., Salmon A.M., Hadchouel, M., J.L., Babinet, C., Tiollais, P. and Pourcel, C. (1987) Proc. Nat. Acad. Sci. U.S.A. 84, 1187-1191.
104 Small, J.A., Scangos, L., Jay, G.A., Cork,G. and Khoury, G. (1986) Cell 46, 13-18.
105 Small, J.A., Khoury, G., Jay, G., Howley, P.M. and Scangos, G.A. (1986) Proc. Nat. Acad. Sci., U.S.A. 83, 8288-8292.

106 Chada, K., Magra 685-688.
107 Kollias, G., Wrig 89-94.
108 Reik, W., Collic M.A. (1987) Natu
109 Swain, J.L., St 719-727.
110 Harbers, K., Ku Proc. Nat. Acad.
111 Hooper, M.L., Ha M. (1987) Nature
112 Kuehn, M.R., Br (1987) Nature 32
113 Brem, G., Breni Kruff, G., Sp Winnacker, E.-L. 251-252.
114 Hammer, R.E., P Bolt, D.J., Ebe (1985) Nature 31
115 Ross, K., Breni FELASA Symposium
116 Strojek, R.M. Hochschule, Hano
117 Nancarrow, C., Ward, K. (1987)
118 Salter, D.W., S Crittenden, L.B.
119 Fabricant, J.D. W.C., Capehart, Bradburg, M. W. 229.
120 Lohse J.K., Robl 23, 205.
121 Loskutoff, N.M., Bowen, M.J., St Theriogenology 2
122 McEvoy, T.G., B J.M. (1987) Ther
123 Minhas, B.S., McCrady, J.D., (1984) Pinkert,
124 Hammer, R.E., P D.J., Wall, R.J 3rd Internat. Sy Aug. 30-Sept. 2,
125 Rexroad, C.E. 611-619.

an, L.M., Alexander,
nster, R.L. (1985)

Adams, J.M. (1986)

Palmiter, R.D. and

and Brinster, R.L.

E., Yagle, M.K. and

Gollahon, K.A. and

(1984) Nature 312,

and Costantini, F.

314, 330-334.
, T. and Baltimore,

, Costantini, F.,
147-259.
, B., Engler, P.,
Inster, R.L. (1986)

torb, U. (19326,

, Capecchi, (1987)
ience 228, 577-580.
and Jay, G. (1986)

Murphy, D.B. (1986)

. and Grosfeld, F.

Ritter, M., Beech,
d. Sci. U.S.A. 84,

(1985) Science 230,

ppi, P., McLachlan,
1985) Science 230,

J.L., Babinet, C.,
c. Nat. Acad. Sci.

c,G. and Khoury, G.

, P.M. and Scangos,
83, 8288-8292.

106 Chada, K., Magran, J. and Costantini, F. (1986) Nature 319, 685-688.

107 Kollias, G., Wrighton, N., Hurst, Grosveld, F. (1986) Cell 46, 89-94.

108 Reik, W., Collick, A., Norris, M.L. Barton, S.C. and Surami, M.A. (1987) Nature 328, 248-251.

109 Swain, J.L., Stewart, T.A. and Leder, P. (1987) Cell 50, 719-727.

110 Harbers, K., Kuehn, M., Delius, H. and Jaenisch, R. (1984) Proc. Nat. Acad. Sci. U.S.A. 81, 1504-1508.

111 Hooper, M.L., Hardy, K., Handyside, A., Hunter, S. and Monk, M. (1987) Nature 326, 292-295.

112 Kuehn, M.R., Bradley, A., Robertson, E.J. and Evans, M.J. (1987) Nature 326, 295-298.

113 Brem, G., Brenig, B., Goodman, H.M., Selden,R.C., Graf, F., Kruff, G., Springmannn, K., Hondale, J., Meyer, J., Winnacker, E.-L. and Kraeusslich, H. (1985) Zuchthygiene 20, 251-252.

114 Hammer, R.E., Pursel, V.G., Rexroad, C.E., Jr., Wall, R.E., Bolt, D.J., Ebert, K.M., Palmiter, R.D. and Brinster, R.L. (1985) Nature 315, 680-683.

115 Ross, K., Brenig, B., Meyer, J. and Brem, G. (1987) 3rd FELASA Symposium, Amsterdam, June 1-5, 1987.

116 Strojek, R.M. (1986) Dissertation Vet. Med., Tieraerztl. Hochschule, Hanover, FRG.

117 Nancarrow, C., Marshall, J., Murray, J., Hazelton, I. and Ward, K. (1987) Theriogenology 27, 263.

118 Salter, D.W., Smith, E.J., Hughes, S.H., Wright, S.E. and Crittenden, L.B. (1987) Virology 157, 236-240.

119 Fabricant, J.D., Nuti, L.C., Minhas, B.S., L.B.S., Baker, W.C., Capehart, J.S., Marrack, P., Chalmers, J.H. Jr., Bradburg, M. W. And Womack, J.E. (1987) Theriogenology 27, 229.

120 Lohse J.K., Robl, J.M. and First, N.L. (1985) Theriogenology 23, 205.

121 Loskutoff, N.M., Coren, B.R., Barritos, D.R., Bessondo, E., Bowen, M.J., Stone, Stack, M., G. and Kraemer, D.C. (1986) Theriogenology 25, 168.

122 McEvoy, T.G., Barry, T., Keane, B. Gonnon, F. and Sreenan, J.M. (1987) Theriogenology 27, 258.

123 Minhas, B.S., Capehart, J.S., Bowen, M.J., Womack, J.E., McCrady, J.D., Harms, P.G., Wagner, T.E. and Kraemer, D.C. (1984) Pinkert, Biol. Reprod. 30, 687-691.

124 Hammer, R.E., Pursel, V.G., Rexroad, C.E. Jr.,C.A., Boit, D.J., Wall, R.J., Palmiter, R.D. and Brinster, R.L. (1987) 3rd Internat. Symp. Cell. Endocrinol., Lake Placid, New York, Aug. 30-Sept. 2, 1987.

125 Rexroad, C.E. and Wall, R.J. (1987) Theriogenology 27, 611-619.

126 Brem, G., Brenig, B., Goodman, H.M., Selden, RF., Kruff, B., Springmann, K., Hondale, J., Meyer, J., Winnacker, E.-L. and Kraeusslich, H. (1986) 3rd World Congress on Genetics Applied to Production, Lincoln, Nebraska, July 16-22, 1986.
127 Shen, Y., Hirschhorn, R.R., Mercer, W.E., Surmacz, E., Tsutsui, Y.,Soprano, K.J. and Basergo, R. (1982) Mol. Cell. Biol. 2, 1145-1154.
128 Wagner, T.E. (1985) Can. J. Anim. Sci. 65, 539-552.
129 Crittenden, L.B. and Salter, D.W. (1985) Can. J. Anim. Sci. 65, 553-562.

PLANT REPORTER GENES:

Richard A. Jef

Department of
Plant Breeding
Maris Lane, Tr
Cambridge, Eng

Much of the attent
ogy is focussed on the
influencing or mediatin
using gene fusions. Ge
tions (performed in vit
sequences from one g
translated under the d
another gene (controlle
an enzyme. Use of repo
sitivity of gene fusic
many types of analysis.

An ideal gene fusi
that is stable, tolerat
simple and versatile as
activity in the organi
sensitive enough to me
abundance in single ce
tion of enzyme activit
tissues and organs. I
tive, cheap and routine
ly varying conditions
and should be tolerant
plant molecular biology
in plants, has been con
marker genes encoding
with this set of proper

To date, at least

Organization TC 1600 CM Bldg./Room

U.S. DEPARTMENT OF COMMERCE
PATENT AND TRADEMARK OFFICE
WASHINGTON, DC 20231
IF UNDELIVERABLE RETURN IN TEN DAYS

OFFICIAL BUSINESS

AN EQUAL OPPORTUNITY EMPLOYER

U.S. OFFICIAL
PENALTY FOR PRIVATE USE $300
$2.90
U.S. POSTAGE
7249720

DELT740 940632011 1A02 16 11/04/03
FORWARD TIME EXP RTN TO SEND
:DELTAGEN INC
1031 BING ST
SAN CARLOS CA 94070-5320

RETURN TO SENDER